Clinicians' Guides to Radionuclide Hybrid Imaging · PET/CT
Series Editors: Jamshed B. Bomanji · Gopinath Gnanasegaran
Stefano Fanti · Homer A. Macapinlac

Archi Agrawal
Venkatesh Rangarajan *Editors*

PET/CT in Lung Cancer

BNMS
BRITISH NUCLEAR MEDICINE SOCIETY

Springer

Clinicians' Guides to Radionuclide Hybrid Imaging

PET/CT

Series Editors

Jamshed B. Bomanji
London, UK

Gopinath Gnanasegaran
London, UK

Stefano Fanti
Bologna, Italy

Homer A. Macapinlac
Houston, Texas, USA

More information about this series at http://www.springernature.com/series/13803

Archi Agrawal
Venkatesh Rangarajan
Editors

PET/CT in Lung Cancer

Springer

BNMS
BRITISH NUCLEAR MEDICINE SOCIETY

Editors
Archi Agrawal
Department of Nuclear Medicine &
Molecular Imaging
Tata Memorial Hospital
Mumbai, Maharashtra
India

Venkatesh Rangarajan
Department of Nuclear Medicine &
Molecular Imaging
Tata Memorial Hospital
Mumbai, Maharashtra
India

ISSN 2367-2439 ISSN 2367-2447 (electronic)
Clinicians' Guides to Radionuclide Hybrid Imaging - PET/CT
ISBN 978-3-319-72660-1 ISBN 978-3-319-72661-8 (eBook)
https://doi.org/10.1007/978-3-319-72661-8

Library of Congress Control Number: 2018930262

Printed on acid-free paper

This Springer imprint is published by Springer Nature
The registered company is Springer International Publishing AG
The registered company address is: Gewerbestrasse 11, 6330 Cham, Switzerland

PET/CT series is dedicated to Prof Ignac Fogelman, Dr Muriel Buxton-Thomas and Prof Ajit K Padhy

Foreword

Clear and concise clinical indications for PET/CT in the management of oncology patients are presented in this series of 15 separate booklets.

The impact on better staging, tailored management and specific treatment of patients with cancer has been achieved with the advent of this multimodality imaging technology. Early and accurate diagnosis will always pay, and clear information can be gathered with PET/CT on treatment responses. Prognostic information is gathered and can forward guide additional therapeutic options.

It is a fortunate coincidence that PET/CT was able to derive great benefits from radionuclide-labelled probes, which deliver good and often excellent target to non-target signals. Whilst labelled glucose remains the cornerstone for the clinical benefit achieved, a number of recent probes are definitely adding benefit. PET/CT is hence an evolving technology, extending its applications and indications. Significant advances in the instrumentation and data processing available have also contributed to this technology, which delivers high throughput and a wealth of data, with good patient tolerance and indeed patient and public acceptance. As an example, the role of PET/CT in the evaluation of cardiac disease is also covered, with emphasis on labelled rubidium and labelled glucose studies.

The novel probes of labelled choline, labelled peptides, such as DOTATATE, and, most recently, labelled PSMA (prostate-specific membrane antigen) have gained rapid clinical utility and acceptance, as significant PET/CT tools for the management of neuroendocrine disease and prostate cancer patients, notwithstanding all the advances achieved with other imaging modalities, such as MRI. Hence, a chapter reviewing novel PET tracers forms part of this series.

The oncological community has recognised the value of PET/CT and has delivered advanced diagnostic criteria for some of the most important indications for PET/CT. This includes the recent Deauville criteria for the classification of PET/CT patients with lymphoma—similar criteria are expected to develop for other malignancies, such as head and neck cancer, melanoma and pelvic malignancies. For completion, a separate section covers the role of PET/CT in radiotherapy planning, discussing the indications for planning biological tumour volumes in relevant cancers.

These booklets offer simple, rapid and concise guidelines on the utility of PET/CT in a range of oncological indications. They also deliver a rapid aide-memoire on the merits and appropriate indications for PET/CT in oncology.

London, UK

Peter J. Ell, FMedSci, DR HC, AΩA

Preface

Hybrid imaging with PET/CT and SPECT/CT combines the best of function and structure to provide accurate localisation, characterisation and diagnosis. There is extensive literature and evidence to support PET/CT, which has made significant impact on oncological imaging and management of patients with cancer. The evidence in favour of SPECT/CT especially in orthopaedic indications is evolving and increasing.

The *Clinicians' Guides to Radionuclide Hybrid Imaging (PET/CT and SPECT/CT)* pocketbook series is specifically aimed at our referring clinicians, nuclear medicine/radiology doctors, radiographers/technologists and nurses who are routinely working in nuclear medicine and participate in multidisciplinary meetings. This series is the joint work of many friends and professionals from different nations who share a common dream and vision towards promoting and supporting nuclear medicine as a useful and important imaging speciality.

We want to thank all those people who have contributed to this work as advisors, authors and reviewers, without whom the book would not have been possible. We want to thank our members from the BNMS (British Nuclear Medicine Society, UK) for their encouragement and support, and we are extremely grateful to Dr. Brian Nielly, Charlotte Weston, the BNMS Education Committee and the BNMS council members for their enthusiasm and trust.

Finally, we wish to extend particular gratitude to the industry for their continuous support towards education and training.

London, UK

Gopinath Gnanasegaran
Jamshed Bomanji

Acknowledgements

The series co-ordinators and editors would like to express sincere gratitude to the members of the British Nuclear Medicine Society, patients, teachers, colleagues, students, the industry and the BNMS Education Committee members, for their continued support and inspiration:

Andy Bradley
Brent Drake
Francis Sundram
James Ballinger
Parthiban Arumugam
Rizwan Syed
Sai Han
Vineet Prakash

Contents

Editors and Contributors

Editors

Archi Agrawal Department of Nuclear Medicine and Molecular Imaging, Tata Memorial Centre, Mumbai, India

Venkatesh Rangarajan Department of Nuclear Medicine and Molecular Imaging, Tata Memorial Centre, Mumbai, India

Contributors

Archi Agrawal Department of Nuclear Medicine and Molecular Imaging, Tata Memorial Centre, Mumbai, India

Athar Haroon Barts Health NHS Trust, London, UK

Sabita Jiwnani Thoracic Surgery, Department of Surgical Oncology, Tata Memorial Hospital, Mumbai, India

George Karimundackal Department of Surgical Oncology, Tata Memorial Hospital, Mumbai, India

Rajiv Kumar Department of Pathology, Tata Memorial Hospital, Mumbai, India

Richard Manber Institute of Nuclear Medicine, University College London Hospital NHS Foundation Trust, London, UK

Aisha Naseer Clinical Radiology, Barts Health NHS Trust, London, UK

Arum Parthipun Department of Nuclear Medicine, Royal Free London NHS Foundation Trust, London, UK

C.S. Pramesh Department of Surgical Oncology, Tata Memorial Hospital, Mumbai, India

Nilendu C. Purandare Department of Nuclear Medicine and Molecular Imaging, Tata Memorial Centre, Mumbai, India

Ameya D. Puranik Department of Nuclear Medicine and Molecular Imaging, Tata Memorial Centre, Mumbai, India

Venkatesh Rangarajan Department of Nuclear Medicine and Molecular Imaging, Tata Memorial Centre, Mumbai, India

Sneha Shah Department of Nuclear Medicine and Molecular Imaging, Tata Memorial Centre, Mumbai, India

April-Louise Smith Institute of Nuclear Medicine, University College London Hospital NHS Foundation Trust, London, UK

Lung Cancer: An Overview

1

Aisha Naseer, Arum Parthipun, Athar Haroon, and Stephen Ellis

Contents

1.1 Introduction

Lung cancer is the most common cancer worldwide with 1.8 million (1,825,000) new cases diagnosed in 2012 [1]. According to statistics from Cancer Research UK, the majority of patients diagnosed with lung cancer present with advanced stage IV disease (NSCLC—non-small cell lung cancer) or extensive disease (SCLC—small cell lung cancer).

The stage of the tumour is used as a prognostic indicator when a potentially curative approach is not feasible and to determine whether adjuvant therapy following

A. Naseer (✉)
Barts Health NHS Trust, London, UK
e-mail: Aisha.Naseer@bartshealth.nhs.uk

A. Parthipun
Department of Nuclear Medicine, Royal Free London NHS Foundation Trust, London, UK
e-mail: arum.parthipun@nhs.net

A. Haroon • S. Ellis
Barts Health NHS Trust, London, UK
e-mail: atharharoon@yahoo.com; Stephen.Ellis@bartshealth.nhs.uk

A. Agrawal, V. Rangarajan (eds.), *PET/CT in Lung Cancer*, Clinicians' Guides to Radionuclide Hybrid Imaging, https://doi.org/10.1007/978-3-319-72661-8_1

treatment with intent to cure is likely to offer a survival benefit. Imaging has always played a vital role in lung cancer staging and typically involves at least a post-contrast CT scan of the chest and abdomen. If treatment with intent to cure is envisaged, the National Institute for Health and Care Excellence (NICE) guidelines recommend PET/CT scanning for patients being considered for treatment with curative intent [2].

The current eighth edition of the stage classification for lung cancer has been the worldwide standard as of January 2017 and has been issued by the AJCC (American Joint Committee on Cancer) and the UICC (Union Internationale Contre le Cancer) and informed by the International Association for the study of lung cancer (IASLC). The data used for this revision was more extensive than that used previously and resulted in some fundamental alterations, the most significant being the alteration to T staging.

1.2 Subtypes of Lung Cancer

Lung cancers are classified according to histological type and tissue of origin. Lung cancers are malignancies arising from epithelial tissue and are carcinomas. The classification of lung cancers is important in defining the optimal management and determines the prognosis. For most purposes, lung cancers are divided into two classes;

Small cell lung cancer (SCLC)
Non-small cell lung cancer (NSCLC)

SCLC is postulated to be of neuroendocrine cell origin and originates submucosally. Classically associated with rapid haematogenous and lymphatic spread, it has traditionally been considered a systemic disease at presentation and is often not amenable to treatment with intent to cure. SCLC almost always occurs in smokers. It is the most common primary lung cancer to cause paraneoplastic syndromes and superior vena cava obstruction.

NSCLC comprises a spectrum of cellular subtypes including:

Squamous cell carcinomas which arise from dysplastic endothelium predominantly in the proximal and segmental bronchi. Histological characteristics are the formation of intracellular bridges. The relative incidence of this subtype of lung cancer is on the decline.

Adenocarcinoma arises from bronchial glands, usually within the lung parenchyma. Histological characteristics are gland formation, mucin secretion and, in 90%, expression of TTF1. Although most cases of adenocarcinoma are associated with smoking, it is the most common form of lung cancer to occur in patients who have never smoked.

Large-cell carcinoma class includes several variants including large-cell neuroendocrine carcinoma and basaloid carcinoma. These tumour types usually have a less favourable prognosis and are less common.

1.3 Risk Factors

Tobacco smoking, particularly cigarettes, is the main risk factor for lung cancer and accounted for 90% of lung cancer deaths in men and 70% of deaths in women in the

year 2000 [3]. Passive smoking, which is the inhalation of smoke from another person's smoking, can be associated with lung cancer in non-smokers.

Other risk factors include exposure to asbestos and occupational exposure to radon, arsenic and chromium. Tobacco smoking and asbestos exposure have a synergistic effect on the formation of lung cancer [4].

The presence of chronic obstructive pulmonary disease or diffuse lung fibrosis is also associated with a higher incidence of lung cancer.

1.4 Clinical Features

Up to 25% of patients are asymptomatic at the time of diagnosis. Symptoms, in those that have them, vary with the extent of disease and are divided into those due to the primary tumour, related to metastatic disease, and those with systemic effects of malignancy.

Symptoms due to primary tumour:

Cough, haemoptysis and recurrent pneumonia.

Mediastinal invasion results in dysphagia, hoarseness, superior vena caval obstruction or diaphragmatic nerve paralysis.

Pleural spread presents with large effusions causing dyspnoea and respiratory compromise.

Chest wall or spinal invasion may cause local or radicular pain.

Apical Pancoast's tumour presents with typical symptoms of brachial plexus invasion or Horner's syndrome.

Nonspecific symptoms include anorexia, weight loss and paraneoplastic syndromes.

1.5 Staging of Non-small Cell Lung Cancer

Staging of the non-small cell lung cancer is based on the tumour, node and metastasis (TNM) classification system. The International Association for the Study of Lung Cancer (IASLC) provided recommendations for the latest eighth edition of the TNM classification of malignant tumours, published by the International Union Against Cancer/Union Internationale Contre Le Cancer (UICC) and American Joint Committee on Cancer (AJCC) [5].

The staging system is described in Table 1.1.

The international staging system for lung cancer stratifies disease extent to determine prognosis. The many possible combinations of T, N and M descriptors are grouped into their appropriate stages to align the stage groupings with prognosis and treatment. The stage groupings for the eighth edition of the TNM classification are seen in Table 1.2.

Table 1.1 Proposed T, N and M descriptors for the eighth edition of the TNM staging for lung cancer

T—primary tumour	
T0	No evidence of primary tumour
Tis	Carcinoma in situ (squamous or adenocarcinoma)
T1	Tumour 3 cm or less in greatest dimension, surrounded by lung or visceral pleura, without bronchoscopic evidence of invasion more proximal than the lobar bronchus (i.e. not in the main bronchus)
T1a (*mi*)	Minimally invasive adenocarcinoma
T1a *ss*	Superficial spreading tumour in central airways (can be of any size but confined to tracheal or bronchial wall)
T1a ≤ *1*	Tumour 1 cm or less in greatest dimension
T1b > *1–2*	Tumour more than 1 cm but not more than 2 cm in greatest dimension
T1c > *2–3*	Tumour more than 2 cm but not more than 3 cm in greatest dimension
T2	Tumour more than 3 cm but not more than 5 cm or tumour with any of the following features:
T2 *Centr*	• Involves main bronchus regardless of distance from the carina, but without involvement of the carina
	• Associated with atelectasis or obstructive pneumonitis that extends to the hilar region, involving part or all of the lung
T2 *Visc*	• Invades visceral pleura
T2a > *3–4*	Tumour more than 3 cm but not more than 4 cm in greatest dimension
T2b > *4–5*	Tumour more than 4 cm but not more than 5 cm in greatest dimension
T3 > *5–7*	Tumour more than 5 cm but not more than 7 cm in greatest dimension
T3 *Inv*	Or directly invades any of the following structures: chest wall (including parietal pleura and superior sulcus tumours), phrenic nerve or pericardium
T3 *Satell*	Or associated with separate tumour nodule(s) in the same lobe as the primary
T4 > *7*	Tumour more than 7 cm in greatest dimension
T4 *Inv*	Or invades any of the following structures: diaphragm, mediastinum, heart, great vessels, trachea, recurrent laryngeal nerve, oesophagus, spine, carina
T4 *Ipsi Nod*	Or associated with separate tumour nodule(s) in a different ipsilateral lobe to that of the primary
N— regional lymph node involvement	
N0	No regional lymph node metastasis
N1	Metastasis in ipsilateral peribronchial and/or ipsilateral hilar lymph nodes and intrapulmonary nodes, including involvement by direct extension
N2	Metastasis in ipsilateral mediastinal and/or subcarinal lymph node(s)
N3	Metastasis in contralateral mediastinal, contralateral hilar, ipsilateral or contralateral scalene or supraclavicular lymph node(s)
M—distant metastasis	
M0	No distant metastasis
M1	Distant metastasis present
M1a *Pl Dissem*	Cytologically proven malignant pleural/pericardial effusions or pleural/pericardial nodules
M1a *Contr Nod*	Or separate tumour nodule(s) in a contralateral lobe
M1b *Single*	Single extrathoracic metastasis
M1c *Multi*	Multiple extrathoracic metastases in one or several organs

Table 1.2 Stage groupings in the eighth edition of the TNM staging system for lung cancer

Stage IA	T1	N0	M0
Stage IA1	T1mi, T1a	N0	M0
Stage IA2	T1b	N0	M0
Stage IA3	T1c	N0	M0
Stage IB	T2a	N0	M0
Stage IIA	T2b	N0	M0
Stage IIB	T1a–c, T2a,b	N1	M0
	T3	N0	M0
Stage IIIA	T1a–c, T2a,b	N2	M0
	T3	N1	
	T4	N0, N1	M0
Stage IIIB	T1a–c, T2a,b	N3	M0
	T3, T4	N2	M0
Stage IIIC	T3, T4	N3	M0
Stage IVA	Any T	Any N	M1a,b
Stage IVB	Any T	Any N	M1c

1.6 Staging of Small Cell Lung Cancer

Traditionally SCLC was considered a systemic disease and classified as either limited or extensive disease according to a modified version of the Veterans Administration Lung Cancer Study Group (VALSG) staging system. This is because at initial diagnosis, approximately 60–70% of patients have metastases [6].

Stage	Description
Limited stage	Disease confined to one hemithorax; includes involvement of mediastinal, contralateral hilar and/or supraclavicular and scalene lymph nodes
Extensive	Disease with spread beyond the definition of limited stage or malignant pleural effusion is present

However, this has now been replaced with the eighth edition lung cancer stage classification described above. This is due to a change in the management of SCLC in that treatment with intent to cure is now considered a viable option.

Key Points

- Lung cancer is the most common cancer worldwide.
- Majority of patients diagnosed with lung cancer present with advanced stage IV disease (NSCLC—non-small cell lung cancer) or extensive disease (SCLC—small cell lung cancer).
- The stage of the tumour is used as a prognostic indicator when a potentially curative approach is not feasible.
- Lung cancers are classified according to histological type and tissue of origin.
- Lung cancers are malignancies arising from epithelial tissue and are carcinomas.
- Lung cancers are divided into two classes: small cell lung cancer (SCLC) and non-small cell lung cancer (NSCLC).
- SCLC is postulated to be of neuroendocrine cell origin and originates submucosally.
- NSCLC comprises a spectrum of cellular subtypes: squamous cell carcinomas, adenocarcinoma and large-cell carcinoma.
- Tobacco smoking, particularly cigarettes, is the main risk factor for lung cancer.
- Tobacco smoking and asbestos exposure have a synergistic effect on the formation of lung cancer.
- The presence of chronic obstructive pulmonary disease or diffuse lung fibrosis is associated with a higher incidence of lung cancer.
- The size of the tumour remains the predominant factor in determining the T stage.
- The international staging system for lung cancer stratifies disease extent to determine prognosis.
- Traditionally SCLC was considered a systemic disease and classified as either limited or extensive disease according to a modified version of the Veterans Administration Lung Cancer Study Group (VALSG) staging system, however this has now been superseded by the eighth edition lung cancer stage classification.

References

1. Ferlay J, Soerjomataram I, Ervik M, et al. GLOBOCAN 2012 v1.0, cancer incidence and mortality worldwide: IARC CancerBase No. 11 [Internet]. Lyon: International Agency for Research on Cancers; 2013.
2. NICE Clinical Guidelines, No. 121. The diagnosis and treatment of lung cancer; 2011.
3. Peto R, Lopez AD, Boreham J, et al. Mortality from smoking in developed countries 1950–2000: Indirect estimates from National Vital Statistics. Oxford University Press; 2006. ISBN 0-19-262535-7.
4. O'Reilly KM, Mclaughlin AM, Beckett WS, Sime PJ. Asbestos-related lung disease. Am Fam Physician. 2007;75(5): 683–8. PMID 17375514.
5. Detterbeck FC, Boffa DJ, Kim AW, et al. The eighth edition lung cancer stage classification. Chest 2017;151(1):193–203.
6. Nicholson SA, Beasley MB, Brambilla E, et al. Small cell lung carcinoma (SCLC): a clinicopathologic study of 100 cases with surgical specimens. Am J Surg Pathol. 2002;26(9):1184–97.

Pathology of Lung Cancer

2

Rajiv Kumar

Contents

2.1 Background

Lung carcinoma is one of the lethal diseases afflicting the global population [1]. Tobacco smoking attributes to majority of cases of lung cancer. Despite decades of efforts to improve outcome through multimodality therapy, survival rates have remained dismal. This is partly attributable to relatively ineffective methods for early detection and lack of curative treatment for advanced disease [2, 3].

2.2 Role of Pathologist in Today's Era of Personalized Medicine

Lung cancer has been traditionally perceived as a relentlessly aggressive, and largely incurable disease, for which the surgical pathologist until recently had a marginal role [2, 4]. Historically, lung cancers have been subdivided by histology

R. Kumar
Department of Pathology, Tata Memorial Hospital, Mumbai, India
e-mail: rajiv.kaushal@gmail.com

A. Agrawal, V. Rangarajan (eds.), *PET/CT in Lung Cancer*, Clinicians' Guides to Radionuclide Hybrid Imaging, https://doi.org/10.1007/978-3-319-72661-8_2

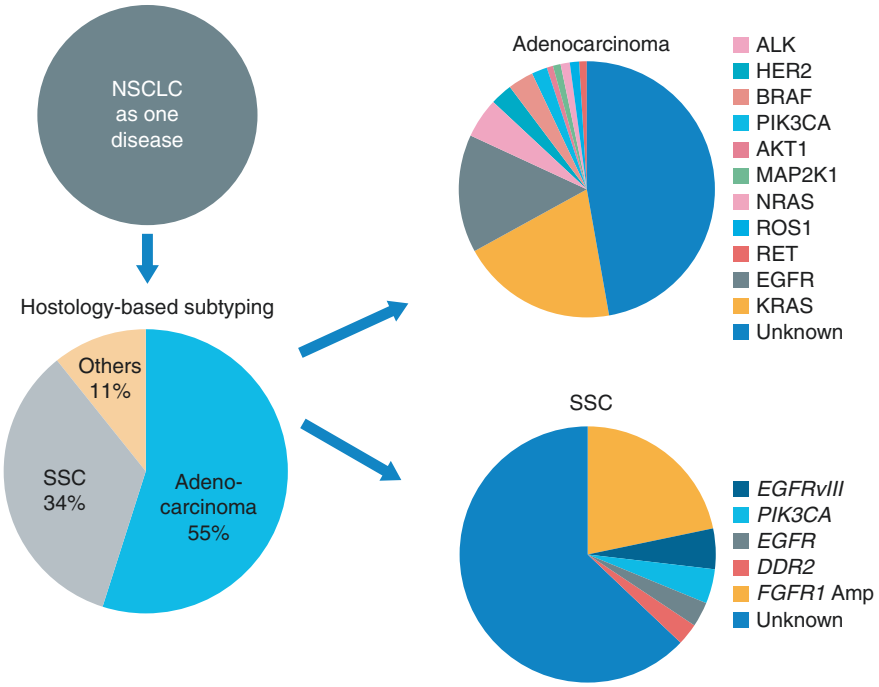

Fig. 2.1 Evolving genomic classification of non-small-cell lung carcinoma (NSCLC)

into small-cell and non-small-cell lung cancers (NSCLCs), with NSCLC further classified into squamous cell carcinoma (SqCC), adenocarcinoma (ADC), and large-cell carcinoma. Prior to the 2004 WHO classification, there have been no therapeutic implications to classify the NSCLCs tumors further, so little attention was been given to the distinction of ADC and SqCC in small tissue samples [2, 4]. The last decade has seen a shift toward molecular-based classification, in which information about genetic alterations and protein expression level is considered alongside histology in order to better understand the pathogenesis of the disease (Fig. 2.1) [5, 6].Now, the patients with NSCLCs are to be classified into more specific types such as ADC or SqCC, whenever possible, as it is important for therapeutic decision-making for several reasons: (1) ADC histology is a strong predictor for improved outcome with pemetrexed therapy compared with SqCC [7], (2) potential life-threatening hemorrhage may occur in patients with SqCC who receive bevacizumab [8], and (3) ADC or NSCLC-not otherwise specified(NSCLC-NOS) should be tested for epidermal growth factor receptor (*EGFR*) mutations and anaplastic lymphoma kinase [ALK] rearrangement as the presence of these mutations is predictive of responsiveness to tyrosine kinase inhibitors [9–13] and crizotinib [14–17].

With the advent of newer predictive biomarkers, tissue is required not only for routine histopathology but also for IHC and molecular analyses [3, 18, 19]. Thus, proper handling of the tissue is the biggest issue in era of personalized medicine, and pathologists' role in the management of lung cancer is becoming more

challenging and demanding, as they are expected to deliver maximal information from these tiny valuable samples. This has resulted in a paradigm shift in the practice of pathologist, who is now holds center stage in the treatment decision process for lung cancer patients [18, 20, 21].

2.3 New 2015 WHO Classification of Lung Cancer Recommendations

A significant change in classification of lung cancer occurred with the landmark publication by collaborative efforts of International Association for the Study of Lung Cancer (IASLC), American Thoracic Society (ATS), and European Respiratory Society(ERS) in 2011 about new lung adenocarcinoma classification [18]. Many good clinical practice guidelines were proposed in this landmark paper (Table 2.1), which were adopted in new 2015 WHO classification with minor alterations [3, 22]. The major changes adopted in the new classifications as compared to 2004 classification are discussed as follows:

Table 2.1 Summary of pathology considerations for good practice applicable to small biopsy and cytology specimens

1. Tissue specimens should be managed not only for diagnosis but also to maximize the amount of tissue available for molecular studies
2. To guide therapy for patients with advanced lung ADC, each institution should develop a multidisciplinary team that coordinates the optimal approach to obtaining and processing biopsy/cytology specimens to provide expeditious diagnostic and molecular results
3. When paired cytology and biopsy specimens exist, they should be reviewed together to achieve the most specific and concordant diagnoses. Cell blocks should be prepared from cytology samples including pleural fluids
4. In order to bring uniformity in routine diagnosis as well as future research and clinical trials for the classification of the disease cohorts in relation to tumor subtypes, similar terminologies should be used for categorization
5. For small biopsies and cytology, NSCLC should be further classified into a more specific type, such as adenocarcinoma or squamous cell carcinoma, whenever possible
6. The term NSCLC-NOS be used as little as possible, and we recommend it be applied only when a more specific diagnosis is not possible by morphology and/or special stains
7. When a diagnosis is made in a small biopsy or cytology specimen in conjunction with special studies, it should be clarified whether the diagnosis was established based on light microscopy alone or if special stains were required
8. The terms AIS and MIA should not be used for diagnosis of small biopsies or cytology specimens. If a noninvasive pattern is present in a small biopsy, it should be referred to as a lepidic growth pattern
9. Neuroendocrine immunohistochemical markers should be performed only in cases where there is suspected neuroendocrine morphology. If neuroendocrine morphology is not suspected, neuroendocrine markers should not be performed
10. The term large-cell carcinoma should not be used for diagnosis in small biopsy or cytology specimens and should be restricted to resection specimens where the tumor is thoroughly sampled to exclude a differentiated component

ADC adenocarcinoma, *AIS* adenocarcinoma in situ, *MIA* minimally invasive adenocarcinoma, *NOS* not otherwise specified, *NSCLC* non-small-cell lung carcinoma, *SQCC* squamous cell carcinoma

(a) Multidisciplinary Approach Is Required for Lung Cancer Diagnosis
One of the central proposals in this new classification is that lung cancer diagnosis is now clearly a multidisciplinary problem [18]. All specialists involved with the diagnosis of lung cancer patients need to work closely together to achieve the correct diagnosis and to obtain appropriate and sufficient tissue for molecular testing [3, 18, 19, 23].

(b) New Criteria and Terminologies for Small Biopsy and Cytology Specimens
Prior classifications were primarily based on the resection specimens, so there were no proposed guidelines for dealing with small biopsies and cytology which are the only available diagnostic material in advance stage [2]. New WHO classification addresses the standardized terminology and criteria for resection specimens, as well as small biopsies and cytology (summarized in Table 2.2) [3, 24, 25].

Table 2.2 Specific terminology and criteria for adenocarcinoma, squamous cell carcinoma, and NSCLC-NOS in small biopsies and cytology

New small biopsy/ cytology terminology	Morphology/stains	2015 WHO classification
Adenocarcinoma (describe identifiable patterns present)	Adenocarcinoma Morphologic adenocarcinoma patterns clearly present	Adenocarcinoma Predominant pattern • Lepidic • Acinar • Papillary • Solid • Micropapillary
Adenocarcinoma with lepidic pattern (if pure, add note: an invasive component cannot be excluded)		Minimally invasive adenocarcinoma, adenocarcinoma in situ, or invasive adenocarcinoma with lepidic component
Invasive mucinous adenocarcinoma (describe patterns present; use term mucinous adenocarcinoma with lepidic pattern if pure lepidic pattern)		Invasive mucinous adenocarcinoma
Adenocarcinoma with colloid /fetal/enteric features		Colloid /fetal/enteric adenocarcinoma
Non-small-cell carcinoma, favor adenocarcinoma	Morphologic adenocarcinoma patterns not present (supported by special stains, i.e., TTF-1)	Adenocarcinoma(solid component may be just one component of tumor)
Squamous cell carcinoma	Morphologic squamous cell patterns clearly present	Squamous cell carcinoma
Non-small-cell carcinoma, favor squamous cell carcinoma	Morphologic squamous cell patterns not present (supported by stains, i.e., p40)	Squamous cell carcinoma (non-keratinizing component may be component of tumor)
Non-small-cell carcinoma, not otherwise specified	No clear adenocarcinoma, squamous or neuroendocrine morphology or staining pattern	Large-cell carcinoma (in resection)
Non-small-cell carcinoma with spindle cell or giant cell carcinoma		Pleomorphic, spindle cell, or giant cell carcinoma

The major changes were focused on the terminology and introduction of new entities for classification of ADC. These include the discontinuation of the terms bronchioloalveolar carcinoma (BAC) and adenocarcinoma, mixed subtype, as well as the introduction of micropapillary as a new histologic subtype, the term adenocarcinoma with lepidic pattern for the former BAC growth pattern and invasive mucinous adenocarcinoma for overtly invasive tumors previously classified as mucinous BAC [3, 18, 22, 24].

For resection specimens, new concepts are introduced such as adenocarcinoma in situ (AIS) and minimally invasive adenocarcinoma (MIA) for small solitary adenocarcinomas (≤3 cm), with either pure lepidic growth (AIS) or predominant lepidic growth with ≤5 mm invasion (MIA) to define patients who, if they undergo complete resection, will have 100% or near 100% disease-free survival, respectively. The invasive component in MIA is defined as follows: (1) histological subtypes other than a lepidic pattern or (2) tumor cells infiltrating myofibroblastic stroma. AIS and MIA terminologies are never to be used in the biopsy specimens [3, 18, 25].

More than 90% of invasive lung adenocarcinomas fall into the mixed subtype in 2004 WHO classification, so it has been proposed to use comprehensive histologic subtyping to make a semiquantitative assessment of percentages (in 5% increments) of the various histologic components: acinar, papillary, micropapillary, lepidic, and solid (Fig. 2.2). Individual tumors are then classified according to the predominant pattern, and the percentages of the subtypes are also reported [18, 25]. This has demonstrated an improved ability to address the complex histologic heterogeneity of lung adenocarcinomas and to improve molecular and prognostic correlations [3, 26].

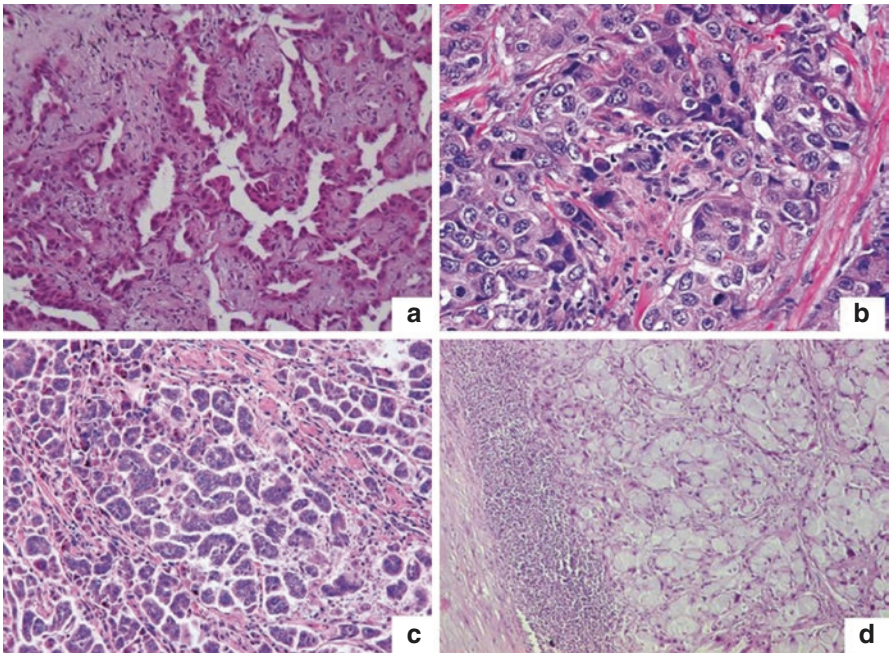

Fig. 2.2 Histological patterns of adenocarcinoma including lepidic (**a**), solid (**b**), micropapillary (**c**), and signet ring cell (**d**) as predominant patterns (hematoxylin-eosin, original magnification ×20)

(c) Diagnostic Approach to Lung Carcinoma with Judicious Use of Immunohistochemistry

In prior WHO classification, lung cancer diagnosis was based mainly on the light microscopy, and role of immunohistochemistry (IHC) was limited to large-cell neuroendocrine tumors and sarcomatoid carcinomas, with no consideration in biopsies [2]. However, a new approach is introduced by recommending limited and judicious use of IHC and/or mucin stains for NSCLC-NOS cases that cannot be categorized definitively on morphological grounds [3, 18, 22]. In the recent past, many algorithms and recommendations to standardize the morphological and IHC classification of lung cancers have been proposed with the aim to optimally preserve the maximum tissue for the molecular testing (Fig. 2.3) [27–29]. The new WHO classification recommended the use of IHC, whenever possible, not only for small biopsies/cytology but also for resected specimens in certain settings such as solid ADC, non-keratinizing SqCC, large-cell carcinoma, neuroendocrine tumors, and sarcomatoid carcinomas [3, 22].

It is recommended to reduce use of the term NSCLC-NOS as minimal as possible using IHC judiciously and classify tumors according to their specific histologic subtype. Tumors that have clear morphologic patterns of ADC (acinar, papillary, lepidic, micropapillary) or SqCC (unequivocal keratinization, well-formed bridges) can be diagnosed, without IHC(Fig. 2.4) [3, 18, 24]. Based on the sensitivity and specificity, the markers which had emerged as preferred classifier of NSCLC include TTF-1 and napsin (for ADC) and p40, p63, and CK5/CK6 (for SqCC) [28, 29]. The reasonable recommendation is that, when IHC is deemed necessary, at least one antibody each for squamous and glandular differentiation, but no more than two antibodies, should be used for an initial work-up (e.g.,TTF-1 or napsin and P40 or P63) (Fig. 2.5) [3, 18, 22]. Of these TTF-1 and p40 are viewed as most useful, and a simple panel of these two markers may be able to classify most NSCC,NOS cases [30–32]. Table 2.3 summarized the various terminologies used, while IHC is used for the categorizing of lung tumors.

If both TTF-1 and p40 are negative in a tumor that lacks clear squamous or glandular morphology, one may consider performing a cytokeratin stain to confirm that the tumor is a carcinoma. If a keratin stain is negative, further stains (S100, CD45, or CD31) may be needed to exclude other tumors [3, 27, 29, 32].

Although primary lung adenocarcinomas can be TTF-1 negative (e.g., mucinous adenocarcinomas), in this setting, one may perform additional IHC markers or suggest clinical evaluation to exclude a metastasis from other sites such as colon or breast. [3, 22, 27]

Even after applying this algorithm, there will remain a minority of specimens where the diagnosis remains NSCLC-NOS, as no clear differentiation can be established by routine morphology and IHC [22, 24].

Recently, the role of EGFR mutation-specific antibodies [32] and ALK [33–35] has been explored. Now, ALK IHC can be used as good screening tool for ALK testing.

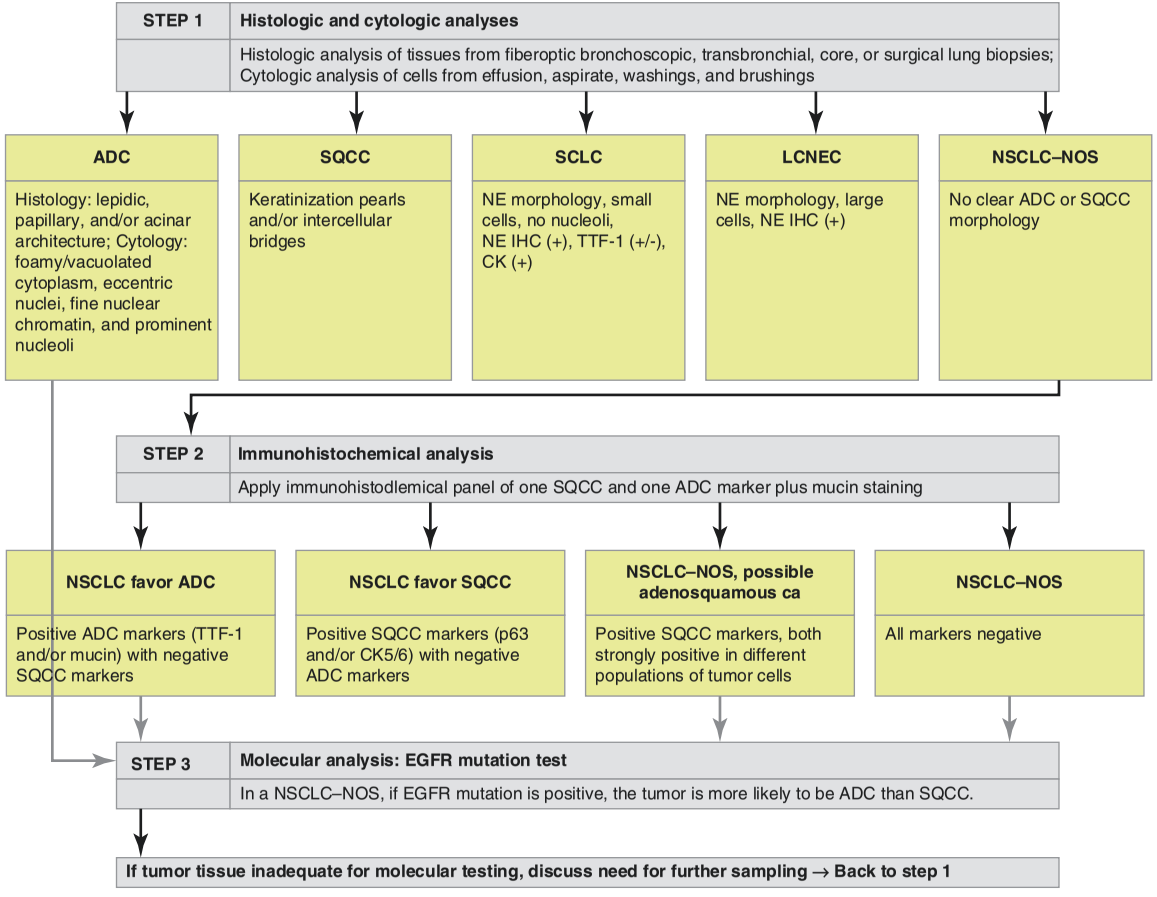

Fig. 2.3 Algorithm for work-up of lung cancer diagnosis in small biopsies and cytology samples. *ADC* adenocarcinoma, *CK* cytokeratin, *IHC* immunohistochemistry, *LCNEC* large-cell neuroendocrine carcinoma, *NE* neuroendocrine, *NSCLC-NOS* non-small-cell lung carcinoma-not otherwise specified, *SCLC* small-cell carcinoma, *SQCC* squamous cell carcinoma, *TTF-1* thyroid transcription factor-1

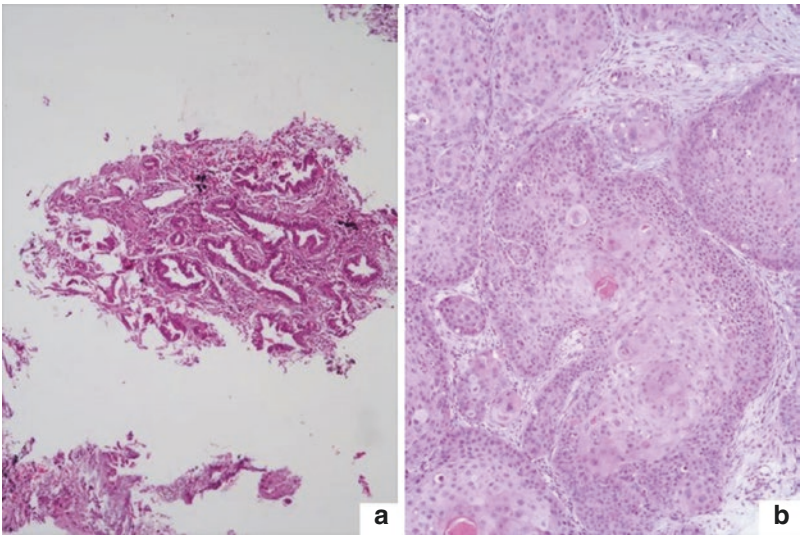

Fig. 2.4 The small biopsy showed fragments of adenocarcinoma with acinar configuration (**a**, hematoxylin-eosin, original magnification ×40) and another case of squamous cell carcinoma with nests of tumor cells that have keratinization and pearls (**b**, hematoxylin-eosin, original magnification ×40).These cases can be diagnosed without immunohistochemistry

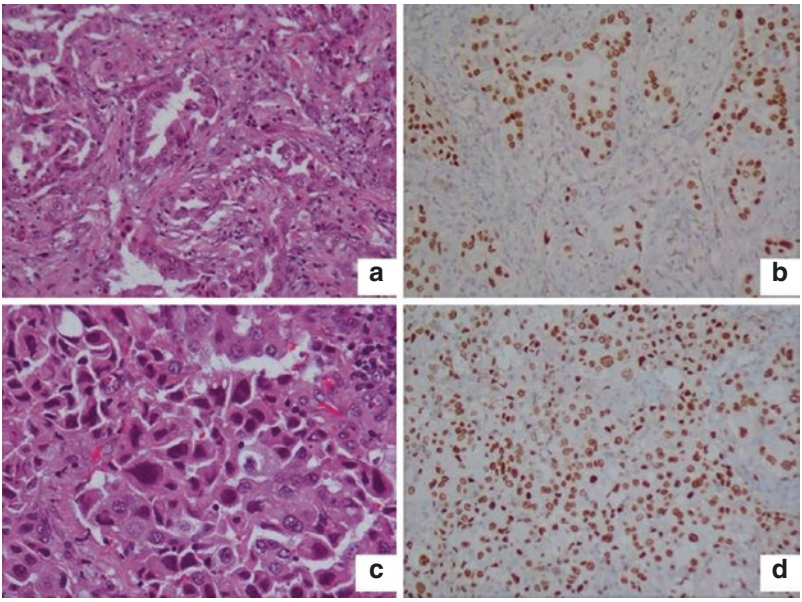

Fig. 2.5 A case of adenocarcinoma with acinar predominant pattern, exhibiting TTF-1 and confirming the primary pulmonary origin (**a**, **b**). Another case of non-small-cell lung carcinoma revealing solid pattern of growth with no clear acinar, papillary, or lepidic growth and no intracytoplasmic mucin. The tumor was thought to have a squamoid morphology and was initially diagnosed as a squamous cell carcinoma (**c**), however, thyroid transcription factor-1 (TTF-1) stain revealed positive immunostaining, favoring adenocarcinoma (**d**) (hematoxylin-eosin, original magnification ×20 (**a**); immunohistochemistry for TTF-1, original magnification ×40 (**b**))

Table 2.3 Algorithm for subtyping of poorly differentiated non-small-cell lung carcinomas according to immunohistochemical staining

TTF-1/ Napsin	P63	P40	CK5/CK6	Diagnosis (Resection)	Diagnosis (Biopsy/ Cytology)
Positive (focal or diffuse)	Negative	Negative	Negative	Adenocarcinoma	NSCLC, favor adenocarcinoma
Positive (focal or diffuse)	Positive (focal or diffuse	Negative	Negative	Adenocarcinoma	NSCLC, favor adenocarcinoma
Positive (focal or diffuse)	Positive (focal or diffuse	Positive (focal)	Negative	Adenocarcinoma	NSCLC, favor adenocarcinoma
Positive (focal or diffuse)	Negative	Negative	Positive (focal)	Adenocarcinoma	NSCLC, favor adenocarcinoma
Positive in different areas	Any one of the above positive in different population as compare to TTF1			Adenosquamous carcinoma(>10% of each component)	NSCLC, possibly adenosquamous carcinoma
Negative	Any one of the above diffusely positive			Squamous cell carcinoma	NSCLC, favor squamous cell carcinoma
Negative	Any one of the above focally positive			Large-cell carcinoma, unclear	NSCLC, NOS
Negative	Negative	Negative	Negative	Large-cell carcinoma	NSCLC, NOS
No stains available	No stains available	No stains available	No stains available	Large-cell carcinoma with no additional stains	NSCLC, NOS

NSCLC non-small-cell lung carcinoma, *NOS* not otherwise specified

2.4 Molecular Work-Up for the Lung

The identification and characterization of molecular targets are having a growing impact on the management of patients with lung cancer [36–38].Due to these developments, lung cancer has now emerged as the role model for the precision cancer medicine for solid tumors [6]. Within the family of lung carcinomas, the molecular underpinnings of lung ADC are best understood at this time (Table 2.4 and Fig. 2.1) [3, 22, 23]. *EGFR* and *ALK* are now widely recognized as therapeutic targets, and thus routine testing for alterations in these genes is a standard of care for advanced lung ADC [9–17].

Guidelines for lung molecular testing recommend that all lung ADCs, regardless of clinical characteristics, undergo molecular testing for *EGFR* mutation and *ALK gene rearrangement* [23]. Other potential driver "events" in NSCLC include ROS1, *KRAS*, *BRAF*, *HER2*, and *FGFR1* and may be tested as recommended by the revised guidelines [5, 6, 22, 38]. The current guidelines recommend to prioritize the tissue for EGFR, ALK, and ROS testing. Molecular testing of other molecular markers is not indicated as a routine stand-alone assay in diagnostic laboratory [6, 38].

Table 2.4 Recurrent molecular alterations in lung adenocarcinoma, squamous cell carcinoma, and small-cell carcinoma

Type of alteration	Adenocarcinoma (%)	Squamous cell carcinoma (%)	Small-cell carcinoma (%)
Mutations			
TP53	30–40	50–80	>90
RB	5–15	5–15	>90
EGFR			
– Caucasian	10–20	<1	<1
– Asian	25–45	<5	<5
KRAS			
– Caucasian	15–35	<5	<1
– Asian	5–10	<5	<1
ERBB2/Her2	<5	0	0
BRAF	<5	0	0
PIK3CA	<5	5–15	<5
Amplifications			
EGFR	5–10	10	<1
ERBB2/Her2	<5	<1	<1
Met	<5	<5	<1
Myc	5–10	5–10	20–30
FGFR1	<5	15–25	<1
Gene rearrangements			
ALK	5	<1	0
ROS	1–2	0	0
RET	1–2	0	0
NTRK1 and NRG1	<1	0	0

However, with the advent of many more potential molecular targets, and the challenges associated with obtaining tissue, there is a growing need to develop and utilize molecular technologies that can determine the expression or mutation status of several genes simultaneously, so-called multiplex testing, in order to obtain the maximum diagnostic information from the limited tumor tissue available. Multiplex PCR assays and high-throughput technologies such as Next Generation Sequencing (NGS) will play an important role in lung carcinoma management and rational therapy selection, but there are many challenges ahead [39]. Further, the role of liquid biopsy in lung cancer is evolving and as per current recommendation can be used to track the disease progression (e.g., EGFR T790M mutational analysis), but not for establishing the diagnosis of malignancy [40].

To conclude, it is now a well-established fact that multidisciplinary approach is essential for establishing a diagnosis of lung cancer and pathologist plays a pivotal role in the lung cancer management in today's era. Modern treatment strategies focus on the pathological classification of NSCLC, which includes assessment of protein expression by IHC as well as the detection of molecular predictive markers.

Key Points

- Lung cancers are subdivided by histology into small-cell and non-small-cell lung cancers (NSCLCs).
- NSCLC are classified into squamous cell carcinoma (SqCC), adenocarcinoma (ADC), and large-cell carcinoma.
- ADC histology is a strong predictor for improved outcome with pemetrexed therapy.
- ADC or NSCLC-not otherwise specified (NSCLC-NOS) should be tested for epidermal growth factor receptor (*EGFR*) mutations and anaplastic lymphoma kinase [ALK] rearrangement.
- New WHO classification addresses the use of standardized terminology and criteria for resection specimens, as well as small biopsies and cytology.
- Currently, terms such as bronchioloalveolar carcinoma (BAC) and adenocarcinoma, mixed subtype, are discontinued.
- Limited and judicious use of immunohistochemistry and/or mucin stains for NSCLC-NOS cases is recommended.
- The identification and characterization of molecular targets play an important role in the management of patients with lung cancer.
- Multiplex PCR assays and high-throughput technologies such as NGS may play important roles in lung carcinoma management and therapy selection.
- The role of liquid biopsy in lung cancer is evolving and is currently recommended to track the disease progression but not for establishing the diagnosis of malignancy.
- Multidisciplinary approach is essential for establishing a diagnosis of lung cancer, and pathologist plays a pivotal role in the lung cancer management in today's era.

References

1. Siegel RL, Miller KD, Jemal A. Cancer statistics, 2016. CA Cancer J Clin. 2016;66:7–30.
2. Travis WD, Brambilla E, Müller-Hermelink HK, Harris CC. Pathology and genetics: tumours of the lung, pleura, thymus and heart. 3rd ed. Lyon: IARC; 2004.
3. Travis WD, Brambilla E, Burke AP, et al. WHO classification of tumours of lung, pleura, thymus and heart. 4th ed. Lyon: IARC; 2015.
4. Travis WD, Brambilla E, Riely GJ. New pathologic classification of lung cancer: relevance for clinical practice and clinical trials. J Clin Oncol. 2013;31:992–1001.
5. Shames DS, Wistuba II. The evolving genomic classification of lung cancer. J Pathol. 2014;232(2):121–33.
6. Sholl LM. Biomarkers in lung adenocarcinoma: a decade of progress. Arch Pathol Lab Med. 2015;139(4):469–80.
7. Scagliotti GV, Parikh P, von Pawel J, et al. Phase III study comparing cisplatin plus gemcitabine with cisplatin plus pemetrexed in chemotherapy-naive patients with advanced-stage non-small-cell lung cancer. J Clin Oncol. 2008;26(21):3543–51.
8. Johnson DH, Fehrenbacher L, Novotny WF, et al. Randomized phase II trial comparing bevacizumab plus carboplatin and paclitaxel with carboplatin and paclitaxel alone in previously untreated locally advanced or metastatic non-small-cell lung cancer. J Clin Oncol. 2004;22(11):2184–91.
9. Kim ES, Herbst RS, Wistuba II, Lee JJ, Blumenschein GR Jr, Tsao A, Stewart DJ, Hicks ME, Erasmus J Jr, Gupta S, Alden CM, Liu S, Tang X, Khuri FR, Tran HT, Johnson BE, Heymach JV, Mao L, Fossella F, Kies MS, Papadimitrakopoulou V, Davis SE, Lippman SM, Hong WK. The BATTLE trial: personalizing therapy for lung cancer. Cancer Discov. 2011;1(1):44–53.
10. Maemondo M, Inoue A, Kobayashi K, et al. Gefitinib or chemotherapy for non-small-cell lung cancer with mutated EGFR. N Engl J Med. 2010;362(25):2380–8.
11. Mitsudomi T, Morita S, Yatabe Y, et al. Gefitinib versus cisplatin plus docetaxel in patients with non-small-cell lung cancer harbouring mutations of the epidermal growth factor receptor (WJTOG3405): an open label, randomised phase 3 trial. Lancet Oncol. 2010;11(2):121–8.
12. Rosell R, Carcereny E, Gervais R, et al. Erlotinib versus standard chemotherapy as first-line treatment for European patients with advanced EGFR mutation-positive non-small-cell lung cancer (EURTAC): a multicentre, open-label, randomised phase 3 trial. Lancet Oncol. 2012;13(3):239–46.
13. Zhou C, Wu YL, Chen G, et al. Erlotinib versus chemotherapy as first-line treatment for patients with advanced EGFR mutation-positive non-small-cell lung cancer (OPTIMAL, CTONG-0802): a multicentre, open-label, randomised, phase 3 study. Lancet Oncol. 2011;12(8):735–42.
14. Soda M, Choi YL, Enomoto M, et al. Identification of the transforming EML4-ALK fusion gene in non-small-cell lung cancer. Nature. 2007;448(7153):561–6.
15. Kwak EL, Bang YJ, Camidge DR, et al. Anaplastic lymphoma kinase inhibition in non-small-cell lung cancer. N Engl J Med. 2010;363(18):1693–703.
16. Sasaki T, Janne PA. New strategies for treatment of ALK rearranged non-small cell lung cancers. Clin Cancer Res. 2011;17(23):7213–8.
17. Shaw AT, Solomon B. Targeting anaplastic lymphoma kinase in lung cancer. Clin Cancer Res. 2011;17(8):2081–6.
18. Travis WD, Brambilla E, Noguchi M, et al. International Association for the Study of Lung Cancer/American Thoracic Society/European Respiratory Society international multidisciplinary classification of lung adenocarcinoma. J Thorac Oncol. 2011;6:244–85.
19. Lee HJ, Lee CH, Jeong YJ, Chung DH, Goo JM, Park CM, Austin JH. IASLC/ATS/ERS International Multidisciplinary Classification of Lung Adenocarcinoma: novel concepts and radiologic implications. J Thorac Imaging. 2012;27(6):340–53.
20. Cagle PT, Allen TC, Dacic S, et al. Revolution in lung cancer: new challenges for the surgical pathologist. Arch Pathol Lab Med. 2011;135(1):110–6.

21. Zugazagoitia J, Enguita AB, Nuñez JA, Iglesias L, Ponce S. The new IASLC/ATS/ERS lung adenocarcinoma classification from a clinical perspective:current concepts and future prospects. J Thorac Dis. 2014;6(Suppl 5):S526–36.
22. Travis WD, Brambilla E, Nicholson AG, Yatabe Y, Austin JH, Beasley MB, Chirieac LR, Dacic S, Duhig E, Flieder DB, Geisinger K, Hirsch FR, Ishikawa Y, Kerr KM, Noguchi M, Pelosi G, Powell CA, Tsao MS, Wistuba I, WHO Panel. The 2015 World Health Organization classification of lung tumors: impact of genetic, clinical and radiologic advances since the 2004 classification. J Thorac Oncol. 2015;10(9):1243–60.
23. Leighl NB, Rekhtman N, Biermann WA, et al. Molecular testing for selection of patients with lung cancer for epidermal growth factor receptor and anaplastic lymphoma kinase tyrosine kinase inhibitors: American Society of Clinical Oncology endorsement of the College of American Pathologists/International Association for the Study of Lung Cancer/Association for Molecular Pathology Guideline. J Clin Oncol. 2014;32:3673–9.
24. Travis WD, Brambilla E, Noguchi M, et al. Diagnosis of lung cancer in small biopsies and cytology: implications of the 2011 International Association for the Study of Lung Cancer/American Thoracic Society/European Respiratory Society classification. Arch Pathol Lab Med. 2013;137:668–84.
25. Travis WD, Brambilla E, Noguchi M, et al. Diagnosis of lung adenocarcinoma in resected specimens: implications of the 2011 International Association for the Study of Lung Cancer/American Thoracic Society/European Respiratory Society classification. Arch Pathol Lab Med. 2013;137:685–705.
26. von der Thüsen JH, Tham YS, Pattenden H, et al. Prognostic significance of predominant histologic pattern and nuclear grade in resected adenocarcinoma of the lung: potential parameters for a grading system. J Thorac Oncol. 2013;8:37–44.
27. Suh J, Rekhtman N, Ladanyi M, Riely GJ, Travis WD. Testing of new IASLC/ATS/ERS criteria for diagnosis of lung adenocarcinoma (AD) in small biopsies: minimize immunohistochemistry (IHC) to maximize tissue for molecular studies. Mod Pathol. 2011;24(1S):424A.
28. Rekhtman N, Ang DC, Sima CS, et al. Immunohistochemical algorithm for differentiation of lung adenocarcinoma and squamous cell carcinoma based on large series of whole-tissue sections with validation in small specimens. Mod Pathol. 2011;24(10):1348–59.
29. Mukhopadhyay S, Katzenstein AL. Subclassification of non-small cell lung carcinomas lacking morphologic differentiation on biopsy specimens: Utility of an immunohistochemical panel containing TTF-1, napsin A, p63, and CK5/6. Am J Surg Pathol. 2011;35(1):15–25.
30. Turner BM, Cagle PT, Sainz IM, Fukuoka J, Shen SS, Jagirdar J. Napsin A, a new marker for lung adenocarcinoma, is complementary and more sensitive and specific than thyroid transcription factor 1 in the differential diagnosis of primary pulmonary carcinoma: evaluation of 1674 cases by tissue microarray. Arch Pathol Lab Med. 2012;136:163–71.
31. Bishop JA, Teruya-Feldstein J, Westra WH, Pelosi G, Travis WD, Rekhtman N. p40 ([DELTA]Np63) is superior to p63 for the diagnosis of pulmonary squamous cell carcinoma. Mod Pathol. 2012;25:405–15.
32. Seo AN, Park TI, Jin Y, et al. Novel EGFR mutation-specific antibodies for lung adenocarcinoma: highly specific but not sensitive detection of an E746_A750 deletion in exon 19 and an L858R mutation in exon 21 by immunohistochemistry [published online ahead of print January 13, 2014]. Lung Cancer.
33. Ali G, Proietti A, Pelliccioni S, et al. ALK rearrangement in a large series of consecutive non-small cell lung cancers: comparison between a new immunohistochemical approach and fluorescence in situ hybridization for the screening of patients eligible for crizotinib treatment. Arch Pathol Lab Med. 2014;138(11):1449–58.
34. Sholl LM, Weremowicz S, Gray SW, et al. Combined use of ALK immunohistochemistry and FISH for optimal detection of ALK-rearranged lung adenocarcinomas. J Thorac Oncol. 2013;8(3):322–8.
35. Wynes MW, Sholl LM, Dietel M, et al. An international interpretation study using the ALK IHC antibody D5F3 and a sensitive detection kit demonstrates high concordance between ALK IHC and ALK FISH and between evaluators. J Thorac Oncol. 2014;9(5):631–8.

36. Larsen JE, Minna JD. Molecular biology of lung cancer: clinical implications. Clin Chest Med. 2011;32:703–40.
37. Cooper WA, Lam DC, O'Toole SA, Minna JD. Molecular biology of lung cancer. J Thorac Dis. 2013;5(Suppl 5):S479–90.
38. Raparia K, Villa C, DeCamp MM, Patel JD, Mehta MP. Molecular profiling in non-small cell lung cancer: a step toward personalized medicine. Arch Pathol Lab Med. 2013;137(4): 481–91.
39. Imielinski M, Berger AH, Hammerman PS, et al. Mapping the hallmarks of lung adenocarcinoma with massively parallel sequencing. Cell. 2012;150(6):1107–20.
40. Sholl LM, Aisner DL, Allen TC, Beasley MB, Cagle PT, Capelozzi VL, Dacic S, Hariri LP, Kerr KM, Lantuejoul S, Mino-Kenudson M, Raparia K, Rekhtman N, Roy-Chowdhuri S, Thunnissen E, Tsao M, Vivero M, Yatabe Y. Liquid biopsy in lung cancer: a perspective from members of the Pulmonary Pathology Society. Arch Pathol Lab Med. 2016;140(8):825–9.

Management of Lung cancer

3

Sabita Jiwnani, George Karimundackal, and C.S. Pramesh

Contents

3.1 Introduction

Lung cancer is the leading cause of cancer-related mortality in both men and women throughout the world, accounting for more than a quarter of the deaths (27%) as per the cancer statistics report 2016 [1]. An estimated 2.2 million new lung cancer cases will be diagnosed in 2016 [1]. Lung cancers are generally divided into small cell lung cancer (SCLC) and non-small cell lung cancer (NSCLC).

S. Jiwnani, MCh, MRCS (✉) • G. Karimundackal, MCh, MRCS
C.S. Pramesh, MS, FRCS
Department of Surgical Oncology, Tata Memorial Hospital, Mumbai, India
e-mail: sabitajiwnani@gmail.com; gkarimundackal@gmail.com; cspramesh@gmail.com

A. Agrawal, V. Rangarajan (eds.), *PET/CT in Lung Cancer*, Clinicians' Guides to Radionuclide Hybrid Imaging, https://doi.org/10.1007/978-3-319-72661-8_3

3.2 Diagnosis

Lung cancer may present with symptoms caused by the primary tumor, locoregional spread, metastatic disease, or ectopic hormone production. Diagnosis should be obtained by the simplest method in patients who have evidence of advanced or metastatic disease.

3.3 Radiological Diagnosis

Chest radiography is usually the preliminary radiographic assessment for persistent respiratory symptoms. Chest radiography is 70–80% accurate in the overall detection of lung cancer [2].

Contrast-enhanced computed tomography (CECT) may help in differentiating between benign and malignant lesions. An increase of 20 HU or more is 98% sensitive and 73% specific in the diagnosis of lung cancer [3]. A peripheral nodule with ill-defined, irregular, and spiculated border is malignant in more than 90% of patients [4].

Positron emission tomography (PET) scanning has been proven to be significantly more accurate than computed tomography (CT) in differentiating benign and malignant lesions as small as 1 cm [5].

Magnetic resonance imaging (MRI) is considered superior to CT in the evaluation of superior sulcus tumors and invasion of the brachial plexus, subclavian vessels, and adjacent vertebral bodies [6]. MRI is also the investigation of choice for brain metastases [7].

3.4 Pathologic Diagnosis

Lung cancer can be diagnosed by using sputum cytology, bronchoscopy, transthoracic needle biopsies, and surgical biopsy [8].

3.5 Staging

The most important prognostic indicator in lung cancer is the extent of disease. All patients with early-stage lung cancer deemed to be operable should undergo staging and complete metastatic work-up. The methods for staging include:

1. Computed tomography
2. PET scan
3. MRI brain
4. Mediastinoscopy/endobronchial ultrasound ± endoscopic ultrasound
5. Bronchoscopy

Table 3.1 TNM staging for lung cancer. Seventh AJCC edition

Category	Description
Primary tumor (T)	
Tis	Carcinoma in situ
T1	Tumor ≤3 cm without invasion more proximal than the lobar bronchus
T1a	Tumor ≤2 cm
T1b	Tumor >2 but ≤3 cm
T2	Tumor >3 cm but ≤7 cm or with any of the following (any tumors with these features are T2a if ≤5 cm): Involves the main bronchus ≥2 cm distal to carina Invades the visceral pleura Associated with atelectasis or obstructive pneumonia that extends to the hilar region but does not involve the whole lung
T2a	Tumor >3 but ≤5 cm
T2b	Tumor >5 but ≤7 cm
T3	Tumor >7 cm or with any of the following: Invades the chest wall, diaphragm, phrenic nerve, mediastinal pleura, parietal pericardium, or main bronchus <2 cm distal to carina but not the carina Atelectasis or obstructive pneumonitis of the entire lung Separate tumor nodules in the same lobe
T4	Tumor of any size with either of the following: Invades the mediastinum, heart, great vessels, trachea, recurrent laryngeal nerve, esophagus, vertebral body, or carina ≥1 Satellite tumors in a different ipsilateral lobe
Regional lymph nodes (N)	
N0	No regional lymph node metastasis
N1	Metastasis to ipsilateral peribronchial or ipsilateral hilar lymph node or both and to intrapulmonary nodes, including that by direct extension of the primary tumor
N2	Metastasis to ipsilateral mediastinal or subcarinal lymph node or both
N3	Metastasis to contralateral mediastinal, contralateral hilar, ipsilateral or contralateral scalene, or supraclavicular lymph node or a combination
Distant metastasis (M)	
M0	No distant metastasis
M1	Distant metastasis
M1a	Tumor with any of the following: ≥1 Tumor nodules in the contralateral lung Pleural nodules Malignant pleural or pericardial effusion
M1b	Distant metastasis

3.6 Lung Cancer Staging System [9] (Table 3.1)

3.7 Management

3.7.1 Early-Stage Lung Cancer

3.7.1.1 Surgery

Surgery is the mainstay of treatment for early-stage (stage I and II) non-small cell lung cancer [10]. Lobectomy is considered as the standard surgical procedure with sublobar resections being reserved for patients with poor pulmonary reserve

[10]. Central tumors may require pneumonectomy or sleeve resection [11].While a randomized trial [12] showed increased local recurrences and lower survival in patients with stage IA tumors, more recent studies [13] have shown equivalent outcomes with lobectomy and anatomical segmentectomy for very early cancers.

Video-assisted thoracoscopic surgery (VATS) has been shown to decrease morbidity, pain, and hospital stay with similar recurrence rates and overall survival compared to open thoracotomy [14]. This approach is also better tolerated in older populations [15] and is associated with fewer delays and dose reductions in adjuvant chemotherapy [16].

The extent of mediastinal lymphadenectomy remains debatable. While two large studies showed discordant results [17–19], a meta-analysis of all studies showed improved survival with SMLND [20].

3.7.1.2 Nonsurgical Management

Radiotherapy and Stereotactic Body Radiotherapy (SBRT)
Medically inoperable patients may be treated with radiation therapy, and a survival of 10–25% has been shown with radiation therapy alone [21]. Stereotactic body radiotherapy can be used for peripheral node-negative tumors less than 5 cm, in medically unfit patients. Studies have shown that patients treated with SBRT had a local recurrence rate of 8.4% and a 5-year overall survival of 70.8% in selected patients [22].

Radiofrequency Ablation
Radiofrequency ablation (RFA) has also been used for inoperable patients and in palliative/metastatic patients. Peripheral tumors less than 3 cm in size are considered suitable, and 2-year survival of up to 75% has been reported [23].

Adjuvant Chemotherapy
The LACE meta-analysis established adjuvant cisplatin-based chemotherapy as the standard of care in completely resected NSCLC. It included 4584 patients with completely resected NSCLC who received cisplatin-based chemotherapy [24]. With a median follow-up time of 5.2 years, the overall HR of death was 0.89 (95% CI, 0.82–0.96; $P = 0.005$), corresponding to a 5-year absolute benefit of 5.4% from chemotherapy.

Adjuvant Radiotherapy
Meta-analysis of nine randomized trials demonstrated a reduction in overall survival with postoperative radiation therapy in stage I and II non-small cell lung cancer [25]. In a subset analysis of the SEER database, Lally et al. showed survival benefit in patients with N2 disease, but was detrimental in those with N0 or N1 disease [26].

3.7.2 Management of N2 Disease

The management of N2 disease is controversial, and combined modality treatment involving surgery, chemotherapy, and radiation is recommended. Several

randomized trials [27–29] and a meta-analysis showed improved survival with a HR = 0.84; (95% confidence interval, 0.77–0.92; $p = 0.0001$) with preoperative chemotherapy followed by surgery [30].Chemoradiotherapy without surgery is an alternative option for the management of patients with N2 nodes [31].

3.7.3 Management of Locally Advanced Unresectable Lung Cancer

An updated Cochrane meta-analysis of concurrent versus sequential chemoradiotherapy published in 2010 showed significant improvement in overall and progression-free survival with concurrent chemoradiotherapy and a survival benefit of 10% at 2 years, but with increased toxicity and nonsignificant increase in mortality in the concurrent group [32].

3.7.4 Management of Stage IV Disease

Patients with stage IV disease and good performance status should be considered for palliative chemotherapy. Chemotherapy improved 1-year survival from 20 to 29% when compared with best supportive care in a meta-analysis. This survival benefit was present irrespective of age or histology [33]. Two drugs have been found to be superior to a single agent, and no benefit was observed with the addition of a third drug [34]. The Elderly Lung Cancer Vinorelbine Italian Study showed 1-year survival of 32% in patients above the age of 70, who received chemotherapy, compared with 14% in patients who received supportive care alone [35]. Cisplatin and pemetrexed is the preferred doublet for first-line chemotherapy with significant improved overall survival in patients with adenocarcinoma [36].

Bevacizumab has shown improved survival combined with carboplatin and paclitaxel in a select subset of patients (non-squamous histology, no hemoptysis, no symptomatic brain metastasis) with stage IV NSCLC, as shown by the ECOG 4599 phase III randomized trial [37]. Maintenance chemotherapy may be considered in responders.

The management of advanced NSCLC has developed significantly over the past decade. Analysis of EGFR mutation and ALK translocation should be attempted in all patients with stage IV disease. Targeted agents such as erlotinib, gefitinib, afatinib, and crizotinib have shown better progression-free survival and improved quality of life in patients with the specific driver mutations/translocations. Immune checkpoint inhibitors have been recently approved for use in advanced lung cancer [38–41]. Although the targeted agents are tolerated better than conventional chemotherapy, they have a different side-effect profile, and resistance to these agents eventually develops (Tables 3.2 and 3.3).

Table 3.2 Management options for non-small cell lung cancer

Stage	Standard treatment	Options
Stage I	Surgery	SBRT
Stage II	Surgery	Adjuvant chemotherapy
Stage IIIA	Multimodality Neoadjuvant chemotherapy + surgery Surgery + adjuvant chemotherapy	Adjuvant radiation may be considered in persistent/multistation N2 disease or positive margins
Stage IIIB	Concurrent chemoradiation	Surgery with neoadjuvant or adjuvant chemoradiation in selected cases
Stage IV	Palliative chemotherapy Targeted therapy in those with driver mutations	Palliative radiation for brain and skeletal metastases Steroids Bisphosphonates

Table 3.3 Targeted therapy approved for clinical use in metastatic non-small cell lung cancer

Target	Approved targeted agents
EGFR mutation (Exons 18, 19, 21)	Erlotinib Gefitinib Afatinib
ALK translocation	Crizotinib Ceritinib
ROS1	Crizotinib Ceritinib
VEGF	Bevacizumab

3.7.5 Small Cell Lung Cancer

SCLC is considered as a separate entity from non-small cell lung cancer due to its aggressive growth, early metastases, and unique sensitivity to chemotherapy and radiation. The Veterans Administration Lung Group proposed the two-stage system used for small cell lung cancer. Patients with disease confined to one hemithorax, with or without mediastinal, contralateral hilar, or ipsilateral supraclavicular or scalene lymph nodes are considered to have limited-stage disease, while those with disease involvement at any other location or pleural effusion are considered to have extensive-stage disease [42]. This staging system was aimed to distinguish disease that could be encompassed within one radiation therapy port. The recent AJCC TNM staging system classifies SCLC similar to NSCLC, but the VA system is still useful in planning treatment [42].

The mainstay of the management of small cell lung cancer is chemotherapy with or without radiation. Surgery may be indicated in patients who present with very early node-negative disease [43]. Management of limited-stage small cell lung cancer involves combination chemotherapy, usually platinum-based and thoracic radiation therapy. If complete remission is achieved, prophylactic cranial irradiation is added. The combination of cisplatin and etoposide (PE) is the widely used regimen in both limited- and extensive-stage small cell lung cancer. A randomized trial reported by Takada and colleagues that compared cisplatin and etoposide with concurrent versus sequential thoracic radiotherapy reported superior 2- and 5-year

survival rates with concurrent approach (2-year survival 35.1% versus 54.4% and 5-year survival 18.3% versus 23.7% in favor of concurrent chemotherapy and radiation) [44]. In a meta-analysis by Auperin et al., prophylactic cranial irradiation showed a 5.4% increase in survival at 3 years [45].

Patients with extensive-stage disease are treated with combination chemotherapy. Even though a combination of cisplatin and etoposide remains most widely used, a randomized trial comparing the combination of cisplatin with either etoposide or irinotecan in extensive-stage small cell lung cancer found the cisplatin/irinotecan to be superior. The 2-year survival rate was also superior at 19.5% versus 5.2% [46].

Key Points

- Chest radiography is 70–80% accurate in the overall detection of lung cancer.
- Contrast-enhanced computed tomography (CECT) may help in differentiating between benign and malignant lesions.
- HU of 20 or more is 98% sensitive and 73% specific in the diagnosis of lung cancer.
- Peripheral nodule with ill-defined, irregular, and spiculated border is malignant in majority of patients.
- ^{18}F-FDG PET/CT is more accurate than CT in differentiating benign and malignant lesions as small as 1 cm.
- MRI is considered superior to CT in the evaluation of superior sulcus tumors and invasion of the brachial plexus, subclavian vessels, and adjacent vertebral bodies.
- MRI is also the investigation of choice for brain metastases.
- Lung cancer can be diagnosed by using sputum cytology, bronchoscopy, transthoracic needle biopsies, and surgical biopsy.
- Patients with early-stage lung cancer deemed to be operable should undergo staging and complete metastatic work-up.

Management of Early-Stage Lung Cancer

- Surgery is the mainstay of treatment for early-stage (stage I and II) non-small cell lung cancer.
- Lobectomy is considered as the standard surgical procedure.
- Sublobar resections are being reserved for patients with poor pulmonary reserve.
- Central tumors may require pneumonectomy or sleeve resection.

- Video-assisted thoracoscopic surgery (VATS) has been shown to decrease morbidity, pain, and hospital stay with similar recurrence rates and overall survival compared to open thoracotomy.
- This approach is also better tolerated in older populations [14] and is associated with fewer delays and dose reductions in adjuvant chemotherapy.
- The extent of mediastinal lymphadenectomy remains debatable.

Nonsurgical Management

- Medically inoperable patients may be treated with radiation therapy.
- Stereotactic body radiotherapy can be used for peripheral node-negative tumors less than 5 cm, in medically unfit patients.
- Radiofrequency ablation (RFA) has also been used for inoperable patients and in palliative/metastatic patients.
- LACE meta-analysis established adjuvant cisplatin-based chemotherapy as the standard of care in completely resected NSCLC.

Management of N2 Disease

- The management of N2 disease is controversial, and combined modality treatment involving surgery, chemotherapy, and radiation is recommended.

Management of Locally Advanced Unresectable Lung Cancer

- Concurrent chemoradiotherapy and a survival benefit of 10% at 2 years, but with increased toxicity and nonsignificant increase in mortality.

Management of Stage IV Disease

- Patients with stage IV disease and good performance status should be considered for palliative chemotherapy.
- III randomized trial [35]. Maintenance chemotherapy may be considered in responders.
- Analysis of EGFR mutation and ALK translocation should be attempted in all patients with stage IV NSCLC disease.
- Immune checkpoint inhibitors have been recently approved for use in advanced lung cancer.
- Targeted agents are tolerated better than conventional chemotherapy, they have a different side-effect profile, and patients eventually develop resistance to these agents.

Small Cell Lung Cancer

- SCLC is considered as a separate entity from non-small cell lung cancer due to its aggressive growth, early metastases, and unique sensitivity to chemotherapy and radiation.
- The mainstay of the management of small cell lung cancer is chemotherapy with or without radiation.
- Surgery may be indicated in patients who present with very early node-negative disease.
- Management of limited-stage small cell lung cancer involves combination chemotherapy.

References

1. Siegel RL, Miller KD, Jemal A. Cancer statistics, 2016. CA Cancer J Clin. 2016;66:7–30.
2. Swensen SJ, Brown LR. Conventional radiography of the hilum and mediastinum in bronchogenic carcinoma. Radiol Clin North Am. 1990;28:521–38, Review.
3. Swensen SJ, Brown LR, Colby TV. Lung nodule enhancement at CT: prospective findings. Radiology. 1996;201:447–55.
4. Zwirewich CV, Vedal S, Miller RR, et al. Solitary pulmonary nodule: high resolution CT and radiologic-patho- logic correlation. Radiology. 1991;179:469–76.
5. Vansteenkiste JF, Stroobants SG. The role of positron emission tomography with 18F-fluoro-2-deoxy-D-glucose in respiratory oncology. Eur Respir J. 2001;17:802–20.
6. Bruzzi JF, Komaki R, Walsh GL, et al. Imaging of non-small cell lung cancer of the superior sulcus: part 1: anatomy, clinical manifestations, and management. Radiographics. 2008;28:551–60, Review.
7. Yokoi K, Kamiya N, Matsuguma H, et al. Detection of brain metastasis in potentially operable non-small cell lung cancer: a comparison of CT and MRI. Chest. 1999;115:714–9.
8. Schreiber G, McCrory DC. Performance characteristics of different modalities for diagnosis of suspected lung cancer: summary of published evidence. Chest. 2003;123:115S–28S, Review.
9. Tsim S, O'Dowd CA, Milroy R, et al. Staging of non-small cell lung cancer(NSCLC): a review. Respir Med. 2010;104:1767–74.
10. Howington JA, Blum MG, Chang AC, et al. Treatment of stage I and II non-small cell lung cancer: diagnosis and management of lung cancer, 3rd ed: American College of Chest Physicians evidence-based clinical practice guidelines. Chest. 2013;143:e278S–313S.
11. Ma Z, Dong A, Fan J, Cheng H. Does sleeve lobectomy concomitant with or without pulmonary artery reconstruction (double sleeve) have favorable results for non-small cell lung cancer compared with pneumonectomy? A meta-analysis. Eur J Cardiothorac Surg. 2007;32:20–8.
12. Ginsberg RJ, Rubinstein LV. Lung Cancer Study Group randomized trial of lobectomy versus limited resection for T1 N0 non-small cell lung cancer. Ann Thorac Surg. 1995;60:615–23.
13. Razi SS, John MM, Sainathan S, et al. Sublobar resection is equivalent to lobectomy for T1a non-small cell lung cancer in the elderly: a Surveillance, Epidemiology, and End Results database analysis. J Surg Res. 2016;200:683–9.
14. Whitson BA, Groth SS, Duval SJ, et al. Surgery for early-stage non-small cell lung cancer: a systematic review of the video-assisted thoracoscopic surgery versus thoracotomy approaches to lobectomy. Ann Thorac Surg. 2008;86:2008–16, Review.

15. Cattaneo SM, Park BJ, Wilton AS, et al. Use of video-assisted thoracic surgery for lobectomy in the elderly results in fewer complications. Ann Thorac Surg. 2008;85:231–5.
16. Cheng D, Downey RJ, Kernstine K, et al. Video-assisted thoracic surgery in lung cancer resection: a meta-analysis and systematic review of controlled trials. Innovations. 2007;2:261–92.
17. Wu Y, Huang ZF, Wang SY, et al. A randomized trial of systematic nodal dissection in resectable non-small cell lung cancer. Lung Cancer. 2002;36:1–6.
18. Allen MS, Darling GE, Pechet TTV, et al. The ACOSOG Z0030 Study Group. Morbidity and mortality of major pulmonary resection in patients with early-stage lung cancer: initial results of the randomised prospective ACOSOG Z0030 trial. Ann Thorac Surg. 2006;81:1013–20.
19. Darling GE, Allen MS, Decker PA, et al. Randomized trial of mediastinal lymph node sampling versus complete lymphadenectomy during pulmonary resection in the patient with N0 or N1 (less than hilar) non-small cell carcinoma: results of the American College of Surgery Oncology Group Z0030 Trial. J Thorac Cardiovasc Surg. 2011;141:662–70.
20. Huang X, Wang J, Chen Q, et al. Mediastinal lymph node dissection versus mediastinal lymph node sampling for early stage non-small cell lung cancer: a systematic review and meta-analysis. PLoS One. 2014;9(10):e109979, eCollection 2014, Review. https://doi.org/10.1371/journal.pone.0109979.
21. Dosoretz DE, Katin MJ, Blitzer PH, et al. Radiation therapy in the management of medically inoperable carcinoma of the lung: results and implications for future treatment strategies. Int J Radiat Oncol Biol Phys. 1992;24:3–9.
22. Onishi H, Shirato H, Nagata Y, et al. Hypofractionated stereotactic radiotherapy (HypoFXSRT) for stage I non-small cell lung cancer: updated results of 257 patients in a Japanese multi-institutional study. J Thorac Oncol. 2007;2:S94–100.
23. Lencioni R, Crocetti L, Cioni R, et al. Response to radiofrequency ablation of pulmonary tumours: a prospective, intention-to-treat, multicentre clinical trial (the RAPTURE study). Lancet Oncol. 2008;9:621–8.
24. Pignon JP, Tribodet H, Scagliotti GV, et al. Lung adjuvant cisplatin evaluation: a pooled analysis by the LACE Collaborative Group. J Clin Oncol. 2008;26:3552–9.
25. PORT Meta-analysis Trialists Group: postoperative radiotherapy for non-small cell lung cancer. Cochrane Database Syst Rev. 2005;(2):CD002142.
26. Lally BE, Zelterman D, Colasanto JM, et al. Postoperative radiotherapy for stage II or III non-small-cell lung cancer using the surveillance, epidemiology, and end results database. J Clin Oncol. 2006;24:2998–3006.
27. Roth JA, Fossella F, Komaki R, et al. A randomized trial comparing perioperative chemotherapy and surgery with surgery alone in respectable stage IIIA non small cell lung cancer. J Natl Cancer Inst. 1994;86:673–80.
28. Rosell R, Gomez-Codina J, Camps C, et al. A randomized trial comparing pre-operative chemotherapy plus surgery with surgery alone in patients with non-small cell lung cancer. N Engl J Med. 1994;330:153–8.
29. Roth JA, Atkinson EN, Fossella F, et al. Long-term follow-up of patients enrolled in a randomized trial comparing perioperative chemotherapy and surgery with surgery alone in resectable stage IIIA non-small-cell lung cancer. Lung Cancer. 1998;21:1–6.
30. Song WA, Zhou NK, Wang W, et al. Survival benefit of neoadjuvant chemotherapy in non-small cell lung cancer: an updated meta-analysis of 13 randomized control trials. J Thorac Oncol. 2010;5:510–6.
31. Martins RG, D'Amico TA, Loo BW Jr, et al. The management of patients with stage IIIA non-small cell lung cancer with N2 mediastinal node involvement. J Natl Compr Canc Netw. 2012;10:599–613, Review.
32. O'Rourke N, Roqué I Figuls M, et al. Concurrent chemoradiotherapy in non-small cell lung cancer. Cochrane Database Syst Rev. 2010;(16):CD002140.
33. NSCLC Meta-Analyses Collaborative Group. Chemotherapy in addition to supportive care improves survival in advanced non-small-cell lung cancer: a systematic review and meta-analysis of individual patient data from 16 randomized controlled trials. J Clin Oncol. 2008;26:4617–25, Review.

34. Delbaldo C, Michiels S, Syz N, et al. Benefits of adding a drug to a single-agent or a 2-agent chemotherapy regimen in advanced non-small-cell lung cancer: a meta-analysis. JAMA. 2004;292:470–84.
35. The Elderly Lung Cancer Vinorelbine Italian Study Group. Effects of vinorelbine on quality of life and survival of elderly patients with advanced non-small-cell lung cancer. J Natl Cancer Inst. 1999;91:66–72.
36. Scagliotti GV, Parikh P, von Pawel J, et al. Phase III study comparing cisplatin plus gemcitabine with cisplatin plus pemetrexed in chemotherapy-naive patients with advanced-stage non-small-cell lung cancer. J Clin Oncol. 2008;26:3543–51.
37. Sandler A, Gray R, Perry MC, et al. Paclitaxel-carboplatin alone or with bevacizumab for non-small-cell lung cancer. N Engl J Med. 2006;355:2542–50.
38. Forde PM, Ettinger DS. Targeted therapy for non-small-cell lung cancer: past, present and future. Expert Rev Anticancer Ther. 2013;13:745–58.
39. Mok TS, Wu YL, Thongprasert S, et al. Gefitinib or carboplatin-paclitaxel in pulmonary adenocarcinoma. N Engl J Med. 2009;361:947–57.
40. Shepherd FA, Rodrigues Pereira J, Ciuleanu T, et al. Erlotinib in previously treated non-small-cell lung cancer. N Engl J Med. 2005;353:123–32.
41. Seetharamu N, Budman DR, Sullivan KM. Immune checkpoint inhibitors in lung cancer: past, present and future. Future Oncol. 2016;12:1151–63.
42. Micke P, Faldum A, Metz T, et al. Staging small cell lung cancer: Veterans Administration Lung Study Group versus International Association for the Study of Lung Cancer–what limits limited disease? Lung Cancer. 2002;37:271–6.
43. Veronesi G, Bottoni E, Finocchiaro G, Alloisio M. When is surgery indicated for small-cell lung cancer? Lung Cancer. 2015;90:582–9.
44. Takada M, Fukuoka M, Kawahara M, et al. Phase III randomized study of concurrent versus sequential thoracic radiotherapy in combination with cisplatin and etoposide for limited-stage small-cell lung cancer: results of the Japan Clinical Oncology Group Study 9104. J Clin Oncol. 2002;20:3054–60.
45. Aupérin A, Arriagada R, Pignon JP, et al. Prophylactic cranial irradiation for patients with small-cell lung cancer in complete remission. Prophylactic Cranial Irradiation Overview Collaborative Group. N Engl J Med. 1999;341:476–84.
46. Noda K, Nishiwaki Y, Kawahara M, et al. Irinotecan plus cisplatin compared with etoposide plus cisplatin for extensive small-cell lung cancer. N Engl J Med. 2002;346:85–91.

Radiological Imaging in Lung Cancer

4

Aisha Naseer, Arum Parthipun, Athar Haroon, and Stephen Ellis

Contents

4.1 Introduction

Lung cancer is the third most common cancer in the UK (2014), but accounts for the most common cause of cancer death, and is responsible for 22% of all cancer-related deaths.

Lung cancer is classified into two categories: small cell lung cancer (SCLC) and non-small cell lung cancer (NSLC). Staging of lung cancer is based on the Eighth

A. Naseer (✉)
Barts Health NHS Trust, London, UK
e-mail: Aisha.Naseer@bartshealth.nhs.uk

A. Parthipun
Department of Nuclear Medicine, Royal Free London NHS Foundation Trust, London, UK
e-mail: arum.parthipun@nhs.net

A. Haroon • S. Ellis
Barts Health NHS Trust, London, UK
e-mail: atharharoon@yahoo.com; Stephen.Ellis@bartshealth.nhs.uk

A. Agrawal, V. Rangarajan (eds.), *PET/CT in Lung Cancer*, Clinicians' Guides to Radionuclide Hybrid Imaging, https://doi.org/10.1007/978-3-319-72661-8_4

Edition of Lung Cancer stage classification from the AJCC (American Joint Committee on Cancer) and the UICC (Union Internationale Contre le Cancer) and informed by the International Association for the Study of Lung Cancer (IASLC) Staging Committee. The National Institute for Health and Care Excellence (NICE) has published guidance on the roles imaging can play in the diagnosis of lung cancer.

The TNM staging of lung cancer is divided into the characteristics of the primary tumour (T), lymph node involvement (N) and the presence of distant metastases (M).

In most cases, the purpose of staging is to determine whether a lung tumour is surgically resectable or can be treated with radiotherapy for curative intent.

4.2 Imaging of the Primary Tumour

The size and location of the primary tumour determine treatment options. Imaging is imperative to assess invasion of the main bronchus (T2), chest wall (T3) and mediastinum (T4), the latter being one of the criteria for irresectable disease. However, where CT and MRI can demonstrate with ease cases where there is extensive tumour involvement, more subtle cases are difficult to define, as loss of fat planes can reflect inflammation, fibrosis or blurring from motion artefact rather than malignant invasion (Figs. 4.1, 4.2, 4.3, 4.4, 4.5, and 4.6).

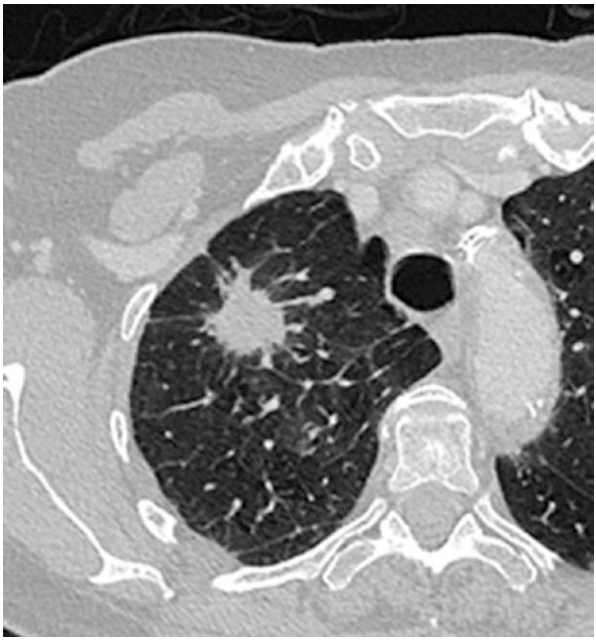

Fig. 4.1 Right upper lobe lung carcinoma with spiculated margins extending to the visceral pleural surface seen on axial thin-section contrast-enhanced CT

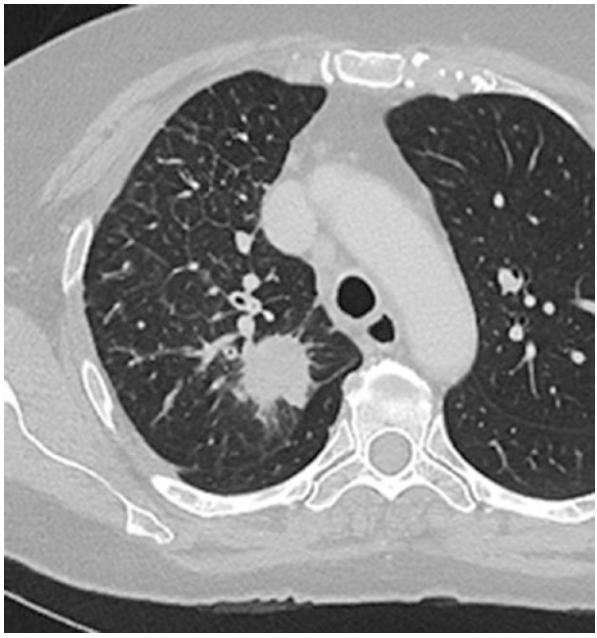

Fig. 4.2 A right upper lobe lung carcinoma abuts the oblique fissure on axial thin-section CT. Within the rest of the right upper lobe, there is interstitial septal thickening which represents lymphangitic carcinomatosis

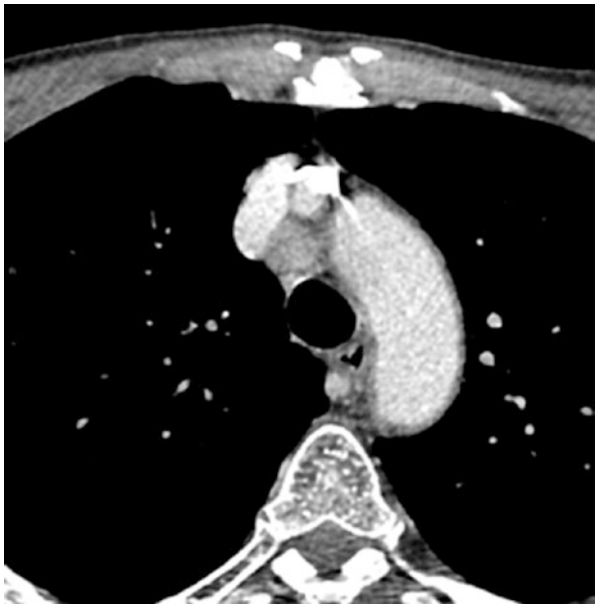

Fig. 4.3 An enlarged paratracheal lymph node on axial contrast-enhanced CT represents N2 disease on TNM staging

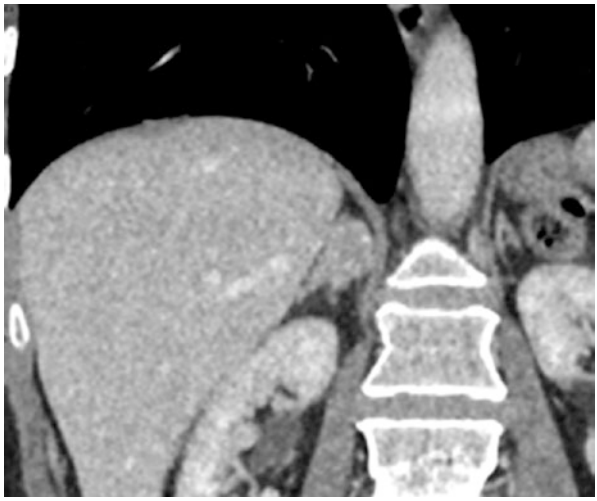

Fig. 4.4 A coronal multiplanar reformat image of a contrast-enhanced CT scan shows an irregularly enhancing metastasis in the right adrenal gland

Fig. 4.5 An axial contrast-enhanced CT scan showing an enlarged paratracheal lymph node metastasis and atelectasis of the right upper lobe

Fig. 4.6 An axial contrast-enhanced CT scan showing a central right lung cancer with mediastinal invasion. There is invasion of the right main bronchus at the level of the carina, the superior vena cava and the azygous vein

4.2.1 CT Features of Mediastinal Invasion on CT

- Greater than 3 cm contact with the mediastinum
- Loss of a fat plane between the tumour and the adjacent mediastinal structures
- Greater than 90° circumferential contact with the aorta [1]

These criteria, coupled with the use of thin-section multiplanar reformats (MPRs), improve the accuracy of detection of mediastinal invasion with a high sensitivity, specificity and positive predictive value (PPV) and a negative predictive value (NPV) of 98% [2].

Cardiac-gated MRI can be used to assess for tumour invasion of the heart or pericardium with the tumour representing a high signal intensity lesion on T1-weighted images [3]. The absence of a sliding motion between the tumour and the underlying structures on dynamic cine MR images may also indicate local invasion [4].

Dynamic imaging with CT and MRI, using variations in the respiratory cycle to assess how fixed the tumour is to underlying structures, would seem to have promise, but benign fibrous adhesions can cause false-positive results reducing the specificity to 23% [5].

On ultrasound, the breach of the echogenic pleural line and absence of tumour movement with respiration have also been proposed as a useful determinant of chest wall invasion.

4.2.2 Superior Sulcus Tumours (Pancoast's Tumours)

Superior sulcus tumours, also known as Pancoast's tumours, are classified as T3 by virtue of the invariable presence of extrathoracic tissue invasion. MRI is the imaging modality of choice to determine the extent of location invasion from superior sulcus tumours. A T3 tumour has limited involvement of the lower thoracic nerve roots (ie T1 or T2 nerve roots) of the brachial plexus. Whereas, more extensive involvement of the brachial plexus cords, nerve roots (ie C8 or higher nerve roots), subclavian vessels, vertebral bodies or spinal canal is classified as T4 disease [6].

4.3 Imaging of Nodal Disease

Fixed anatomical landmarks are used to localise individual nodal stations based on the recently unified American Thoracic Society (ATS) and American Joint Committee on Cancer (AJCC) classification [7, 8]. One would expect lymph node spread to be sequential: first to ipsilateral segmental, interlobar or lobar intrapulmonary nodes, then to ipsilateral hilar nodes (all N1) and thereafter to ipsilateral mediastinal nodes (N2). However, skip metastases to mediastinal nodes without hilar nodal involvement are seen in up to one third of cases.

On contrast-enhanced CT, lymph node size is the only recognised determinant of metastases, with a short-axis diameter of greater than 1 cm suggestive of involvement. However, studies have shown that in the context of NSCLC, lymph node size alone is not a reliable indicator of tumour involvement with a PPV of only 56% [9]. In practice FDG PET/CT uptake of lymph nodes is taken as the best determinant of lymph node involvement, with avid nodes less than 1 cm on CT considered to be involved with tumour and enlarged nodes with little or no avidity assumed to be clear of tumour provided the primary tumour is FDG avid. A meta-analysis comparing the performance of FDG-PET with CT in the nodal staging for NSCLC found an overall sensitivity and specificity of 83% and 92%, respectively, for FDG-PET compared to 59% and 78% for CT [10]. Agreement between PET and CT regarding tumour involvement has a better positive predictive value than modality alone. This demonstrable value of FDG-PET has led to its inclusion in the NICE guidelines for the management of NSCLC with the intention to cure [11]. However, FDG-PET is an adjunct rather than a stand-alone imaging technique as the false-positive rate is significant [12, 13].

Diffusion-weighted MRI in the diagnosis of mediastinal lymph node metastasis in NSCLC has been proposed as an alternative to FDG-PET in identifying lymph nodes with tumour infiltration [14]. However, further research is required before this is implemented in regular clinical practice.

4.3.1 Nodal Sampling

Mediastinal lymph node sampling is offered to confirm or exclude nodal metastases in patients with PET-positive lymph nodes, except when there is definite distant metastatic disease or there is a high probability that nodal disease is metastatic.

Most equivocal mediastinal lymph nodes are station 4 (lower paratracheal), 7 (subcarinal) and 10 (hilar) nodes, and the technique of choice for sampling these is now endobronchial ultrasound-guided fine-needle aspiration (EBUS-FNA). Previously station 7 lymph nodes were sampled using conventional bronchoscopy utilising trans-carinal FNA.

Previously, the technique of choice for sampling station 1 (low cervical, supraclavicular and sternal notch), 2 (upper paratracheal) and 4 (lower paratracheal) nodes was mediastinoscopy. This requires a general anaesthetic, is more invasive than EBUS and is therefore reserved for station 1 and 2 nodes and for station 4 nodes when EBUS-FNA has failed to provide an adequate sample.

Transoesophageal fine-needle aspiration (EUS-FNA) uses the endoscopic equivalent of EBUS and can sample nodes adjacent to the oesophagus at stations 3P (prevertebral), 7 (subcarinal), 8 (paraoesophageal) and 9 (pulmonary ligament).

Percutaneous transthoracic needle aspiration or biopsy can be performed for nodes at station 5 (sub-aortic) or 6 (para-aortic) which are not amenable to sampling by other techniques. Overall, minimally invasive techniques such as EBUS-FNA and EUS-FNA are used in preference as first-line investigations.

4.4 Imaging of Metastatic Disease

Around 40% of NSCLCs have metastasized at presentation, and 90% of these have clinical symptoms, which would indicate the site and specific imaging can be performed to identify these. The most common extrathoracic sites are:

Brain
Lymph nodes
Adrenal
Liver
Bone—Particularly vertebral body metastases, which may present with spinal cord compression

Potential sites of metastases are the liver and adrenals; these are usually included in the initial staging CT scan of the chest and upper abdomen. The sensitivity and specificity of CT for detection of adrenal lesions are 41% and 84.5% [15] and for liver lesions 93% and 75%, respectively [16]. If this initial study suggests the cancer is curable, NICE guidelines recommend an FDG PET/CT scan to fully stage the cancer, identifying metastases outside the range of the staging CT scan and clarifying the FDG avidity of any equivocal abnormalities identified on the staging CT that would alter the stage, i.e. adrenal lesions, additional lung lesions and lymph nodes [11].

Whole body MRI has been considered as an alternative to FDG PET/CT and was found to be at least as effective in detecting metastases with a slightly increased sensitivity and specificity in the identification of head and neck and bone metastases [17].

4.5 Restaging of Tumours

Patients with either T4 or N2 disease can undergo tumour or nodal downstaging, respectively, to qualify as candidates for treatment with intent to cure.

Tumour downstaging can be determined by CT or MRI (in the case of a superior sulcus tumour). However, determining nodal downstaging has proven challenging. It can be investigated with FDG-PET coupled with contrast-enhanced CT to assess for a decrease in the metabolic activity of previously involved nodes and to assess size criteria. However, this has proven to be a less sensitive modality at detecting metastatic disease posttreatment than at initial staging [18–20].

4.6 Imaging of Recurrent Disease

Recurrent disease following surgical resection can be either loco-regional or metastatic, the latter being more common. The likelihood of recurrence increases as the T and N stage of the resected tumour increases. Adjuvant chemotherapy may be offered to patients with postresection stage II or above with some survival benefit.

FDG-PET/CT is the most useful assessment tool for identifying either local or metastatic disease recurrence after a 4–5-month posttreatment window, in which inflammation and fibrosis may give false-positive results [21]. However, CT scanning is usually used as the first-line assessment tool if there is clinical suspicion of recurrent disease, with FDG-PET reserved for equivocal cases. In cases where treatment with intent to cure has not involved resection, e.g. radical radiotherapy, cyberKnife, radiofrequency or microwave ablation, FDG-PET may be used to establish the success of the treatment through the absence of metabolic activity.

Key Points

- The size and location of the primary tumour determine treatment options, and therefore imaging is imperative to assess for the presence of main bronchus (T2), chest wall (T3) and mediastinal (T4) invasion.
- CT and MRI can demonstrate with ease cases where there is extensive tumour involvement in most cases.
- CT features of mediastinal invasion on CT include (a) greater than 3 cm contact with the mediastinum, (b) loss of a fat plane between the tumour and the adjacent mediastinal structures and (c) greater than 90° circumferential contact with the aorta.
- Cardiac-gated MRI can be used to assess for tumour invasion of the heart or pericardium with the tumour representing a high signal intensity lesion on T1-weighted images.
- On ultrasound, the breach of the echogenic pleural line and absence of tumour movement with respiration have also been proposed as useful determinants of chest wall invasion.
- MRI is the imaging modality of choice to determine the extent of location invasion from superior sulcus tumours.
- Fixed anatomical landmarks are used to localise individual nodal stations based on the recently unified American Thoracic Society (ATS) and American Joint Committee on Cancer classification.
- One would expect lymph node spread to be sequential. However, skip metastases to mediastinal nodes without hilar nodal involvement are seen in up to one third of cases.
- On contrast-enhanced CT, lymph node size is the only recognised determinant of metastases, with a short-axis diameter of greater than 1 cm suggestive of involvement.
- Lymph node size alone is not a reliable indicator of tumour involvement in NSCLC.
- Diffusion-weighted MRI in the diagnosis of mediastinal lymph node metastasis in NSCLC has been proposed as an alternative to FDG-PET in identifying lymph nodes with tumour infiltration.
- Mediastinal lymph node sampling is offered to confirm or exclude nodal metastases in patients with PET-positive lymph nodes.

- Most equivocal mediastinal lymph nodes are station 4, 7 and 10 nodes, and the technique of choice for sampling these is now endobronchial ultrasound-guided fine-needle aspiration (EBUS-FNA).
- Transoesophageal fine-needle aspiration (EUS-FNA) uses the endoscopic equivalent of EBUS and can sample nodes adjacent to the oesophagus at stations 3P, 7, 8 and 9.
- Percutaneous transthoracic needle aspiration or biopsy can be performed for nodes at station 5 or 6 which are not amenable to sampling by other techniques.
- Tumour downstaging can be determined by CT or MRI (in the case of a superior sulcus tumour).
- CT scanning is usually used as the first-line assessment tool if there is clinical suspicion of recurrent disease, with FDG-PET reserved for equivocal cases.

References

1. Higashino T, Ohno Y, Takenaka D, Watanabe H, Nogami M, Ohbayashi C, et al. Thin-section multiplanar reformats from multidetector-row CT data: utility for assessment of regional tumor extent in non-small cell lung cancer. Eur J Radiol. 2005;56(1):48–55.
2. Ohno Y, Sugimura K, Hatabu H. MR imaging of lung cancer. Eur J Radiol. 2002;44(3):172–81.
3. White CS. MR evaluation of the pericardium and cardiac malignancies. Magn Reson Imaging Clin N Am. 1996;4(2):237–51.
4. Seo JS, Kim YJ, Choi BW, Choe KO. Usefulness of magnetic resonance imaging for evaluation of cardiovascular invasion: evaluation of sliding motion between thoracic mass and adjacent structures on cine MR images. J Magn Reson Imaging. 2005;22(2):234–41.
5. Sakai S, Murayama S, Murakami J, Hashiguchi N, Masuda K. Bronchogenic carcinoma invasion of the chest wall: evaluation with dynamic cine MRI during breathing. J Comput Assist Tomogr. 1997;21(4):595–600.
6. Detterbeck FC, Boffa DJ, Kim AW, et al. The eighth edition lung cancer stage classification. Chest 2017;151(1):193–203.
7. Ko JP, Drucker EA, Shepard JA, Mountain CF, Dresler C, Sabloff B, et al. CT depiction of regional nodal stations for lung cancer staging. AJR Am J Roentgenol. 2000;174(3):775–82.
8. Mountain CF, Dresler CM. Regional lymph node classification for lung cancer staging. Chest. 1997;111(6):1718–23.
9. Glazer GM, Gross BH, Aisen AM, Quint LE, Francis IR, Orringer MB. Imaging of the pulmonary hilum: a prospective comparative study in patients with lung cancer. AJR Am J Roentgenol. 1985;145(2):245–8.
10. De Leyn P, Vansteenkiste J, Cuypers P, Deneffe G, Van Raemdonck D, Coosemans W, et al. Role of cervical mediastinoscopy in staging of non-small cell lung cancer without enlarged mediastinal lymph nodes on CT scan. Eur J Cardiothorac Surg. 1997;12(5):706–12.
11. Lung cancer: diagnosis and treatment. Guidance and guidelines. NICE [Internet]. [cited 2017 Jun 5]. Available from https://www.nice.org.uk/guidance/cg24.
12. Dietlein M, Weber K, Gandjour A, Moka D, Theissen P, Lauterbach KW, et al. Cost-effectiveness of FDG-PET for the management of potentially operable non-small cell lung cancer: priority for a PET-based strategy after nodal-negative CT results. Eur J Nucl Med. 2000;27(11):1598–609.

13. Scott WJ, Shepherd J, Gambhir SS. Cost-effectiveness of FDG-PET for staging non-small cell lung cancer: a decision analysis. Ann Thorac Surg. 1998;66(6):1876–83; discussion 1883–5.
14. Xu L, Tian J, Liu Y, Li C. Accuracy of diffusion-weighted (DW) MRI with background signal suppression (MR-DWIBS) in diagnosis of mediastinal lymph node metastasis of nonsmall-cell lung cancer (NSCLC). J Magn Reson Imaging. 2014;40(1):200–5.
15. Allard P, Yankaskas BC, Fletcher RH, Parker LA, Halvorsen RA. Sensitivity and specificity of computed tomography for the detection of adrenal metastatic lesions among 91 autopsied lung cancer patients. Cancer. 1990;66(3):457–62.
16. Schrevens L, Lorent N, Dooms C, Vansteenkiste J. The role of PET scan in diagnosis, staging, and management of non-small cell lung cancer. Oncologist. 2004;9(6):633–43.
17. Ohno Y, Koyama H, Nogami M, Takenaka D, Yoshikawa T, Yoshimura M, et al. STIR turbo SE MR imaging vs. coregistered FDG-PET/CT: quantitative and qualitative assessment of N-stage in non-small-cell lung cancer patients. J Magn Reson Imaging. 2007;26(4):1071–80.
18. Pignon JP, Arriagada R, Ihde DC, Johnson DH, Perry MC, Souhami RL, et al. A meta-analysis of thoracic radiotherapy for small-cell lung cancer. N Engl J Med. 1992;327(23):1618–24.
19. Akhurst T, Downey RJ, Ginsberg MS, Gonen M, Bains M, Korst R, et al. An initial experience with FDG-PET in the imaging of residual disease after induction therapy for lung cancer. Ann Thorac Surg. 2002;73(1):259–64; discussion 264–6.
20. Ryu JS, Choi NC, Fischman AJ, Lynch TJ, Mathisen DJ. FDG-PET in staging and restaging non-small cell lung cancer after neoadjuvant chemoradiotherapy: correlation with histopathology. Lung Cancer. 2002;35(2):179–87.
21. Israel O, Kuten A. Early detection of cancer recurrence: 18F-FDG PET/CT can make a difference in diagnosis and patient care. J Nucl Med. 2007;48(Suppl 1):28S–35S.

^{18}F-FDG PET/CT in Lung Cancer

5

Archi Agrawal, Venkatesh Rangarajan,
and Nilendu Purandare

Contents

5.1 Introduction

Lung cancer is the leading cause of cancer death—worldwide [1]. Lung cancer can be clinically divided into non-small cell lung cancer (NSCLC), which forms about 85% of all lung cancer, and small cell lung cancer (SCLC) which forms about 15% [2].

A. Agrawal, MBBS, DMRE, DRM, DNB (✉) • V. Rangarajan, MBBS, DRM, DNB
N. Purandare, MBBS, DMRD, DNB
Department of Nuclear Medicine and Molecular Imaging, Tata Memorial Hospital, Mumbai, India
e-mail: drarchi23@gmail.com; drvrangarajan@gmail.com; nilpurandare@gmail.com

A. Agrawal, V. Rangarajan (eds.), *PET/CT in Lung Cancer*, Clinicians' Guides to Radionuclide Hybrid Imaging, https://doi.org/10.1007/978-3-319-72661-8_5

[^{18}F] 2-Fluoro-2-deoxy-D-glucose (^{18}F-FDG) PET/CT (positron-emission tomography/computed tomography) is a noninvasive imaging modality which combines metabolic and anatomic information in the evaluation of cancer.

FDG PET combined with contrast-enhanced CT (CECT) is a useful imaging modality in staging, treatment response evaluation, radiotherapy planning, restaging, and prognostication of lung cancer. In this chapter, we shall discuss these roles of ^{18}F-FDG PET/CT in the management of lung cancer.

5.2 Role of ^{18}F-FDG PET/CT in the Evaluation of Solitary Pulmonary Nodule

Solitary pulmonary nodule (SPN) is a lesion which is less than 3 cm in diameter and is surrounded by lung parenchyma and is not associated with atelectasis, pleural effusion, or hilar adenopathy [3–5]. It is important to differentiate between benign and malignant nodules by noninvasive imaging techniques, so that unnecessary interventions can be avoided in investigating a benign nodule and appropriate treatment be started for malignant lesions. Approximately 55% of SPNs are malignant, and there is a direct relationship between the increasing size of the nodule and the likelihood of malignancy [3–5]. FDG PET is a noninvasive imaging modality used for the evaluation of SPN (Fig. 5.1). Fletcher et al. demonstrated sensitivity and specificity of 91.7% and 82.3% for PET and 95.6% and 40.6% for CT [6]; clearly the accuracy of PET is better than CT in the evaluation of a SPN. Also PET correctly identified 58% of benign nodules that were incorrectly labeled as malignant by CT [6].

5.3 Staging of NSCLC

Staging of NSCLC includes evaluation of the primary tumor (T staging), regional nodal involvement (N staging), and assessment of distant metastatic sites (M staging). PET/CECT being a whole-body imaging modality ensures the assessment of T, N, and M staging in a single examination.

5.3.1 T Staging

CECT is the imaging modality of choice for delineation of size and extent of the primary lung lesion. Magnetic resonance imaging (MRI) is useful in delineation of superior sulcus and mediastinal involvement due to superior spatial resolution. PET/CT outperforms CT and MRI in the evaluation of the tumor size when there is surrounding post-obstructive atelectasis (Fig. 5.2). This is very important for proper radiotherapy planning as well [7–9]. PET/CT also identifies chest wall invasion accurately [10].

5.3.2 N Staging

To decide upon an appropriate management plan for a patient with NSCLC, it is important to stage the mediastinal nodes accurately. Lymph node status is an

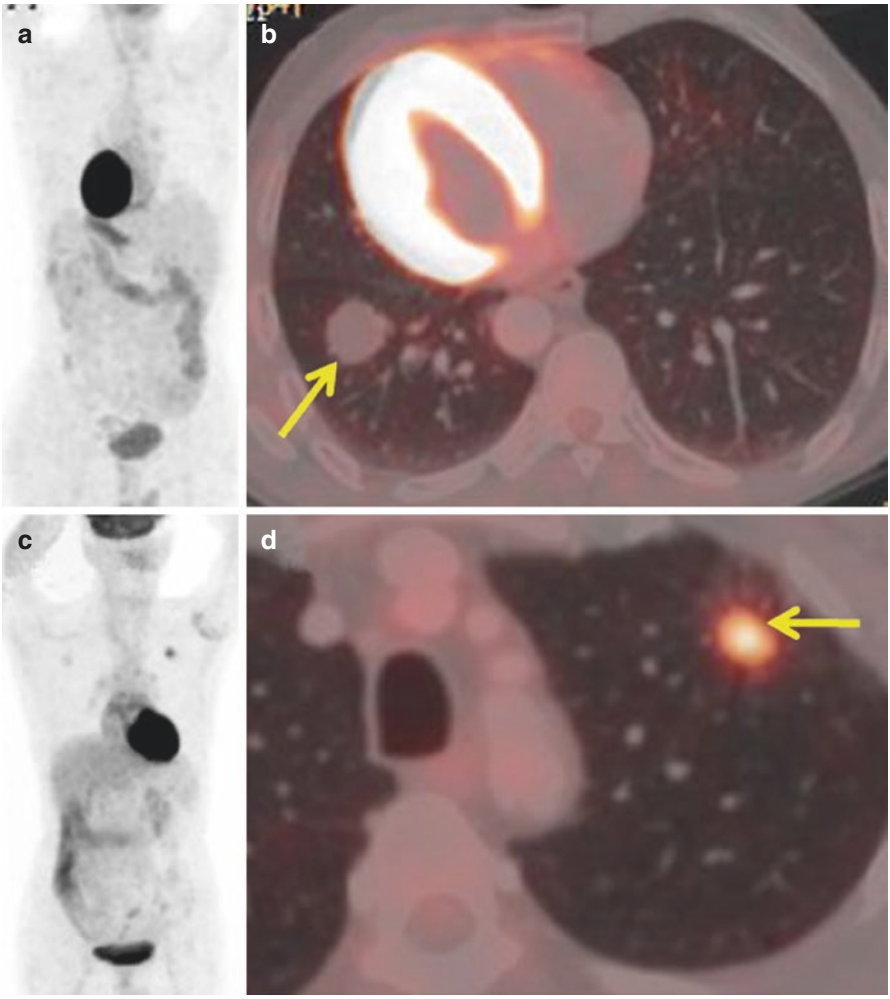

Fig. 5.1 (**a**, **b**) A patient of situs inversus being evaluated for a solitary pulmonary nodule (SPN). No FDG uptake in the SPN in the lower lobe of right-sided lung (arrow). No metabolic activity indicates the possibility of a benign lesion which was confirmed by biopsy. (**c**, **d**) Hypermetabolic SPN in the upper lobe of the left lung (arrow)—likely to represent a malignant lesion. Biopsy was adenocarcinoma confirming the PET/CT finding

important prognosticator in lung cancer. The morphological criterion for a positive mediastinal node is based on size. Short-axis diameter greater than 1 cm indicates an involved node on CECT [11]. PET/CT has a higher sensitivity and specificity than CT in the staging of mediastinal lymph nodes [81% and 90% for PET vs. 59% and 79% for CT, respectively] [12]. PET is not dependent on size criteria and detects metastasis in lymph nodes of size less than 1 cm (Fig. 5.3). PET has a low positive predictive value of 64%, and thus it is mandatory that PET-positive nodes undergo mediastinoscopic sampling for histopathologic confirmation of metastatic involvement [13–17]. However, invasive mediastinoscopy can be omitted in PET-negative nodes as PET has a high negative predictive value of 95% [16, 17]. PET reduces the total number of thoracotomies as well as futile thoracotomies [18]. It is also

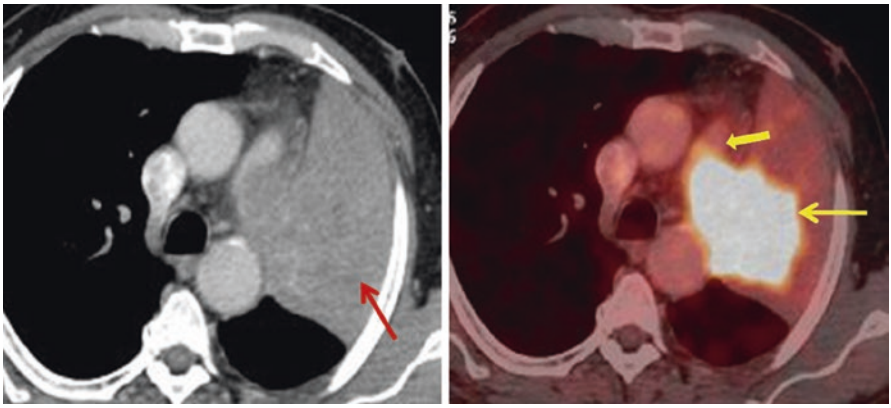

Fig. 5.2 CECT component of the PET/CT showing consolidation/mass (arrow) in upper lobe of the left lung. There is no clear demarcation between the mass and the consolidation making it difficult for radiotherapy planning. A PET/CT image clearly showing the hypermetabolic malignant lung mass (arrow), with surrounding benign consolidation. Invasion of the pulmonary artery (block arrow) is also clearly visible

important to note that in cases where the mass is centrally situated, a mediastinoscopy should always be done as perilesional mediastinal nodes may be masked due to high metabolic activity in the primary tumor [19].

5.3.3 M Staging

The incidence of distant metastases in NSCLC at initial presentation varies from 18 to 36% [20]. The commonest sites of distant metastases are the adrenal glands, bones, liver, and brain. Being a whole-body imaging modality, ^{18}F-FDG PET/CT is more accurate for the detection of distant metastatic disease, as compared to conventional imaging modalities. PET has the ability to detect occult metastatic disease in 29% of cases [21]. A recent meta-analysis showed a pooled sensitivity of 87% and a pooled specificity of 96% of FDG PET/CT for the detection of distant metastatic disease [22].

FDG PET/CT is a noninvasive imaging technique to differentiate benign from malignant adrenal lesions depending on metabolic activity. It has a high sensitivity (93%), specificity (90%), and accuracy (92%) for detecting metastatic adrenal lesions [23] (Fig. 5.4). Due to high sensitivity and specificity of FDG PET/CT for the detection of adrenal metastases, the need for an invasive biopsy can often be obviated [24, 25]. A biopsy or adrenalectomy may be warranted in cases of isolated adrenal lesion with equivocal PET/CT findings.

FDG PET/CT is the best modality for the detection of skeletal metastases [26, 27]. This has been demonstrated by a meta-analysis, which compared the ability of bone scintigraphy, MRI, and PET/CT for evaluating bone metastases. PET/CT

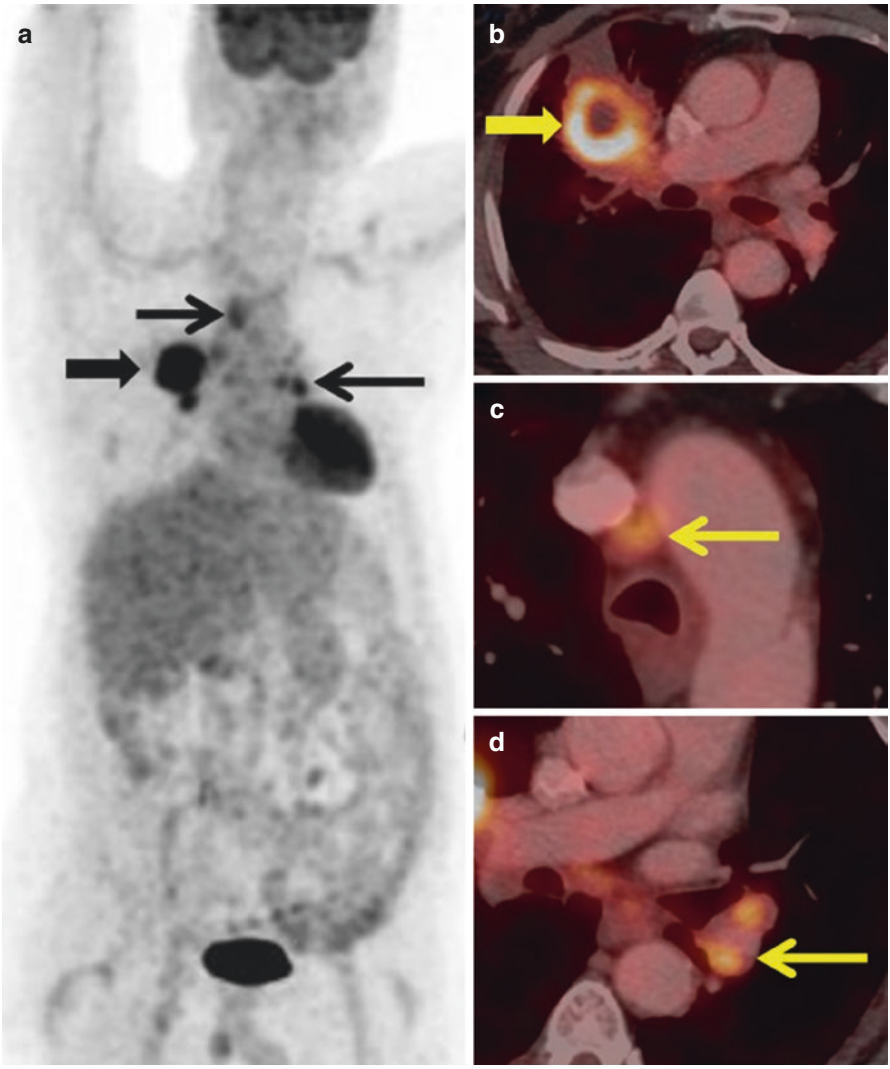

Fig. 5.3 Hypermetabolic right middle lobe mass (block arrow in **a**, **b**) biopsy proven squamous cell carcinoma. Hypermetabolic ipsilateral paratracheal (arrow in **a**, **c**) and contralateral hilar nodes (arrow in **a**, **d**) are noted. These were suspicious for metastatic involvement. This was confirmed by mediastinoscopy-guided sampling

demonstrated the highest pooled sensitivity and specificity of 92% and 98%. The pooled sensitivity and specificity of MRI were 77% and 92% and 86% and 88% for bone scintigraphy. They concluded that PET/CT had the highest diagnostic value for the detection of bone metastases from lung cancer compared to any other conventional imaging modality [26].

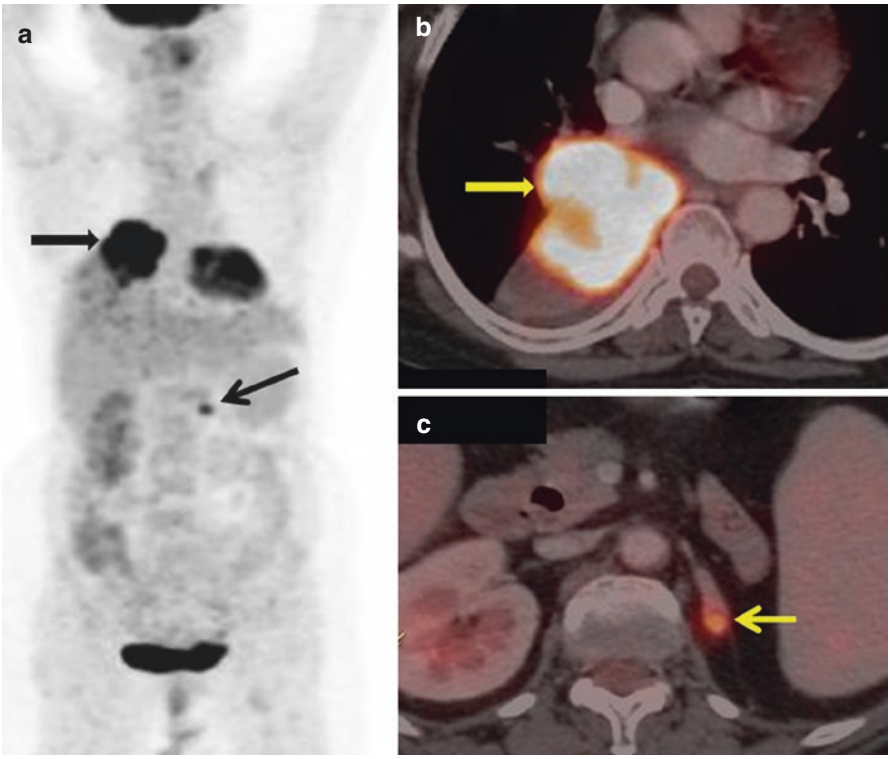

Fig. 5.4 Hypermetabolic mass in the right lung (block arrow in **a**, **b**) with tiny FDG-avid nodule in the left adrenal (arrow in **a**, **c**) which was confirmed histopathologically to be metastasis from the lung primary

Due to high physiological uptake of FDG in gray matter of the brain, FDG PET/CT is not an ideal modality for detection of brain metastases. MRI is the imaging modality of choice for detection of brain metastases [28].

PET/CT is the best modality for detection of pleural metastases. CT and MRI can detect pleural nodules and thickening but lack the ability to differentiate benign pleural thickening from malignant disease. PET/CT has a sensitivity and specificity of 95% and 67%, respectively, for detection of pleural metastases. It has a high positive predictive value and accuracy of 95% and 92%, respectively [29]. Few studies have also shown that PET/CT can noninvasively and reliably distinguish between benign and malignant pleural effusion depending upon uptake of FDG [30]. It has a sensitivity, specificity, and accuracy of 88.8%, 94.1%, and 91.4% with a high positive predictive value of 94.1% and a negative predictive value of 88.8% in the detection of malignant pleural effusion [29]. This is an important indication as thoracocentesis may be false negative in 30–40% of cases with malignant pleural effusion [31].

Detection of unsuspected metastases leads to change in stage in 27–62% of patients and leads to change in management in about 19–52% of patients [32–34]. In a study of 153 patients with diagnosed NSCLC, Hicks et al. showed that FDG

PET led to upstaging of the disease in 33% and downstaging in 10%. It led to change in the therapy plan in 35% of cases; more often the change in therapy was from curative to palliative [34].

5.4 Radiotherapy (RT) Planning

Metabolic information obtained from FDG PET/CT studies can be utilized for accurate radiotherapy planning. CT may not always be very helpful in delineation of the tumor when there is associated atelectasis. CT also has limitation in detection of involved nodes. PET/CT-based RT planning leads to improved tumor delineation and enhanced tumor coverage, thereby reducing radiation dose to the surrounding uninvolved tissues. It also reduces the interobserver variability associated with CT-based RT planning. It leads to treatment strategy medication in >50% of patients [7, 35]. PET/CT facilitates escalation of radiation dose to the tumor as the tumor volumes derived by PET/CT are smaller compared to CT [36].

5.5 Prediction of Response and Treatment Response Evaluation

A newer indication of PET/CT which is being evaluated these days is prediction of response to neoadjuvant chemotherapy (NACT). NACT precedes surgery in patients who have stage III disease. It is necessary to assess the response to NACT in order to identify nonresponders from responders. This helps in reducing the cost as well as toxic effects of an ineffective therapy. Morphologic imaging techniques like CT have limitations in differentiating residual tumor from fibrotic or posttreatment changes [37]. PET/CT being a functional imaging technique has the advantage of predicting response earlier than morphologic imaging methods [38]. A reduction of >20% in metabolic activity is considered as response (Fig. 5.5). Most studies have shown that SUV decrease of >35% is characterized by longer time to disease progression and longer median overall survival [39, 40].

5.6 Restaging/Recurrence

PET/CT is the best imaging technique for the detection of recurrences. It can differentiate between recurrent disease and posttreatment changes efficiently, which can be challenging with conventional imaging methods like CT due to anatomical distortion. The recurrence rate is quite high in patients of NSCLC, even in those who are treated with curative intent. It is advisable that FDG PET/CT be done after 12 weeks of completion of treatment, as false-positive inflammatory changes may confound the interpretation [41–43]. FDG PET/CT has high sensitivity and specificity of 93% and 89% for detection of recurrence [43]. A recent meta-analysis has shown pooled sensitivity and specificity of 90% for detection of lung cancer

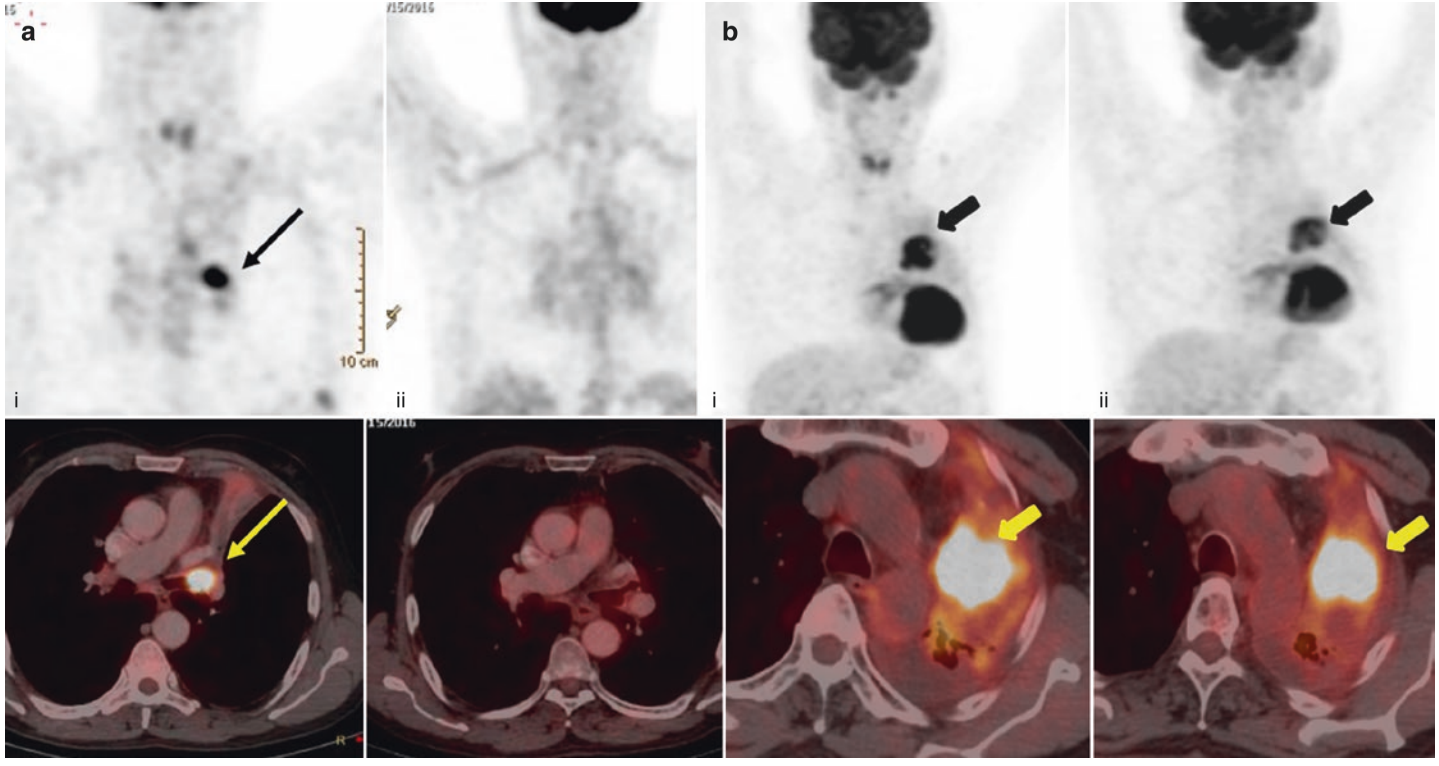

Fig. 5.5 (**a**) Coronal and axial images of PET/CT of a 66-year-old male showing hypermetabolic left hilar mass (arrow in [*i*]). Post-chemoradiotherapy there is complete resolution of the mass as seen in [*ii*]. (**b**) Coronal and axial images of PET/CT of another patient with adenocarcinoma of the left lung, showing hypermetabolic left hilar mass (block arrow in [*i*]). Post-chemoradiotherapy there is neither metabolic nor morphologic response (block arrow in [*ii*])

recurrence, whereas the pooled sensitivity and specificity were 78% and 80% for conventional imaging modalities [44]. Due to high negative predictive value of FDG PET/CT to detect recurrent disease, imaging with conventional techniques is not required, except for brain MRI.

5.7 Prognostication

There are conflicting reports regarding the value to SUVmax (maximum standardized uptake value) in prediction of prognosis [45–48]. Few studies have reported that MTV (metabolic tumor volume) and TLG (total lesion glycolysis) are better predictors as compared to SUVmax [49, 50]. But a recent meta-analysis has shown that high values of SUVmax, MTV, and TLG are associated with higher risk of recurrence and death in patients with operable NSCLC [51].

5.8 Small Cell Lung Cancer (SCLC)

SCLC is an aggressive malignancy with a rapid doubling time and usually is disseminated at the time of presentation. It accounts for about 15–20% of all lung cancers [2]. It is important to differentiate SCLC into limited-stage (LS) disease or extensive-stage (ES) disease, depending on whether the disease is confined to one hemithorax or is disseminated. Intention of treatment is different in both groups; the intent is palliative if the disease is ES and CT-RT if it is limited disease. PET/CT has a high sensitivity and specificity of 98% for the detection of disseminated disease [52]. It also leads to change in stage and management in 12–26% of cases [52, 53]. The data pertaining to SCLC and PET/CT is limited.

Key Points

- FDG PET combined with contrast-enhanced CT (CECT) is a useful imaging modality in lung cancer.
- FDG PET is a noninvasive imaging modality used for the evaluation of SPN and demonstrates sensitivity and specificity of 91.7% and 82.3% for PET and 95.6% and 40.6% for CT.

T Staging

- CECT is the imaging modality of choice for the delineation of size and extent of the primary lung lesion.
- Magnetic resonance imaging (MRI) is useful in the delineation of superior sulcus and mediastinal involvement due to superior spatial resolution.
- PET/CT outperforms CT and MRI in the evaluation of the tumor size when there is surrounding post-obstructive atelectasis.

N Staging

- PET/CT has a higher sensitivity and specificity than CT in staging of mediastinal lymph nodes [81% and 90% for PET vs. 59% and 79% for CT, respectively].
- PET is not dependent on size criteria and detects metastasis in lymph nodes of size less than 1 cm.
- PET has a low positive predictive value of 64%, and thus it is mandatory that PET-positive nodes undergo mediastinoscopic sampling for histopathologic confirmation of metastatic involvement.
- Invasive mediastinoscopy can be omitted in PET-negative nodes as PET has a high negative predictive value of 95%.

M Staging

- ^{18}F-FDG PET/CT is more accurate for the detection of distant metastatic disease, as compared to conventional imaging modalities.
- FDG PET/CT is a noninvasive imaging technique to differentiate benign from malignant adrenal lesions depending on metabolic activity. It has a high sensitivity (93%), specificity (90%), and accuracy (92%) for detecting metastatic adrenal lesions.

Detection of Metastases

- FDG PET/CT is the best modality for the detection of skeletal metastases.
- Due to high physiological uptake of FDG in gray matter of the brain, FDG PET/CT is not an ideal modality for the detection of brain metastases.
- PET/CT is the best modality for the detection of pleural metastases.

Radiotherapy Planning

- FDG PET/CT studies can be utilized for accurate radiotherapy planning.
- PET/CT-based RT planning leads to improved tumor delineation and enhanced tumor coverage, thereby reducing radiation dose to the surrounding uninvolved tissues.

Prediction of Response and Treatment Response Evaluation

- A reduction of >20% in metabolic activity is considered as response.
- SUV decrease of >35% is characterized by longer time to disease progression and longer median overall survival.

Restaging/Recurrence

- PET/CT is the best imaging technique for the detection of recurrences.
- FDG PET/CT should be performed at 12 weeks after of completion of treatment, as false-positive inflammatory changes may confound the interpretation.
- Due to high negative predictive value of FDG PET/CT to detect recurrent disease, imaging with conventional techniques is not required, except for brain MRI.

References

1. DeSantis CE, Lin CC, Mariotto AB, Siegel RL, Stein KD, Kramer JL, et al. Cancer treatment and survivorship statistics, 2014. CA Cancer J Clin. 2014;64:252–71.
2. Rodriguez E, Lilenbaum RC. Small cell lung cancer: past, present, and future. Curr Oncol Rep. 2010;12:327–34.
3. Ost D, Fein AM, Feinsilver SH. Clinical practice. The solitary pulmonary nodule. N Engl J Med. 2003;348(25):2535–42.
4. Visioni A, Kim J. Positron emission tomography for benign and malignant disease. Surg Clin North Am. 2001;91:249–66.
5. Grgic A, Yüksel Y, Gröschel A, et al. Risk stratification of solitary pulmonary nodules bymeans of PET using (18)F-fluorodeoxyglucose and SUV quantification. Eur J Nucl Med Mol Imaging. 2010;37:1087–94.
6. Fletcher JW, Kymes SM, Gould MK, et al. A comparison of the diagnostic accuracy of 18F-FDG PET and CT in the characterization of solitary pulmonary nodules. J Nucl Med. 2008;49:179–85.
7. Bradley J, Bae K, Choi N, Forster K, Siegel BA, Brunetti J, et al. A phase II comparative study of gross tumor volume definition with or without PET/CT fusion in dosimetric planning for non-small-cell lung cancer (NSCLC): primary analysis of Radiation Therapy Oncology Group (RTOG) 0515. Int J Radiat Oncol Biol Phys. 2012;82:435–41.e1.
8. Nestle U, Walter K, Schmidt S, Licht N, Nieder C, Motaref B, et al. 18F-deoxyglucose positron emission tomography (FDG-PET) for the planning of radiotherapy in lung cancer: high impact in patients with atelectasis. Int J Radiat Oncol Biol Phys. 1999;44:593–7.
9. Pawaroo D, Cummings NM, Musonda P, Rintoul RC, Rassl D, Beadsmoore C. Non-small cell lung carcinoma: accuracy of PET/CT in determining the size of T1 and T2 primary tumors. AJR Am J Roentgenol. 2011;196:1176–18.
10. Kligerman S, Digumarthy S. Staging of non-small cell lung cancer using integrated PET/CT. AJR Am J Roentgenol. 2009;193:1203–11.
11. Silvestri GA, Gould MK, Margolis ML, Tanoue LT, McCrory D, Toloza E, Detterbeck F. Noninvasive staging of non-small cell lung cancer: ACCP evidenced-based clinical practice guidelines (2nd edition). Chest. 2007;132:178S–201S.
12. Gould MK, Kuschner WG, Rydzak CE, Maclean CC, Demas AN, Shigemitsu H, et al. Test performance of positron emission tomography and computed tomography for mediastinal staging in patients with non-small-cell lung cancer: a meta-analysis. Ann Intern Med. 2003;139:879–92.
13. Toloza EM, Harpole L, McCrory DC. Noninvasive staging of non-small cell lung cancer: a review of the current evidence. Chest. 2003;123(Suppl):137S–46S.

14. Fischer BM, Mortensen J, Højgaard L. Positron emission tomography in the diagnosis and staging of lung cancer: a systematic, quantitative review. Lancet Oncol. 2001;2:659–66.
15. Dwamena BA, Sonnad SS, Angobaldo JO, Wahl RL. Metastases from non-small cell lung cancer: mediastinal staging in the 1990s-meta-analytic comparison of PET and CT. Radiology. 1999;213:530–6.
16. Darling GE, Maziak DE, Inculet RI, Gulenchyn KY, Driedger AA, Ung YC, et al. Positron emission tomography-computed tomography compared with invasive mediastinal staging in non-small cell lung cancer: results of mediastinal staging in the early lung positron emission tomography trial. J Thorac Oncol. 2011;6:1367–72.
17. Silvestri GA, Gonzalez AV, Jantz MA, Margolis ML, Gould MK, Tanoue LT, et al. Methods for staging non-small cell lung cancer: Diagnosis and management of lung cancer, 3rd ed: American College of Chest Physicians evidence-based clinical practice guidelines. Chest. 2013;143(Suppl):e211–50S.
18. Fischer B, Lassen U, Mortensen J, Larsen S, Loft A, Bertelsen A, et al. Preoperative staging of lung cancer with combined PET/CT. N Engl J Med. 2009;361:32–9.
19. Sahiner I, Vural GU. Positron emission tomography/computerized tomography in lung cancer. Quant Imaging Med Surg. 2014;4:195–206.
20. Quint LE. Staging non-small cell lung cancer. Cancer Imaging. 2007;7:148–59.
21. Schrevens L, Lorent N, Dooms C, Vansteenkiste J. The role of PET scan in diagnosis, staging, and management of non-small cell lung cancer. Oncologist. 2004;9:633–43.
22. Li J, Xu W, Kong F, Sun X, Zuo X. Meta-analysis: accuracy of ^{18}FDG PET/CT for distant metastasis staging in lung cancer patients. Surg Oncol. 2013;22:151–5.
23. Kumar R, Xiu Y, Yu JQ, Takalkar A, El-Haddad G, Potenta S, Kung J, Zhuang H, Alavi A. 18F-FDG PET in evaluation of adrenal lesions in patients with lung cancer. J Nucl Med. 2004;45:2058–62.
24. Brady MJ, Thomas J, Wong TZ, Franklin KM, Ho LM, Paulson EK. Adrenal nodules at FDG PET/CT in patients known to have or suspected of having lung cancer: a proposal for an efficient diagnostic algorithm. Radiology. 2009;250:523–30.
25. Cho AR, Lim I, Na II, du Choe H, Park JY, Kim BI, et al. Evaluation of adrenal masses in lung cancer patients using F-18 FDG PET/CT. Nucl Med Mol Imaging. 2011;45:52–8.
26. Qu X, Huang X, Yan W, Wu L, Dai K. A meta-analysis of ^{18}FDG-PET/CT, ^{18}FDG-PET, MRI and bone scintigraphy for diagnosis of bone metastases in patients with lung cancer. Eur J Radiol. 2012;81:1007–15.
27. Chang MC, Chen JH, Liang JA, Lin CC, Yang KT, Cheng KY, et al. Meta-analysis: comparison of F-18 fluorodeoxyglucose-positron emission tomography and bone scintigraphy in the detection of bone metastasis in patients with lung cancer. Acad Radiol. 2012;19:349–57.
28. Yi CA, Shin KM, Lee KS, Kim BT, Kim H, Kwon OJ, et al. Non-small cell lung cancer staging: efficacy comparison of integrated PET/CT versus 3.0-T whole-body MR imaging. Radiology. 2008;248:632–42.
29. Erasmus JJ, McAdams HP, Rossi SE, Goodman PC, Coleman RE, Patz EF. FDG PET of pleural effusions in patients with non-small cell lung cancer. AJR Am J Roentgenol. 2000;175:245–9.
30. Gupta NC, Rogers JS, Graeber GM, Gregory JL, Waheed U, Mullet D, Atkins M. Clinical role of F-18 fluorodeoxyglucose positron emission tomography imaging in patients with lung cancer and suspected malignant pleural effusion. Chest. 2002;122:1918–24.
31. Light RW, Erozan YS, Ball WC. Cells in pleural fluid. Their value in differential diagnosis. Arch Intern Med. 1973;132:854–60.
32. Shim SS, Lee KS, Kim BT, Chung MJ, Lee EJ, Han J, et al. Non-small cell lung cancer: prospective comparison of integrated FDG PET/CT and CT alone for preoperative staging. Radiology. 2005;236:1011–9.
33. De Wever W, Ceyssens S, Mortelmans L, Stroobants S, Marchal G, Bogaert J, et al. Additional value of PET/CT in the staging of lung cancer: comparison with CT alone, PET alone and visual correlation of PET and CT. Eur Radiol. 2007;17:23–32.
34. Hicks RJ, Kalff V, MacManus MP, Ware RE, Hogg A, McKenzie AF, et al. ^{18}F-FDG PET provides high-impact and powerful prognostic stratification in staging newly diagnosed non-small cell lung cancer. J Nucl Med. 2001;42:1596–604.

35. Pommier P, Touboul E, Chabaud S, Dussart S, Le Pechoux C, Giammarile F, et al. Impact of (18) F-FDG PET on treatment strategy and 3D radiotherapy planning in non-small cell lung cancer: a prospective multicenter study. AJR Am J Roentgenol. 2010;195:350–5.
36. Bradley J, Thorstad WL, Mutic S, Miller TR, Dehdashti F, Siegel BA, et al. Impact of FDG-PET on radiation therapy volume delineation in non-small-cell lung cancer. Int J Radiat Oncol Biol Phys. 2004;59:78–86.
37. Skoura E, Datseris IE, Platis I, Oikonomopoulos G, Syrigos KN. Role of positron emission tomography in the early prediction of response to chemotherapy in patients with non-small-cell lung cancer. Clin Lung Cancer. 2012;13:181–7.
38. Therasse P, Eisenhauer EA, Verweij J. RECIST revisited: a review of validation studies on tumour assessment. Eur J Cancer. 2006;42:1031–9.
39. Park JO, Lee SI, Song SY, et al. Measuring response in solid tumors: comparison of RECIST and WHO response criteria. Jpn J Clin Oncol. 2003;33:533–7.
40. de Geus-Oei L, van der Heijden H, Visser PE, et al. Chemotherapy response evaluation with 18F-FDG PET in patients with non-small cell lung cancer. J Nucl Med. 2007;48:1592–8.
41. Koenig TR, Munden RF, Erasmus JJ, Sabloff BS, Gladish GW, Komaki R, et al. Radiation injury of the lung after three-dimensional conformal radiation therapy. AJR Am J Roentgenol. 2002;178:1383–8.
42. Larici AR, del Ciello A, Maggi F, Santoro SI, Meduri B, Valentini V, et al. Lung abnormalities at multimodality imaging after radiation therapy for non-small cell lung cancer. Radiographics. 2011;31:771–89.
43. Hellwig D, Gröschel A, Graeter TP, Hellwig AP, Nestle U, Schäfers HJ, et al. Diagnostic performance and prognostic impact of FDG-PET in suspected recurrence of surgically treated non-small cell lung cancer. Eur J Nucl Med Mol Imaging. 2006;33:13–21.
44. He YQ, Gong HL, Deng YF, Li WM. Diagnostic efficacy of PET and PET/CT for recurrent lung cancer: a meta-analysis. Acta Radiol. 2014;55:309–17.
45. Sasaki R, Komaki R, Macapinlac H, Erasmus J, Allen P, Forster K, et al. [18F] fluorodeoxyglucose uptake by positron emission tomography predicts outcome of non-small-cell lung cancer. J Clin Oncol. 2005;23:1136–43.
46. Na F, Wang J, Li C, Deng L, Xue J, Lu Y. Primary tumor standardized uptake value measured on F18-fluorodeoxyglucose positron emission tomography is of prediction value for survival and local control in non-small-cell lung cancer receiving radiotherapy: meta-analysis. J Thorac Oncol. 2014;9:834–42.
47. Agarwal M, Brahmanday G, Bajaj SK, Ravikrishnan KP, Wong CY. Revisiting the prognostic value of preoperative 18F-fluoro-2-deoxyglucose (18F-FDG) positron emission tomography (PET) in early-stage (I & II) non-small cell lung cancers (NSCLC). Eur J Nucl Med Mol Imaging. 2010;37:691–8.
48. Hoang JK, Hoagland LF, Coleman RE, Coan AD, Herndon JE 2nd, Patz EF Jr. Prognostic value of fluorine-18 fluorodeoxyglucose positron emission tomography imaging in patients with advanced-stage non-small-cell lung carcinoma. J Clin Oncol. 2008;26:1459–64.
49. Park SY, Cho A, Yu WS, Lee CY, Lee JG, Kim DJ, et al. Prognostic value of total lesion glycolysis by 18F-FDG PET/CT in surgically resected stage IA non-small cell lung cancer. J Nucl Med. 2015;56:45–9.
50. Im HJ, Pak K, Cheon GJ, Kang KW, Kim SJ, Kim IJ, et al. Prognostic value of volumetric parameters of 18F-FDG PET in non-small-cell lung cancer: a meta-analysis. Eur J Nucl Med Mol Imaging. 2015;42:241–51.
51. Liu J, Dong M, Sun X, Li W, Xing L, Yu J. Prognostic value of 18F-FDG PET/CT in surgical non-small cell lung cancer: a meta-analysis. PLoS One. 2016;11(1):e0146195.
52. Lu YY, Chen JH, Liang JA, Chu S, Lin WY, Kao CH. 18F-FDG PET or PET/CT for detecting extensive disease in small-cell lung cancer: a systematic review and meta-analysis. Nucl Med Commun. 2014;35:697–703.
53. Azad A, Chionh F, Scott AM, Lee ST, Berlangieri SU, White S, et al. High impact of 18F-FDG PET on management and prognostic stratification of newly diagnosed small cell lung cancer. Mol Imaging Biol. 2010;12:433–51.

^{18}F-FDG PET/CT: Normal Variants, Artifacts, and Pitfalls in Lung Cancer

6

Archi Agrawal and Venkatesh Rangarajan

Contents

6.1 Introduction

^{18}F-2-Fluoro-2-deoxyglucose (FDG) is the workhorse of oncological PET/CT departments. Its role in staging, restaging, and response assessment of various cancers is already established. But FDG is a marker of glycolysis and, thus, is neither specific for malignancy nor for a particular tumor. Its accumulation can be seen in benign process which may be difficult to differentiate from a neoplastic etiology. It is imperative that nuclear physicians and radiologists know about these FDG-avid benign pathologies and few FDG-negative malignant etiologies, which may confound correct interpretation in PET/CT reporting.

In this chapter we will look at few artifacts and benign variants in lung cancer, which can be potential pitfalls while reporting FDG PET/CT scans.

A. Agrawal, MBBS, DMRE, DRM, DNB (✉) • V. Rangarajan, MBBS, DRM, DNB
Department of Nuclear Medicine and Molecular Imaging,
Tata Memorial Hospital, Mumbai, India
e-mail: drarchi23@gmail.com; drvrangarajan@gmail.com

A. Agrawal, V. Rangarajan (eds.), *PET/CT in Lung Cancer*, Clinicians' Guides to Radionuclide Hybrid Imaging, https://doi.org/10.1007/978-3-319-72661-8_6

6.2 Normal Variants, Artifacts, and Pitfalls in Lung Cancer

These can be divided into:

1. Technical artifacts due to integration of PET and CT
2. Various false positives due to infection and inflammation
3. Incidental findings
4. Benign etiologies which can mimic distant metastases in lung cancer
5. False-negative neoplastic pathology

6.2.1 Technical Artifacts

(a) *Respiratory artifacts*—These are seen due to mismatch of PET and CT data during respiration. It occurs due to images being acquired during different stages of the respiration, leading to a mismatch between CT data which is acquired during breath-hold and the PET data which is acquired during normal tidal breathing [1]. This manifests as a curvilinear photon-deficient (cold) defect at the interface of the lung and diaphragm leading to incorrect anatomic localization of the focus of increased FDG activity. This artifact can lead to a metabolically active hepatic lesion being wrongly localized to the lung, mimicking a lung nodule (Fig. 6.1) or sometimes a lung nodule in the lung base appearing as

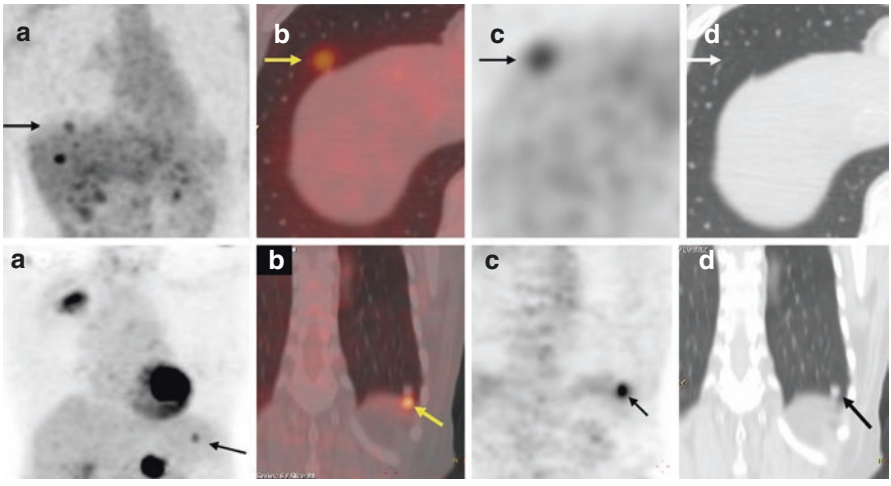

Fig. 6.1 (**1i**) (*a*) MIP (maximum intensity projection) of FDG PET/CT scan artifactually shows the hypermetabolic liver lesions in the right lower thorax (arrow) due to respiratory artifact. (*b*, *c*) Axial fused PET/CT and PET images show a hypermetabolic focus in the base of the right lung (arrow). No corresponding lesion is noted in the lung in the axial CT image (*d*). (**1ii**) (*a*) MIP image of FDG PET/CT artifactually shows a hypermetabolic lesion in the spleen (arrow) due to respiratory artifact. (*b*, *c*) Coronal fused PET/CT and PET images show a hypermetabolic focus in the spleen (arrow). (*d*) Coronal CT image clearly shows a nodule in the base of the left lung (arrow) which is artifactually seen as a hypermetabolic focus in the spleen in image *b*, *c*. This occurs due to acquisition of PET and CT data during different phases of respiration

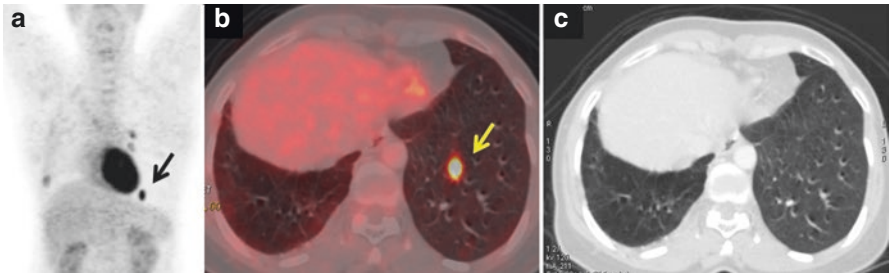

Fig. 6.2 (**a**) MIP of FDG PET/CT scan shows an intensely FDG-avid focus in the base of the left lung (arrow). Axial fused PET/CT image (**b**) shows the hypermetabolic focus in the lower lobe of the left lung (arrow). No corresponding lesion is noted in the left lung in the axial CT image (**c**). This is seen due to faulty injection leading to formation of a microembolus mixed with the radiotracer which then gets trapped in the pulmonary microcirculation giving this a typical appearance

a focus of increased FDG activity in the liver or spleen. A review of the CT images for a nodule in the lung or liver/spleen lesion usually solves the dilemma.

(b) *Attenuation artifacts*—Artifacts due to high CT attenuation materials such as intravenous or oral contrast, metals, ports, and catheters. This occurs due to overestimation of FDG concentration in areas of high attenuation due to application of high attenuation correction factors [2].

(c) *Artifacts due to faulty injection technique*—Very rarely, an intense well-defined focal uptake is seen in the lung without any morphologic abnormality in the lung. This is likely due to paravenous injection which leads to endothelial injury which in turn leads to the formation of clots at the injury site, which get trapped in the pulmonary microcirculation. As these clots are admixed with the radioactive tracer, they demonstrate intense FDG uptake [3–5] (Fig. 6.2). These disappear on re-scanning the patient. Sometimes a paravenous injection can also lead to FDG uptake in the ipsilateral nodes in the axilla due to lymphatic uptake of the tracer. These artifacts can be avoided by preparing the patient with a good venous access prior to injection of the radiotracer.

6.2.2 Various False Positives Due to Infection and Inflammation

(a) Infection and Inflammation

In evaluation of lung cancer, the commonest causes of false-positive uptakes in the lung are due to infection and inflammation. As inflammatory cells like activated macrophages, neutrophils, and lymphocytes utilize glucose and have a high glycolytic rate, these benign conditions are usually FDG avid [6, 7]. Therefore, pulmonary infections can often be misinterpreted as neoplastic etiology. It is not always easy to differentiate between benign and malignant process on imaging findings alone, and a biopsy may be necessary for confirmation. This includes infections such as *pneumonia* (Fig. 6.3), tuberculosis, sarcoidosis, and amyloidosis.

Increased FDG uptake is almost always seen in active *tuberculosis* of the lung. It may be seen as patchy areas of consolidation or a solitary nodule (Fig. 6.4) or even lobar consolidation (Fig. 6.5). Cavitation may or may not be

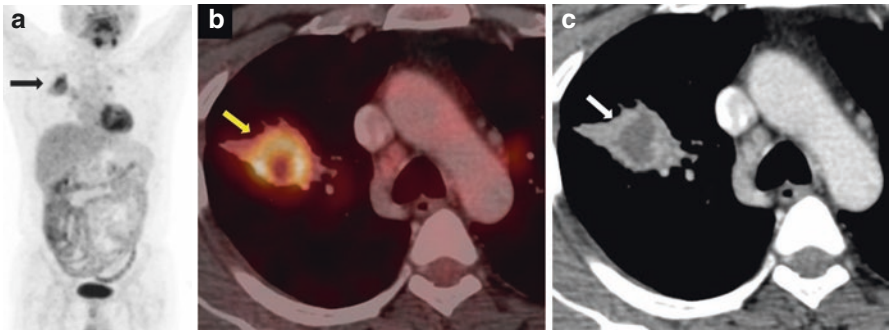

Fig. 6.3 Whole-body FDG PET/CT MIP (**a**) image shows a hypermetabolic mass in the right lung (arrow) in a 52-year-old gentleman, being evaluated for a solitary pulmonary nodule in the right lung. Axial fused PET/CT and CT (**b**, **c**) show increased FDG uptake (maxSUV 7.92) in the periphery of a thick-walled cavity with central liquefaction, in the right upper lobe (arrow). The findings on biopsy of this lesion were consistent with organizing inflammation. On immunohistochemistry there was absence of cytokeratin AE1/AE3 confirming the absence of tumor

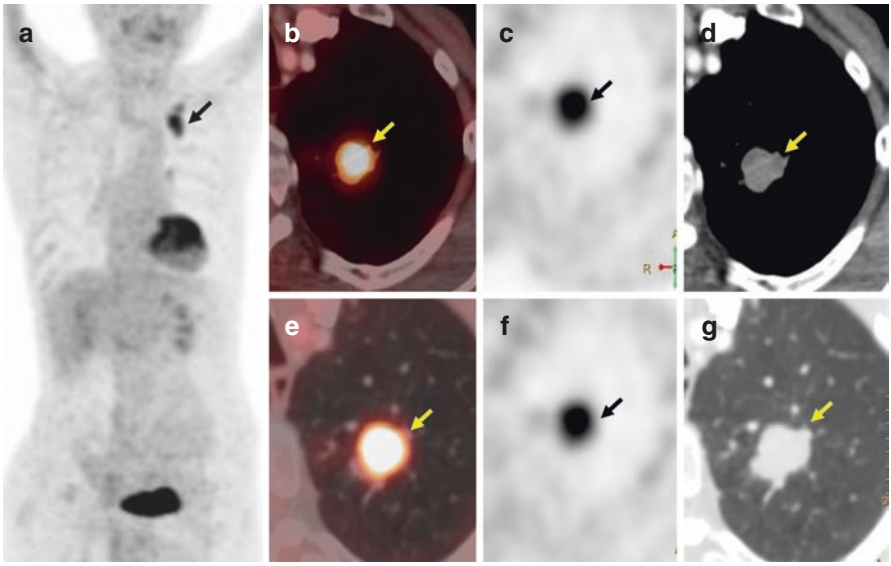

Fig. 6.4 FDG PET/CT MIP (**a**) and axial (**b–g**) images show intensely FDG-avid nodule in the left upper lobe (arrow). Biopsy showed epithelioid granulomas with fibrosis. Patient responded to antituberculous treatment

present. Extrapulmonary involvement of tuberculosis may involve the lymph nodes, liver, spleen, and bones [8, 9].

Granulomatous disease like *sarcoidosis* is FDG avid and commonly affects the lungs and mediastinal and bilateral hilar nodes [10, 11] (Fig. 6.6). Similar to tuberculosis, this chronic inflammatory disease may involve other organs as

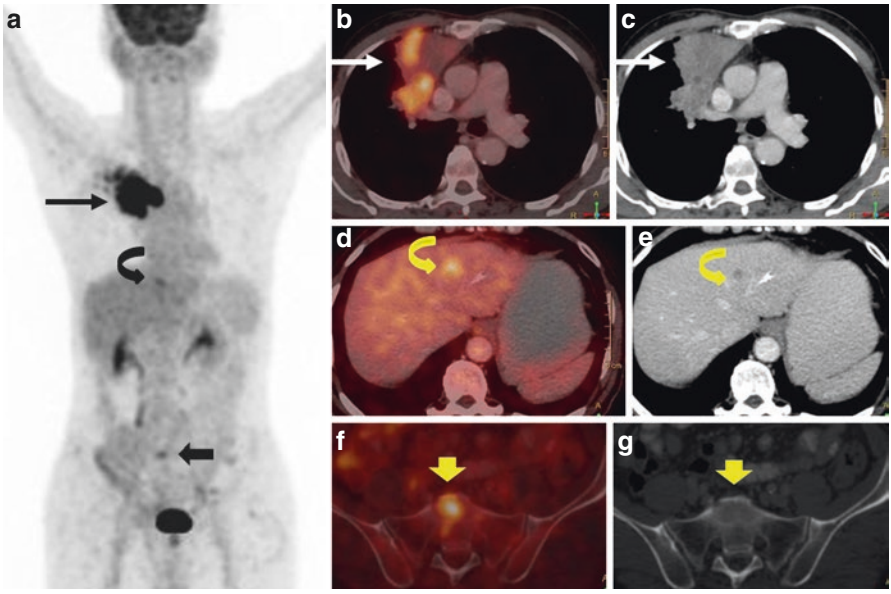

Fig. 6.5 FDG PET/CT MIP (**a**) and axial images show a large area of FDG-avid consolidation in the right upper lobe (maxSUV 12.93) (**b**, **c**). FDG-avid hypodense lesion is noted in the left lobe of the liver (curved arrow in **d**, **e**) and a marrow lesion in the sacrum (block arrow in **f**, **g**). Biopsy of all the lesions showed granulomatous inflammation with epithelioid granulomas and multinucleated Langhans and foreign body giant cells, consistent with tuberculosis

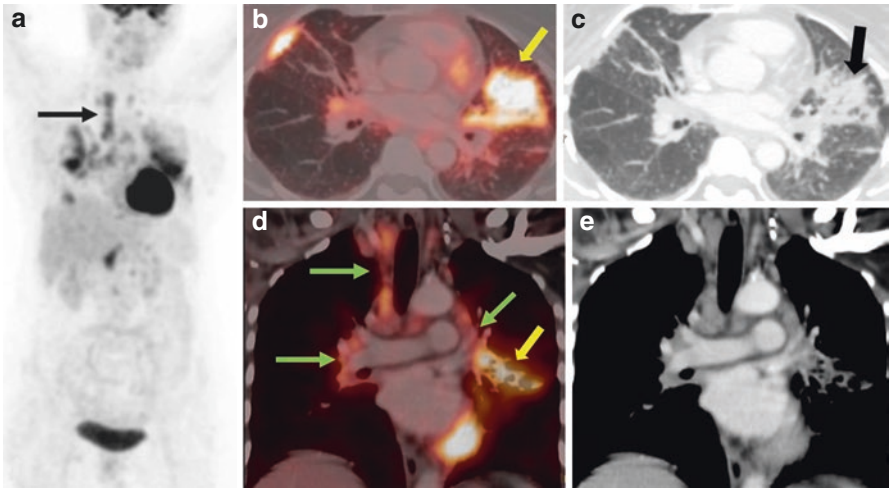

Fig. 6.6 MIP, axial, and coronal images of whole-body PET/CT scan of a 43-year-old lady who had been treated for carcinoma right breast and was being evaluated for suspected recurrence. The images show hypermetabolic enlarged bilateral hilar and paratracheal nodes with FDG-avid interstitial thickening and nodular opacities predominantly in the left lung (**a–e**). Biopsy confirmed sarcoidosis

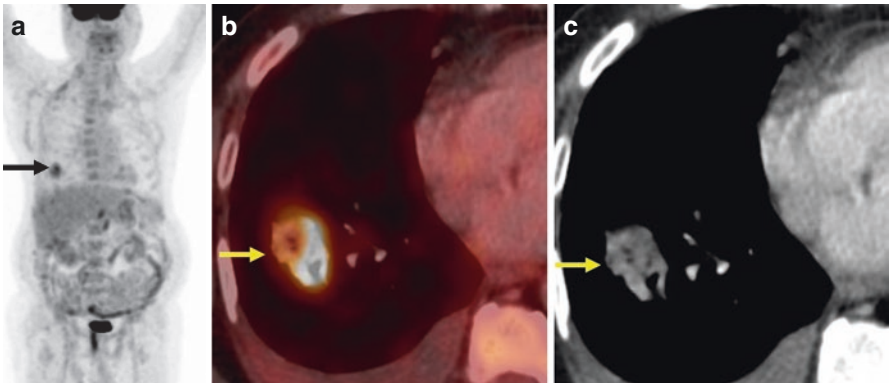

Fig. 6.7 A 68-year-old male under evaluation for a mass in the lower lobe of the right lung. Whole-body PET/CT MIP (**a**) and axial images (**b**, **c**) show FDG-avid mass in lower lobe of the right lung with few areas of calcification and cavitation (arrow). Histological examination showed extracellular amorphous eosinophilic material with apple green birefringence with foci of calcification. The findings were consistent with primary amyloidosis

well like the liver, spleen, and skeletal system. Lesions of sarcoidosis show intense and diffuse FDG uptake [12, 13].

Another benign pathology which can mimic pulmonary amyloidosis in the lung is *amyloidosis*. Pulmonary amyloidosis can be either nodular or diffuse and may show increased FDG uptake. Nodular pulmonary amyloidosis (Fig. 6.7) is more common than diffuse and may manifest as a single mass lesion or multiple nodules. The nodules usually show foci of calcifications and may cavitate. The differentials are primary lung cancer or metastasis. Histopathological confirmation is usually needed. Histologically these nodules are laden with amorphous, eosinophilic material which stains with Congo red and under polarizing microscopy shows apple-green birefringence [14, 15].

FDG uptake is also seen in *inflammatory process* like post mediastinoscopy at the site of incision in the suprasternal region (Fig. 6.8), post-thoracoscopy and post-tracheostomy at the site of intercostal drainage for pleural effusions, and scar sites post-biopsy or post-surgery representing healing changes (Fig. 6.9). A detailed history before acquisition of the scan helps in correct interpretation. In addition to these invasive procedures, few therapeutic interventions such as chemotherapy, radiation therapy, and talc pleurodesis can also cause certain false-positive results on PET/CT imaging. *Talc pleurodesis* is performed for patients who have recurrent benign or malignant pleural effusion or persistent pneumothorax. Talc pleurodesis results in obliteration of the pleural space due to adherence of the visceral and parietal pleura caused by the inflammatory reaction due to instillation of the talc. This is FDG avid due to the inflammatory reaction in the pleura (Fig. 6.10). This persists for years and may mimic pleural metastases on PET/CT. But the CT findings of focal areas of high attenuation in the pleura are diagnostic of talc pleurodesis. Appropriate clinical history and correlation with

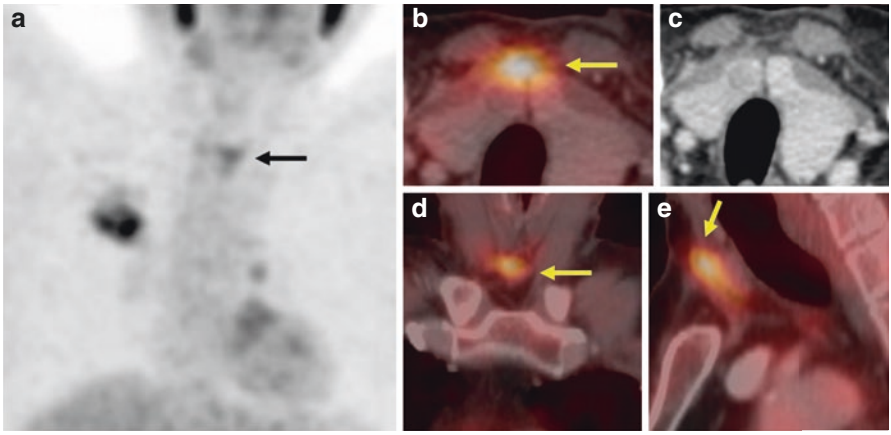

Fig. 6.8 Whole-body PET/CT MIP (**a**), axial (**b**, **c**), coronal (**d**), and sagittal (**e**) images of a 49-year-old male with adenocarcinoma in the right lung. The patient had undergone mediastinoscopy 3 weeks prior to the PET scan for nodal assessment. Increased FDG uptake is noted in the suprasternal region at site of incision of the mediastinoscopy (arrow), due to inflammation

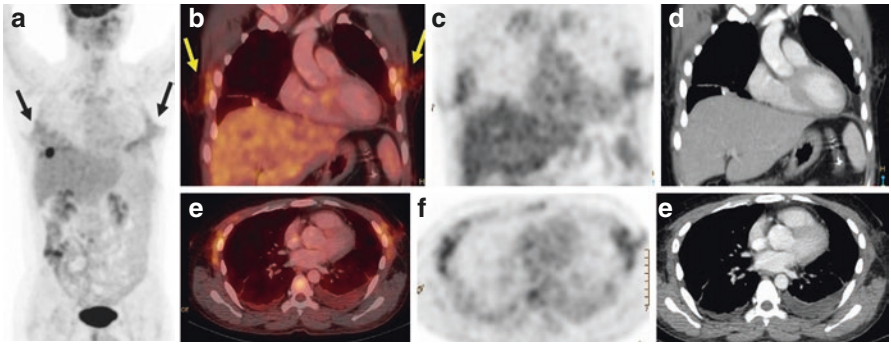

Fig. 6.9 MIP (**a**), coronal (**b–d**), and axial (**e–g**) images of whole-body FDG PET/CT scan of a 40-year-old male with adenocarcinoma rectum, who had undergone metastatectomy for bilateral lung nodules 4 months prior to the PET scan. Low-grade diffuse FDG uptake is noted in noted at the site of thoracotomy incision in bilateral anterolateral chest wall (arrows)

CT findings help in differentiating this benign condition from a malignant one [16, 17].

Radiation-induced pneumonitis is commonly seen in patients of lung cancer treated with external beam radiotherapy. Though the intention is to radiate the involved areas with maximal dose and to minimize the dose to the adjacent normal tissues, normal tissues are affected invariably. This type of injury is seen as FDG -avid consolidation or ground glass opacity within the radiation port of the involved lung (Fig. 6.11). These inflammatory changes can persist for many months and may be seen as early as 2 weeks. Radiation pneumonitis usually has a linear

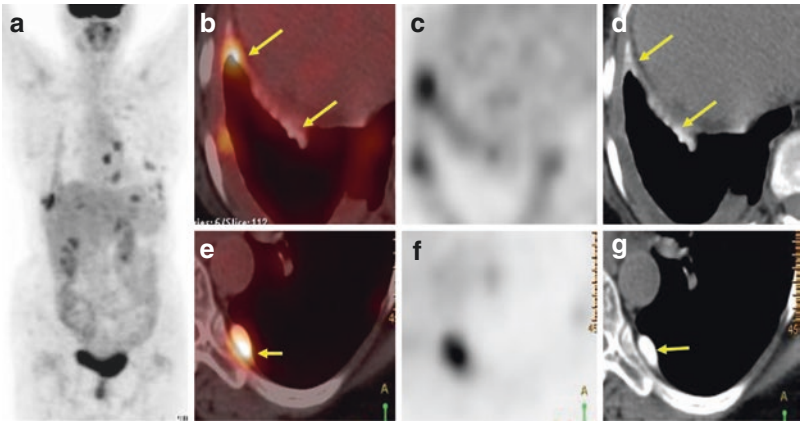

Fig. 6.10 Whole-body FDG PET/CT scan of a 65-year-old lady with recurrent malignant bilateral pleural effusion. She had undergone pleurodesis 5 months prior to the FDG PET scan. MIP (**a**) and axial images (**b–g**) show FDG-avid linear and nodular areas of talc deposition which are seen as high attenuation areas in the CT image (**d**, **g**). This occurs due to the inflammatory reaction in the pleura due to instillation of talc to obliterate the pleural space

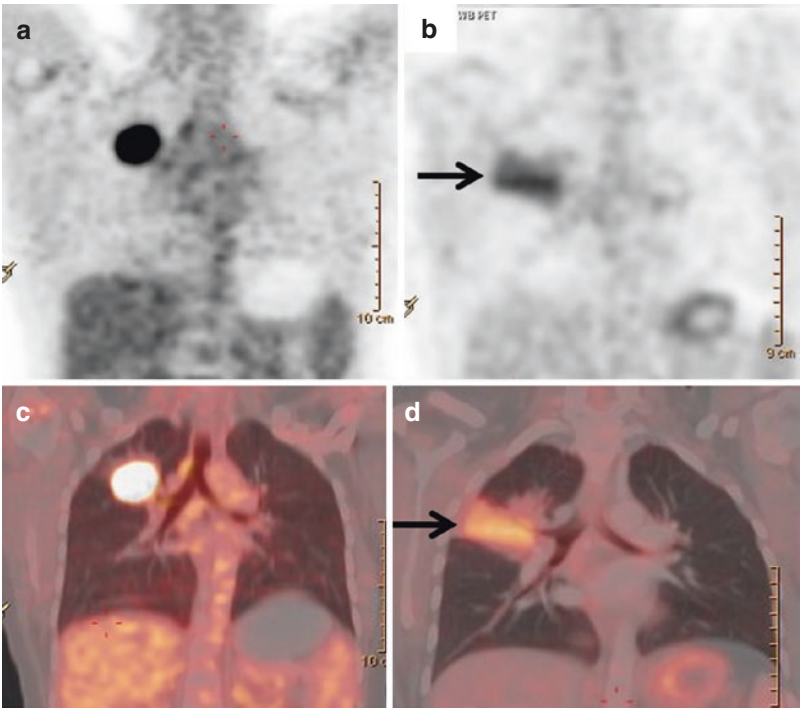

Fig. 6.11 Whole-body FDG PET/CT scan of a 50-year-old gentleman with adenocarcinoma of the right lung (**a**, **c**). PET/CT scan was done 3 months post-external beam radiotherapy. The coronal PET and PET/CT images (**b**, **d**) show FDG-avid consolidation in the radiation port of the involved lung. The consolidation typically has a linear configuration typical of radiation-induced pneumonitis

configuration along the radiation port. It is important to differentiate radiation pneumonitis from infections and neoplastic etiologies of the lung [18, 19].

6.2.3 Incidental Findings

6.2.3.1 Asymmetrical Vocal Cord Uptake

Normally the physiologic uptake of FDG in the vocal cords is bilaterally symmetrical. However, in patients of lung cancer, when the mass lies in the aortopulmonary region and infiltrates the left recurrent laryngeal nerve, it causes paralysis of the ipsilateral vocal cord with compensatory muscular activation of the contralateral normal vocal cord. This causes asymmetric FDG uptake in the non-paralyzed vocal cord (Fig. 6.12) and cricoarytenoid muscle [20, 21]. Knowledge about this physiologic variant is necessary for correct interpretation.

6.2.4 Benign Etiologies Mimicking Distant Metastases in Lung Cancer

Few benign tumors of the parotid gland, like pleomorphic adenoma and Warthin's tumor, may cause a problem in FDG PET/CT interpretation. Warthin's tumor is seen as a FDG-avid, well-defined, high-attenuation nodule in the parotid gland on FDG

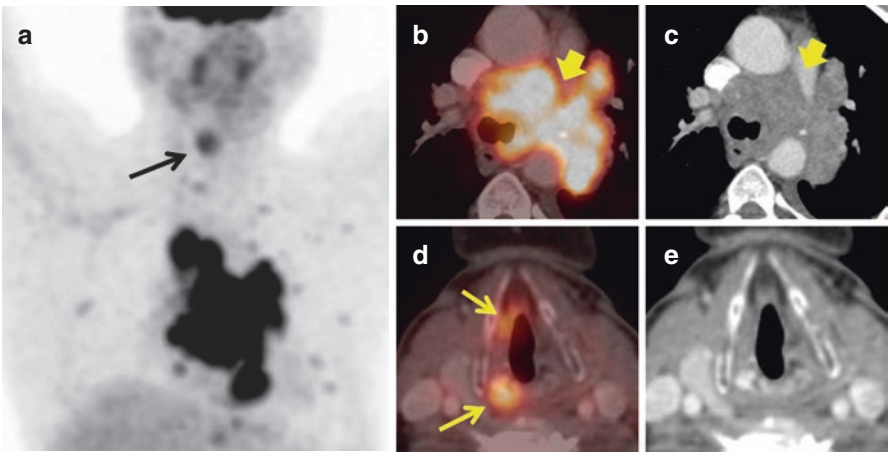

Fig. 6.12 FDG PET/CT scan of a 58-year-old gentleman with carcinoma in the upper lobe of the left lung. MIP and transaxial images (**a–c**) show a large FDG-avid mass in the left upper lobe infiltrating the mediastinum and involving the aortic pulmonary window (block arrows in **b**, **c**) through which the left recurrent laryngeal nerve traverses thereby involving it and causing paralysis of the left vocal cord. This in turn causes compensatory hypertrophy of the contralateral (right) vocal cord seen as increased FDG uptake in the right vocal cord and cricoarytenoid muscle (arrows in **a**, **d**)

PET/CT imaging (Fig. 6.13). They are usually solitary but may be bilateral occasionally. These are more common in smokers and may be confused with a metastatic lesion. The imaging findings on CT scan and ultrasonography are usually characteristic [22, 23].

Physiological bone marrow uptake is usually homogenous and low grade. Diffusely increased uptake in the marrow may occur due to *anemia* (Fig. 6.14) and *hematopoietic diseases* or in patients receiving colony-stimulating factors. Bone marrow involvement can also occur due to metastatic disease arising from tumors of the lung, breast, and prostate, and differentiation from benign marrow involvement is necessary. Sometimes a marrow biopsy may be necessary to come to the correct diagnosis [24].

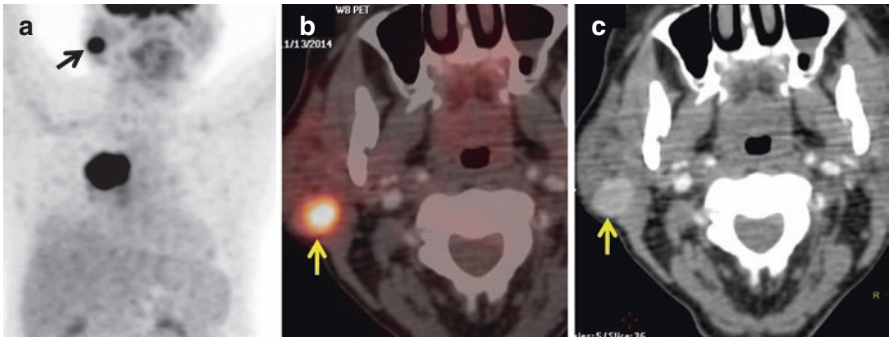

Fig. 6.13 FDG PET/CT scan done in a 60-year-old gentleman with poorly differentiated non-small cell carcinoma in the upper lobe of the right lung (MIP **a**). The scan shows enhancing FDG-avid nodule in the right parotid gland (arrow in **a–c**). Though the imaging findings were favoring the possibility of a benign Warthin's tumor, a biopsy was advised in view of the poorly differentiated nature of the tumor. Biopsy confirmed Warthin's tumor in the right parotid gland

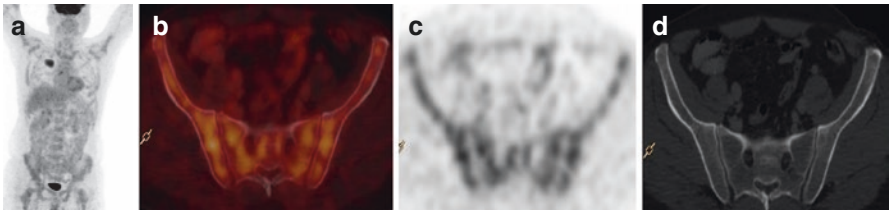

Fig. 6.14 Whole-body FDG PET/CT scan in a 61-year-old gentleman with adenocarcinoma in the right lung (MIP image **a**) with diffuse increased FDG uptake in the axial and appendicular skeleton seen in MIP image (**a**) and transaxial images of the pelvis (**b–d**) due to anemia. The hemoglobin was 8 g/dL [normal range, 13–17 g/dL]

6.2.5 False-Negative Neoplastic Pathology

Few adenocarcinomas of the lung like bronchoalveolar cell carcinoma show very-low-grade FDG uptake due to low GLUT1 expression in these malignancies [25]. Carcinoids (Fig. 6.15), which have neuroendocrine differentiation, may have variable FDG uptake ranging from no to low-grade uptake due to slow growth pattern [26]. Also small lung nodules less than 10mm in diameter which is below the spatial resolution of current PET scanner may result in false-negative studies [27, 28].

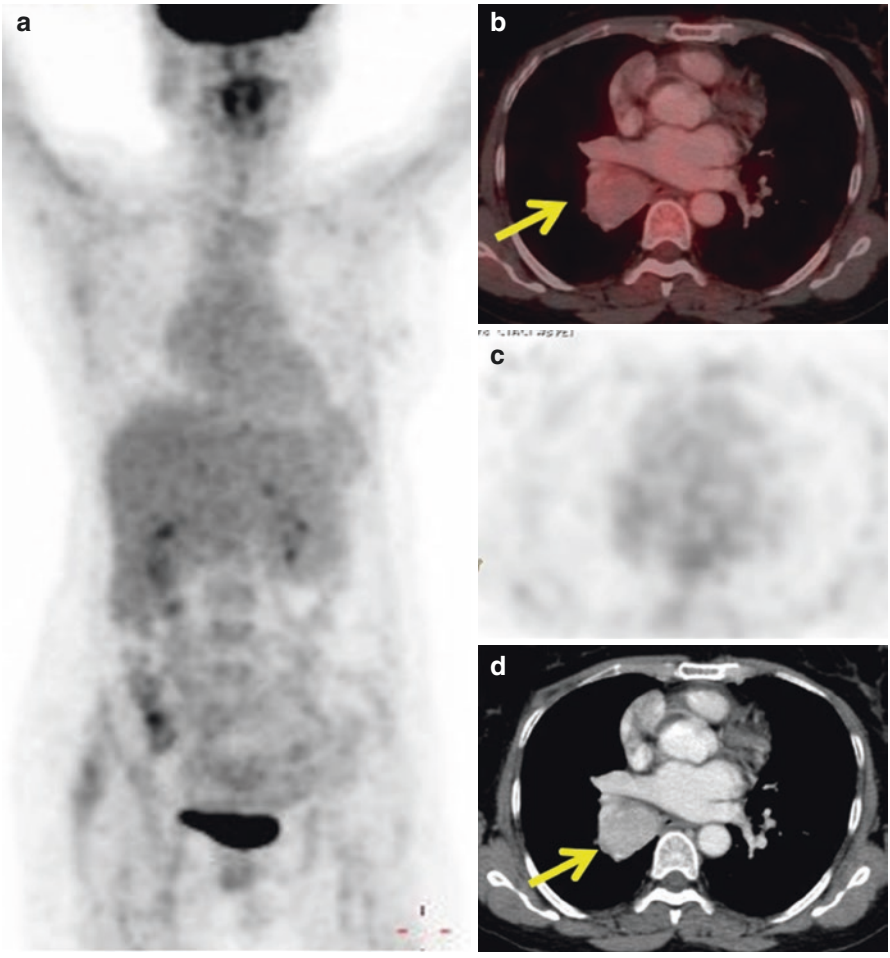

Fig. 6.15 Whole-body FDG PET/CT scan of a 52-year-old lady with right infracarinal mass involving the right lower lobe bronchus. No FDG uptake is noted in the lesion (**a** and arrow in the transaxial images **b–d**). Biopsy of the lesion was a carcinoid tumor. A 68Ga-DOTANOC study done subsequently showed intense uptake in the lesion typical of low-grade carcinoids

Conclusion

PET/CT is an amalgamation of functional and anatomical imaging modalities which should be used constructively benefitting the medical imaging field. Knowledge of the normal variants and benign pathologic conditions will help us in correct interpretation of false-positive lesions which confound the results with malignancy and vice versa.

Key Points

- FDG is a marker of glycolysis and, thus, is neither specific for malignancy nor for a particular tumor.
- FDG accumulates in benign process and is difficult to differentiate from a neoplastic etiology.

Respiratory artifacts:

- Due to mismatch of PET and CT data during respiration.
- Seen as curvilinear photon-deficient (cold) defect at the interface of the lung and diaphragm leading to incorrect anatomic localization of the focus of increased FDG activity.
- A review of the CT images for a nodule in the lung or liver/spleen lesion usually solves the dilemma.

Attenuation artifacts:

- High CT attenuation materials such as intravenous or oral contrast, metals, ports, and catheters can cause attenuation artifacts.

Artifacts due to faulty injection technique:

- Paravenous injection may lead to endothelial injury, which in turn leads to the formation of clots at the injury site, which get trapped in the pulmonary microcirculation.
- Paravenous injection can also lead to FDG uptake in the ipsilateral nodes in the axilla due to lymphatic uptake of the tracer.

Infection and inflammation:

- In the evaluation of lung cancer, the commonest causes of false-positive uptakes in the lung are due to infection and inflammation.
- It is not always easy to differentiate between benign and malignant process on imaging findings alone, and a biopsy may be necessary for confirmation (includes infections such as pneumonia, tuberculosis, sarcoidosis, and amyloidosis).

- Talc pleurodesis is FDG avid due to the inflammatory reaction in the pleura and can show increased uptake for years and may mimic pleural metastases on PET/CT.
- Radiation-induced pneumonitis is commonly seen in patients of lung cancer treated with external beam radiotherapy and is seen as FDG-avid consolidation or ground glass opacity within the radiation port of the involved lung.

Incidental findings:

- Asymmetrical vocal cord uptake is often seen in patients with paralysis of the ipsilateral vocal cord with compensatory muscular activation of the contralateral normal vocal cord.
- Warthin's tumor is seen as a FDG-avid, well-defined, high-attenuation nodule in the parotid gland on FDG PET/CT imaging.
- Physiological bone marrow uptake is usually homogenous and low grade. Diffusely increased uptake in the marrow may occur due to anemia and hematopoietic diseases or in patients receiving colony-stimulating factors.

False-negative neoplastic pathology:

- Adenocarcinomas of the lung like bronchoalveolar cell carcinoma show very-low-grade FDG uptake due to low GLUT1 expression in these malignancies [25].
- Carcinoids, which have neuroendocrine differentiation, may have variable FDG uptake ranging from no to low-grade uptake due to slow growth pattern.
- Small lung nodules less than 10 mm in diameter which is below the spatial resolution of current PET scanner may result in false-negative studies.
- Knowledge of the normal variants and benign pathologic conditions will help in correct interpretation of false-positive lesions.

References

1. Beyer T, Antoch G, Blodgett T, et al. Dual-modality PET/CT imaging: the effect of respiratory motion on combined image quality in clinical oncology. Eur J Nucl Med Mol Imaging. 2003;30:588–96.
2. Nehmeh SA, Erdi YE, Kalaigian H, et al. Correction for oral contrast artifacts in CT attenuation corrected PET images obtained by combined PET/CT. J Nucl Med. 2003;44:1940–4.
3. Liu Y, Ghesani NV, Zuckier LS. Physiology and pathophysiology of incidental findings detected on FDG-PET scintigraphy. Semin Nucl Med. 2010;40(4):294–315.
4. Farsad M, Ambrosini V, Nanni C, et al. Focal lung uptake of 18F-fluorodeoxyglucose (18F-FDG) without computed tomography findings. Nucl Med Commun. 2005;26(9):827–30.
5. Ozdemir E, Poyraz NY, Keskin M, Kandemir Z, Turkolmez S. Hot-clot artifacts in the lung parenchyma on F-18 fluorodeoxyglucose positron emission tomography/CT due to faulty injection techniques: two case reports. Korean J Radiol. 2014;15(4):530–3.

6. Kubota R, Yamada S, Kubota K, et al. Intratumoral distribution of fluorine-18-fluorodeoxyglucose in vivo: high accumulation in macrophages and granulation tissues studied by microautoradiography. J Nucl Med. 1992;33:1972–80.
7. Paik JY, Lee KH, Choe YS, et al. Augmented 18F-FDG uptake in activated monocytes occurs during the priming process and involves tyrosine kinases and protein kinase C. J Nucl Med. 2004;45:124–8.
8. Bakheet SM, Powe J, Ezzat A, et al. F-18-FDG uptake in tuberculosis. Clin Nucl Med. 1998;23:739–42.
9. Skoura E, Zumla A, Bomanji J. Imaging in tuberculosis. Int J Infect Dis. 2015;32:87–93.
10. Lewis PJ, Salama A. Uptake of fluorine-18-deoxyglucose uptake in sarcoidosis. J Nucl Med. 1994;35:1647–9.
11. Yasuda S, Shothsu A, Ide M, et al. High fluorine-18-deoxyglucose uptake in sarcoidosis. Clin Nucl Med. 1996;21:983–4.
12. El-Haddad G, Zhuang H, Gupta N, et al. Evolving role of positron emission tomography in the management of patients with inflammatory and other benign disorders. Semin Nucl Med. 2004;34(4):313–29.
13. Sobic-Saranovic D, Artiko V, Obradovic V. FDG PET imaging in sarcoidosis. Semin Nucl Med. 2013;43(6):404–11.
14. Quan XQ, Yin TJ, Zhang CT, Liu J, Qiao LF, Ke CS. (18)F-FDG PET/CT in patients with nodular pulmonary amyloidosis: case report and literature review. Case Rep Oncol. 2014;7(3):789–98.
15. Wachsmann JW, Gerbaudo VH. Thorax: normal and benign pathologic patterns in FDG-PET/CT imaging. PET Clin. 2014;9(2):147–68.
16. Kwek BH, Aquino SL, Fischman AJ. Fluorodeoxyglucose positron emission tomography and CT after talc pleurodesis. Chest. 2004;125:2356–60.
17. Ahmadzadehfar H, Palmedo H, Strunk H, Biersack HJ, Habibi E, Ezziddin S. False positive 18F-FDG-PET/CT in a patient after talc pleurodesis. Lung Cancer. 2007;58(3):418–21.
18. Ulaner GA, Lyall A. Identifying and distinguishing treatment effects and complications from malignancy at FDG PET/CT. Radiographics. 2013;33(6):1817–34.
19. de Prost N, Tucci MR, Melo MF. Assessment of lung inflammation with 18F-FDG PET during acute lung injury. AJR Am J Roentgenol. 2010;195(2):292–300.
20. Kamel EM, Goerres GW, Burger C, et al. Recurrent laryngeal nerve palsy in patients with lung cancer: detection with PET/CT image fusion—report of six cases. Radiology. 2002;224:153–6.
21. Lee M, Ramaswamy MR, Lilien DL, et al. Unilateral vocal cord paralysis causes contralateral false-positive positron emission tomography scans of the larynx. Ann Otol Rhinol Laryngol. 2005;114:202–6.
22. Peter Klussmen J, Wittekindt C, Florian Preuss S, et al. High risk for bilateral warthin tumor in heavy smokers - review of 185 cases. Acta Otolaryngol. 2006;126:1213–7.
23. Lee SK, Rho BH, Won KS. Parotid incidentaloma identified by combined 18F-fluorodeoxyglucose whole-body positron emission tomography and computed tomography: findings at gray-scale and power Doppler ultrasonography and ultrasound-guided fine-needle aspiration biopsy or core biopsy. Eur Radiol. 2009;19:2268–74.
24. Inoue K, Okada K, Harigae H, et al. Diffuse bone marrow uptake on F-18 FDG PET in patients with myelodysplastic syndromes. Clin Nucl Med. 2006;31:721–3.
25. Higashi K, Ueda Y, Sakurai A, et al. Correlation of Glut-1 glucose transporter expression with [^{18}F]FDG uptake in non-small cell lung cancer. Eur J Nucl Med. 2000;27:1778–85.
26. Stefani A, Franceschetto A, Nesci J, Aramini B, Proli C, Kaleci S, et al. Integrated FDG-PET/CT imaging is useful in the approach to carcinoid tumors of the lung. J Cardiothorac Surg. 2013;8:223.
27. Nomori H, Watanabe K, Ohtsuka T, et al. Evaluation of F-18 fluorodeoxyglucose (FDG) PET scanning for pulmonary nodules less than 3 cm in diameter, with special reference to the CT images. Lung Cancer. 2004;45:19–27.
28. Cook GJ, Wegner EA, Fogelman I. Pitfalls and artifacts in 18FDG PET and PET/CT oncologic imaging. Semin Nucl Med. 2004;34(2):122–33.

Physics of PET and Respiratory Gating

7

April-Louise Smith and Richard Manber

Contents

7.1 PET Physics

Positron emission tomography (PET) is an imaging technique that detects radiolabelled drugs, which have been injected into the body. PET uses radioisotopes which emit energy in the form of positrons (β^+). Positrons are positively charged energetic electrons emitted from nuclei. As the positron interacts with the surrounding tissue, it quickly loses energy. Once the majority of energy is lost, it will combine with an electron and converts energy annihilating, subsequently forming two gamma rays (γ) of equal energy (511 keV) in opposite directions (Fig. 7.1). These gamma rays can then be detected by external detectors and used to produce a 3D image.

PET scanners have multiple detectors positioned in a ring around the patient, which allows simultaneous gamma ray detection (Fig. 7.2). These two gamma rays

A.-L. Smith (✉)
Institute of Nuclear Medicine, University College London Hospital NHS Foundation Trust, London, UK
e-mail: April-Louise.Smith@nhs.net

R. Manber
Institute of Nuclear Medicine, University College London Hospital NHS Foundation Trust, London, UK
e-mail: manber.richard@gmail.com

A. Agrawal, V. Rangarajan (eds.), *PET/CT in Lung Cancer*, Clinicians' Guides to Radionuclide Hybrid Imaging, https://doi.org/10.1007/978-3-319-72661-8_7

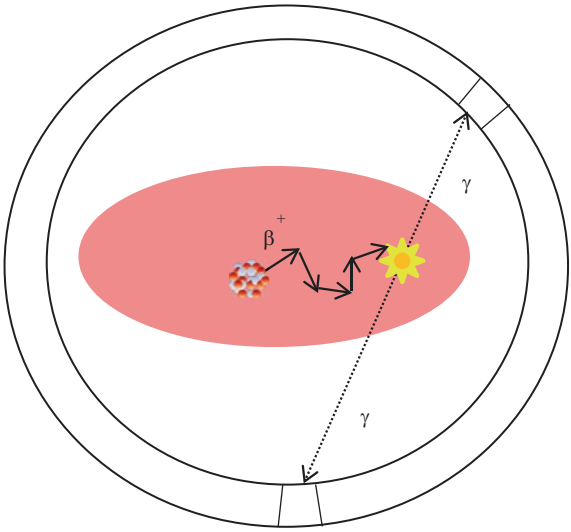

Fig. 7.1 Diagram to show radioisotope decay via β^+ emission, the interaction with surrounding tissue and annihilation producing two 511 keV gamma rays that are detected on the PET ring of detectors (diagram not to scale)

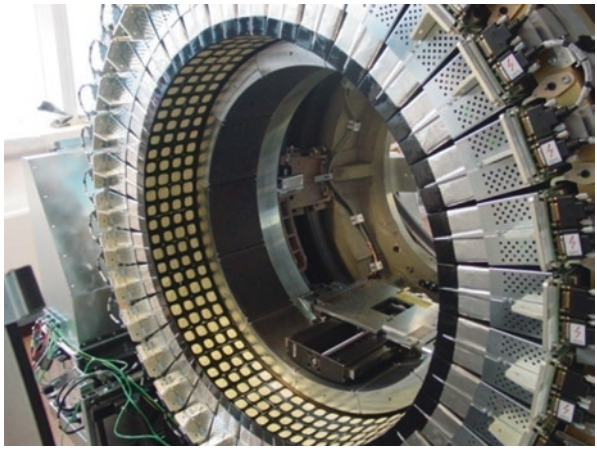

Fig. 7.2 Inside a multi-detector ring PET scanner

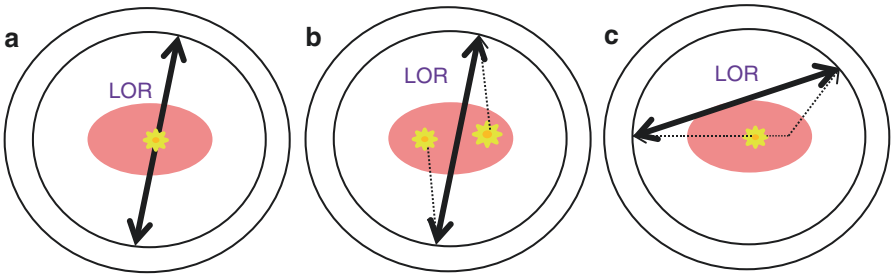

Fig. 7.3 Diagrams showing different coincidence events. (**a**) True event showing a correct LOR, (**b**) random event where two separate events are detected within the coincidence window, giving an incorrect LOR. (**c**) Scatter event, where one photon is scattered and both photons are then detected, also giving an incorrect LOR

create a line of response (LOR) indicating a pathway where the annihilation has occurred. If the gamma rays are detected within a set timing window (~10 ns), this is called a 'coincidence event'.

If the event detected is due to an annihilation (back-to-back gamma rays), it is known as a 'true event' giving a correct LOR (Fig. 7.3a). If, however, two separate interactions occur simultaneously and are detected, this is considered a 'random event' (Fig. 7.3b). Scatter events occur when the positron annihilates and either one or both the gamma rays are scattered by the surrounding tissue, changing their path (Fig. 7.3c). Scattered and random events result in incorrect LOR, which can introduce noise into the image.

There are a number of correction methods for scattered and random events that can be applied to improve the image quality. In addition, normalisation corrections are applied to account for different sensitivities of the detector blocks and dead-time corrections to compensate for high count rates. Another important correction is for attenuation. In PET acquisitions, some of the emitted photons are attenuated by the surrounding tissue and not detected. This gives rise to artefacts showing the outer edge with increased intensity and central areas with lower intensity. Computed tomography (CT) images can be used to create a map of this attenuation which can be used to correct the PET data. Magnetic resonance (MR) data can also be used to create an attenuation correction map in PET/MR systems, by segmenting the images and assigning corresponding attention factors for that specific tissue. In older scanners, attenuation correction is performed using a transmission scan with an external rod source.

7.2 Reconstruction

Once injected with a radiopharmaceutical, a number of interactions will occur in the patient tissue which can be accumulated over time. This gives projections at different angles, representing the distribution of radioactivity within the tissue (Fig. 7.4a, b).

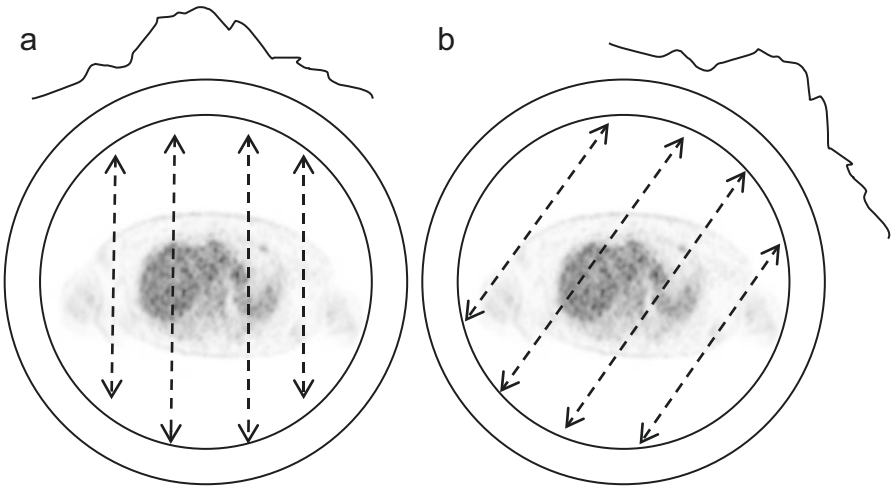

Fig. 7.4 PET reconstruction. The detected events generate lines of response (LOR); these give projections of the distribution at different angles (**a**) and (**b**). A number of projections surrounding the patient are then reconstructed to build a 3D image

Table 7.1 Some examples of radionuclides that can be used in PET

Radioisotope	Half-life	β^+ energy, max (keV)	β^+ range (mm)	Mode of production
^{18}F	110 m	633 (97%)	0.6	Cyclotron
^{11}C	20.4 m	960 (100%)	1.1	Cyclotron
^{13}N	9.97 m	1199 (100%)	1.5	Cyclotron
^{15}O	2.04 m	1732 (100%)	2.5	Cyclotron
^{68}Ga	73 m	822 (1%)	2.9	Generator
		1899 (88%)		
^{82}Rb	75 s	1523 (83.3%)	5.9	Generator
		1157 (10.2%)		

Data references: ^{18}F [1]; ^{11}C, ^{13}N, ^{15}O, ^{68}Ga [2]; ^{82}Rb [3]

The images are then reconstructed using either filter back projection (FBP) or iterative reconstruction using ordered-subset expectation maximization (OSEM) or maximum likelihood expectation maximization (MLEM).

7.3 PET Tracers

There are a number of radiopharmaceuticals available for PET imaging. ^{18}F (Fluorine-18)-labelled compounds are most commonly used; ^{18}F has a slightly longer half-life compared to other PET tracers which allows it to be transported and not require an onsite cyclotron. In addition to half-life, different radionuclides vary in properties that can have effects on imaging parameters. Positron range affects the spatial resolution, since the annihilation can occur at a distance away from where the positron was produced. The abundance of positrons produced from each decay can also have effects on the sensitivity. Also, affecting imaging parameters, the different radionuclides have different radiochemistry, allowing them to be labelled to desired pharmaceuticals. Some examples of PET isotopes are outlined in Table 7.1.

7.4 PET Images

The reconstructed images can be viewed in a number of ways. A stack of images is created and can be viewed in the different planes, as shown in Fig. 7.5. Hybrid imaging also allows fused data for anatomical localisation, as shown in Fig. 7.6. Because PET data are corrected for physical processes, quantitative data of activity concentration per unit volume (kBq/mL) can be calculated. When normalised to available activity concentration by factoring in, e.g. patient body mass, the standardized uptake values (SUV) can be determined. This allows longitudinal comparisons—taking into account variations between injected activity and patient's weight between time points—to give a representation of the uptake in the lesion.

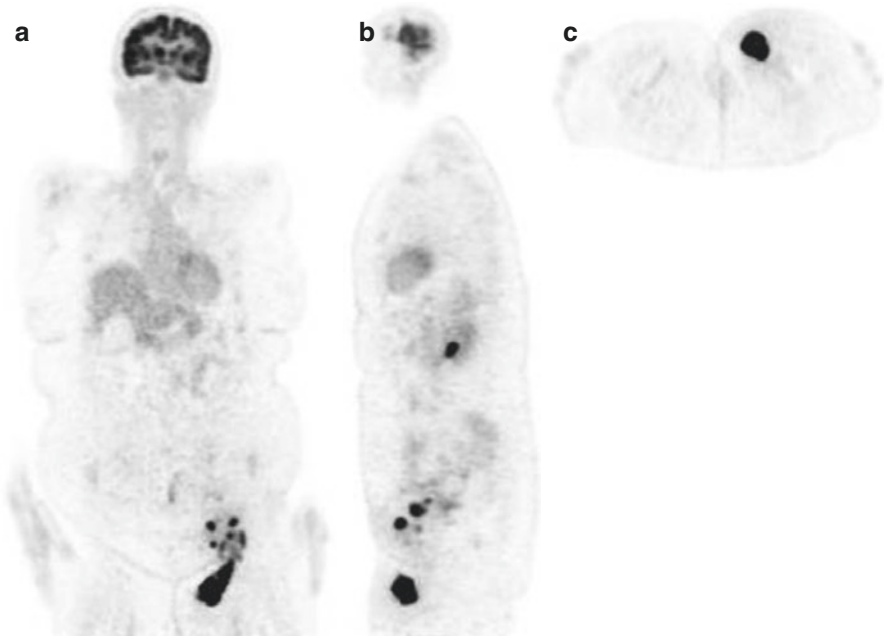

Fig. 7.5 An example of ^{18}F-FDG whole body PET acquisition using OSEM with TOF. (**a**) Coronal slices, (**b**) sagittal slices and (**c**) transaxial slices

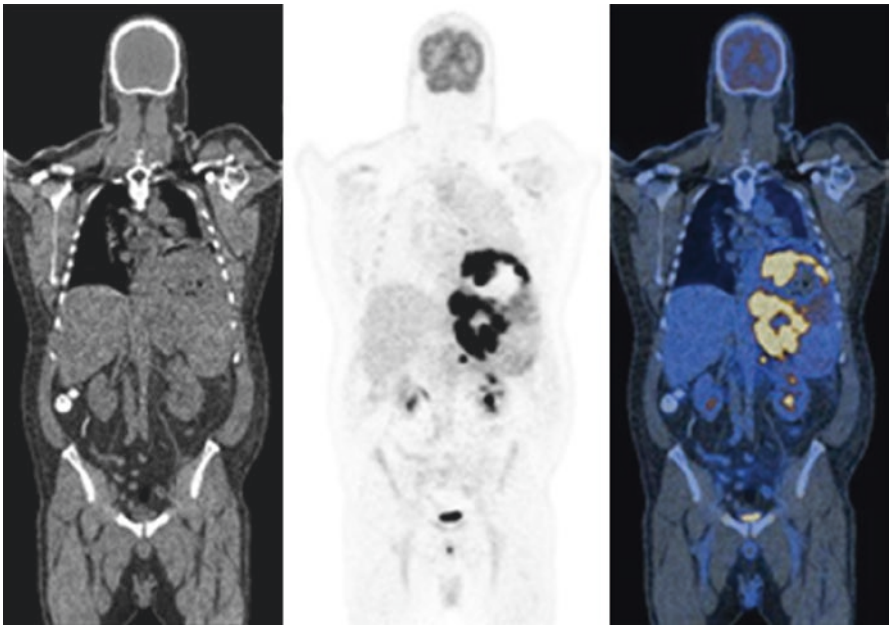

Fig. 7.6 ^{18}F-FDG whole body PET/CT acquisition showing CT, PET, fused PET/CT in the coronal plane

7.5 Respiratory Gating

There are many artefacts that can affect image quality—one of which is motion. This can cause potential spatial mismatch between CT and PET, which can give attenuation correction artefacts as CT images are acquired in seconds compared to PET which is time averaged over a number of minutes. In addition to this, respiratory motion may introduce further errors, particularly when imaging the thorax or abdomen. Figure 7.7 shows mismatch between PET and MR data of the liver due to respiratory motion. PET data is acquired over several minutes, covering many respiratory cycles, which can introduce blurring into resultant images. One approach to overcome this problem is to acquire a respiratory signal and split the PET data into different respiratory states, either viewing separately or retrospectively combining, to form one motion-corrected image.

In order to track respiration, diaphragm displacement can be examined, using imaging techniques. Or external sensors can be used, to detect motion. Pressure sensor belts are clinically available, identifying low pressure during expiration and high pressure during inspiration. In addition, Real-time Position Management (RPM) uses a camera to track two infrared markers on a box positioned on the patient's chest.

Using these tracking techniques, the breathing signal can be synchronised with the imaging data, by binning or gating into groups of data at similar respiratory

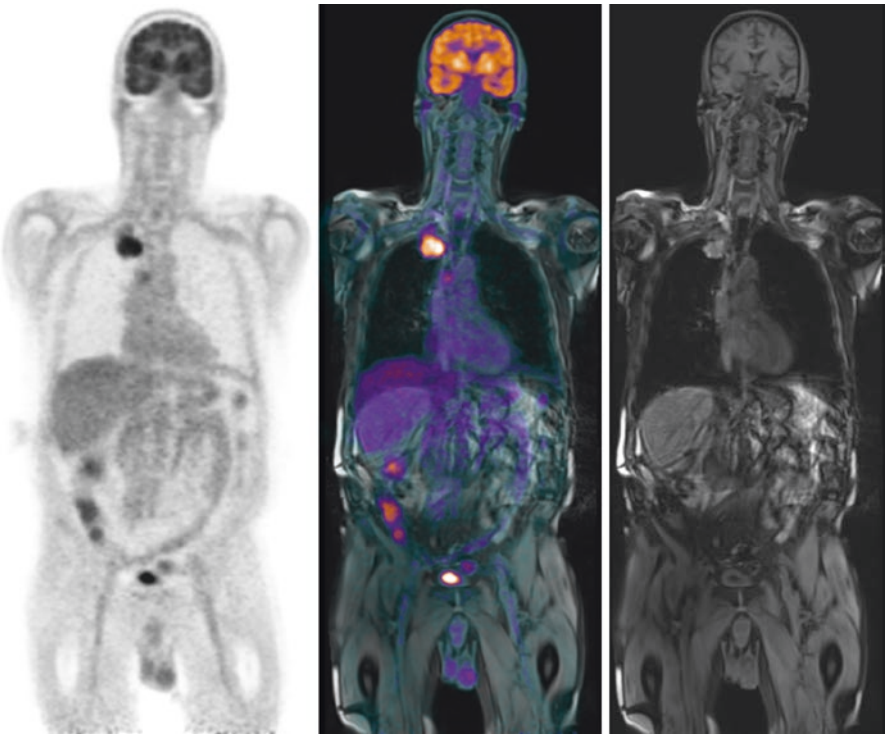

Fig. 7.7 ^{18}F-FDG whole body PET/MR showing PET, PET/MR fused and MR in the coronal plane

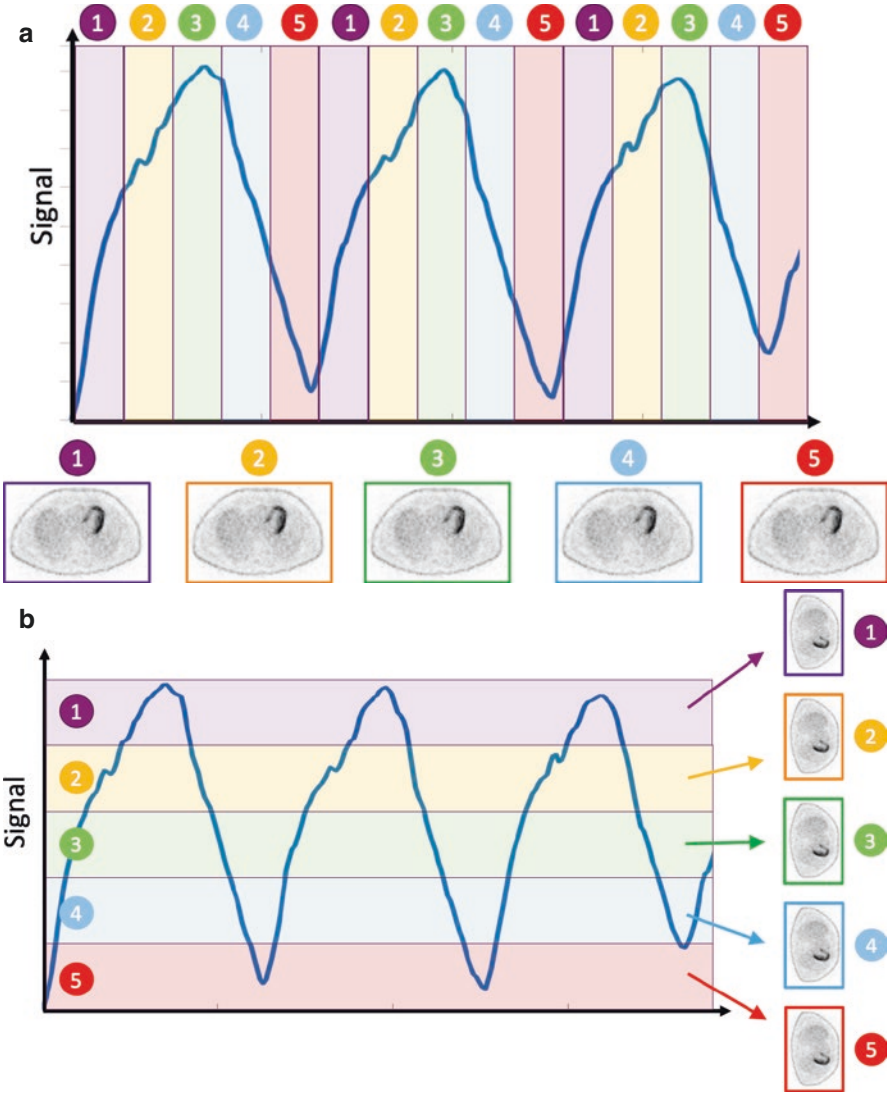

Fig. 7.8 Gating respiratory data using numbers of bins (**a**) or amplitude (**b**)

states. The main methods are gating by amplitude or phase. Phase gating splits the data within each respiratory cycle into a number of bins between each inhalation peak (Fig. 7.8a), whereas amplitude gating splits the data based on the value of respiratory signal (Fig. 7.8b). Once the data is binned, one option is to create one 'exhale' image using the data from one gate. This will reduce sensitivity; therefore, increased scan time is required to achieve the same contrast. Another method is to use all the data for the different gates and register them to one gate, preserving full image contrast.

7.6 Recent Developments

There are various software advances that improve image quality which can be factored into PET reconstructions. These include time of flight (TOF) [4], which looks at the time at which two photons are received from the annihilation compared to each other, to give a better estimation of where the annihilation occurred along the LOR. There are also reconstruction algorithms that take into account the detector geometry, point spread function (PSF) [5], and an algorithm that can iteratively reconstruct going to full convergence, Bayesian Penalised Likelihood (BPL), algorithm [6]. In addition to this, recent advances in detectors have seen the use of solid-state detectors, initially pioneered for PET/MR systems as the use of photomultiplier tubes (PMT) is not compatible with the magnetic field. These detectors replace photomultiplier tubes with semiconductor readout arrays allowing more compact design and improved detecting capabilities.

Key Points

- PET scanners have multiple detectors positioned in a ring around the patient, which allows simultaneous gamma ray detection.
- There are many artefacts that can affect image quality—one of which is motion.
- Patient motion can cause potential spatial mismatch between CT and PET, which can give attenuation correction artefacts as CT images are acquired in seconds compared to PET which is time averaged over a number of minutes.
- Respiratory motion may introduce errors, particularly when imaging the thorax or abdomen.
- PET data is acquired over several minutes, covering many respiratory cycles, and can introduce blurring into resultant images.

References

1. Jolla L. Radionuclide data sheets. University of California; 2009. https://ehs.ucsd.edu/rad/radionuclide/radionuclide_datasheets.html. Accessed May 2016.
2. Delacroix D, Guerre JP, Leblanc P, Hickman C. Radionuclide and radiation protection handbook, Vol. 98. Ashford: Nuclear Technology Publishing; 2002.
3. Jadvar H, Parker JA. Clinical PET and PET/CT – Chap 2 Radiotracers. Berlin: Springer; *2005*. p. 45–67.
4. Vandenberghe E, Mikhaylova E, D'Hoe E, Mollet P, Karp JS. Recent developments in time-of-flight PET. EJNMMI Phys. 2016;3:3.
5. Rahmima A, Qi J, Sossi V. Resolution modelling in PET imaging: theory, practice, benefits and pitfalls. Med Phys. 2013;40:6.
6. Ross S. GE Healthcare Q. Clear, White paper; 2014, rev 3.

Lung Cancer Pictorial Atlas

8

Nilendu C. Purandare, Archi Agrawal, Sneha Shah, and Venkatesh Rangarajan

Contents

N.C. Purandare (✉) • A. Agrawal • S. Shah • V. Rangarajan
Department of Nuclear Medicine and Molecular Imaging, Tata Memorial Hospital, Mumbai, India
e-mail: nilpurandare@gmail.com; drarchi23@gmail.com; snehahv@gmail.com; drvrangarajan@gmail.com

A. Agrawal, V. Rangarajan (eds.), *PET/CT in Lung Cancer*, Clinicians' Guides to Radionuclide Hybrid Imaging, https://doi.org/10.1007/978-3-319-72661-8_8

8.1 Case 1: Lung Cancer and Tuberculosis

Teaching point: Both tuberculosis and lung cancer can present as cavitating lesions.

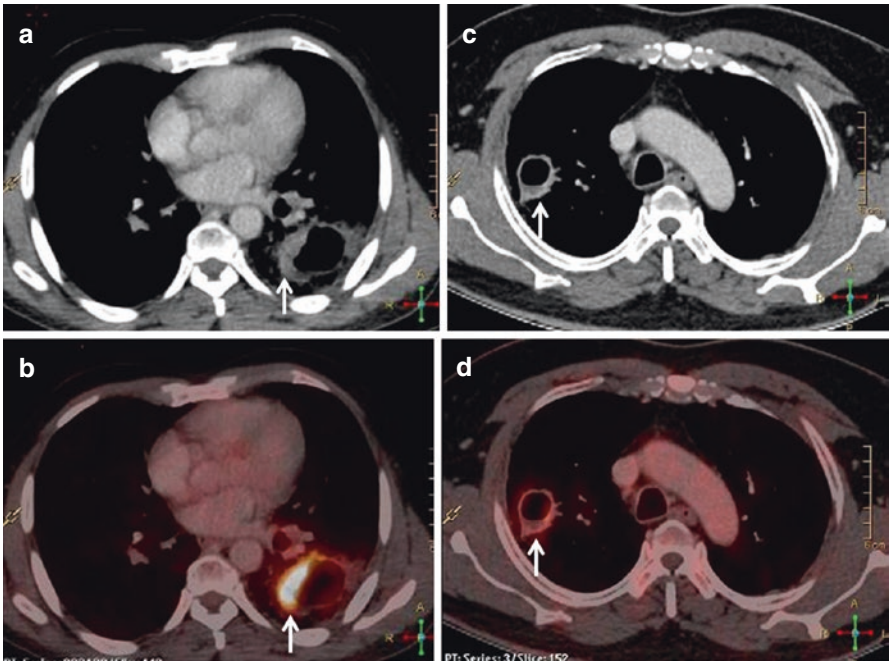

Fig. 8.1 Cavitating lesions. Axial CT and fusion PET/CT (arrows in **a**, **b**) images in a patient of non-small cell lung cancer show a thick irregular walled cavity showing FDG uptake in the wall. Axial CT and fusion PET/CT (arrows in **c**, **d**) images in a patient of pulmonary tuberculosis show a thin-walled cavity

8.2 Case 2: Mass-Like Lesions of Tuberculosis and Lung Cancer

Teaching point: Tuberculosis occasionally presents as a mass-like lesion.

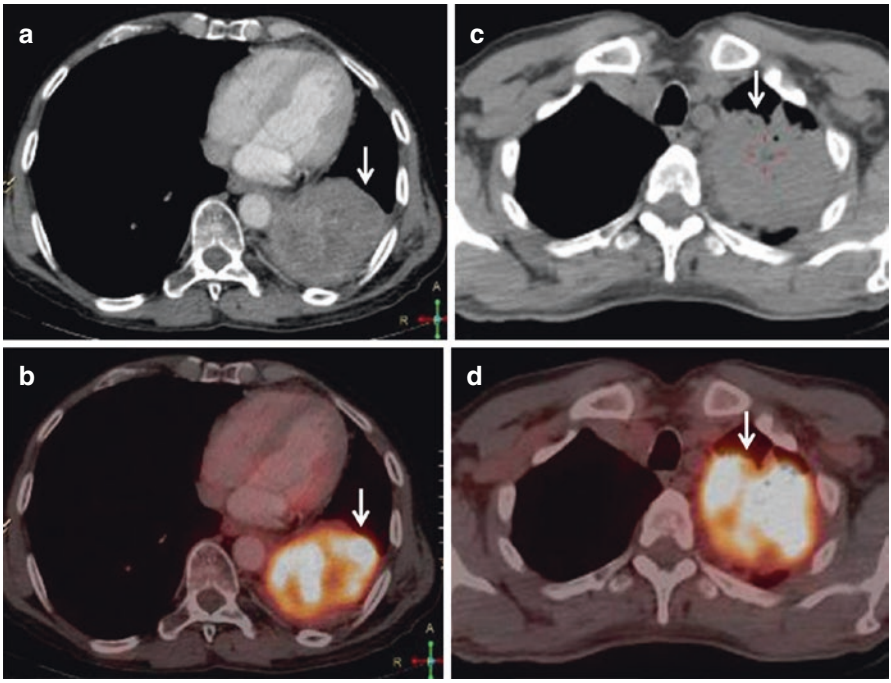

Fig. 8.2 Axial CT and fusion PET/CT (arrows in **a**, **b**) images in a patient of non-small cell lung cancer show a FDG-avid mass lesion. Axial CT and fusion PET/CT (arrows in **c**, **d**) images show pulmonary tuberculosis presenting as a mass-like lesion

8.3 Case 3: Various Appearances of Adenocarcinoma In Situ: AIS (Bronchioloalveolar Carcinoma, BAC)

Teaching point: AIS/BAC can present in several patterns and often show low FDG uptake.

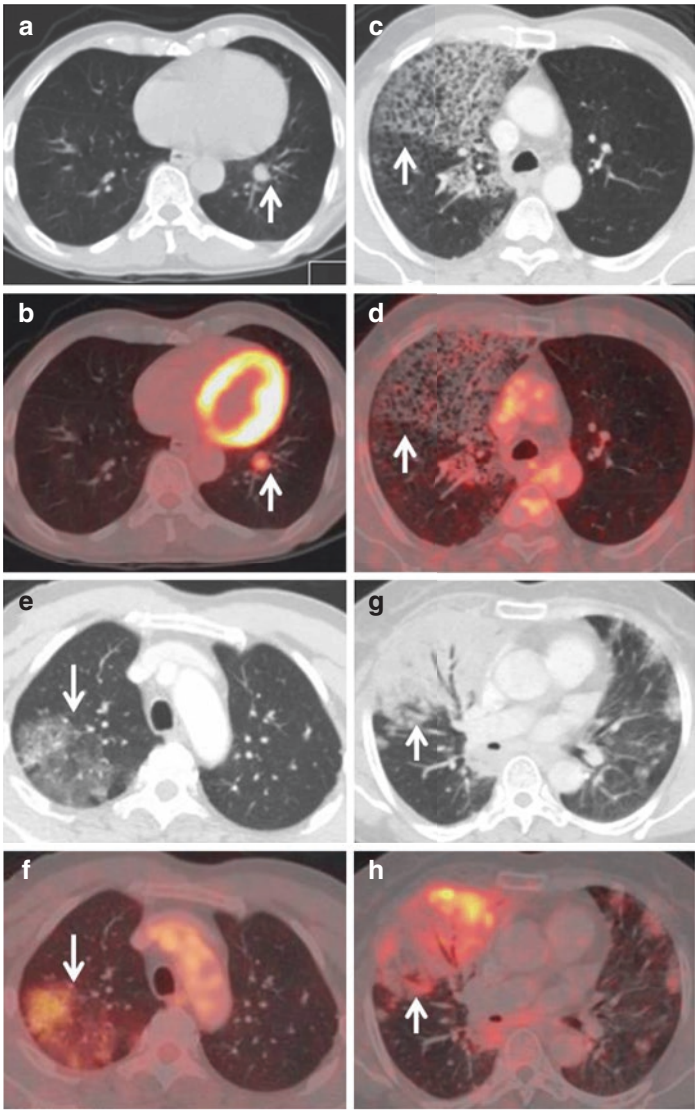

Fig. 8.3 (**a**, **b**) Solitary pulmonary nodule (SPN), (**c**, **d**) crazy paving pattern due to ground glass opacities with superimposed interlobular septal thickening. (**e**, **f**) Ground-glass pattern, (**g**, **h**) consolidation with air bronchogram

8.4 Case 4: Use of PET to Direct the Appropriate Site of Biopsy

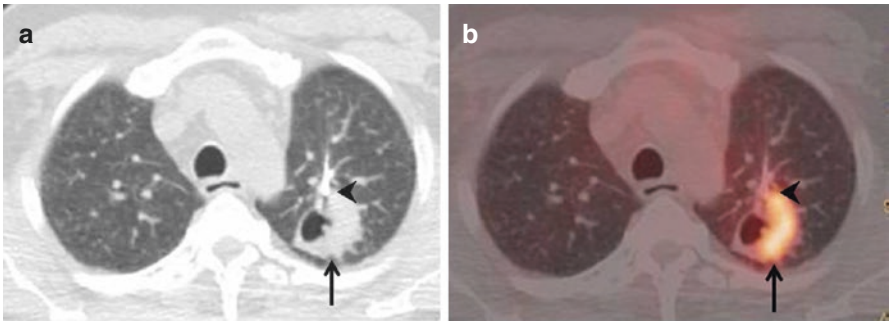

Fig. 8.4 Axial CT and fusion PET/CT (arrows in **a**, **b**) images show a cavitating lung neoplasm **Teaching point**: FDG PET/CT directs the site of biopsy from the hypermetabolic component in the wall of the cavity (arrowhead in **a**, **b**) leading to a correct diagnosis

8.5 Case 5: Staging PET/CT in Lung Cancer Detects Asymptomatic Distant Metastases

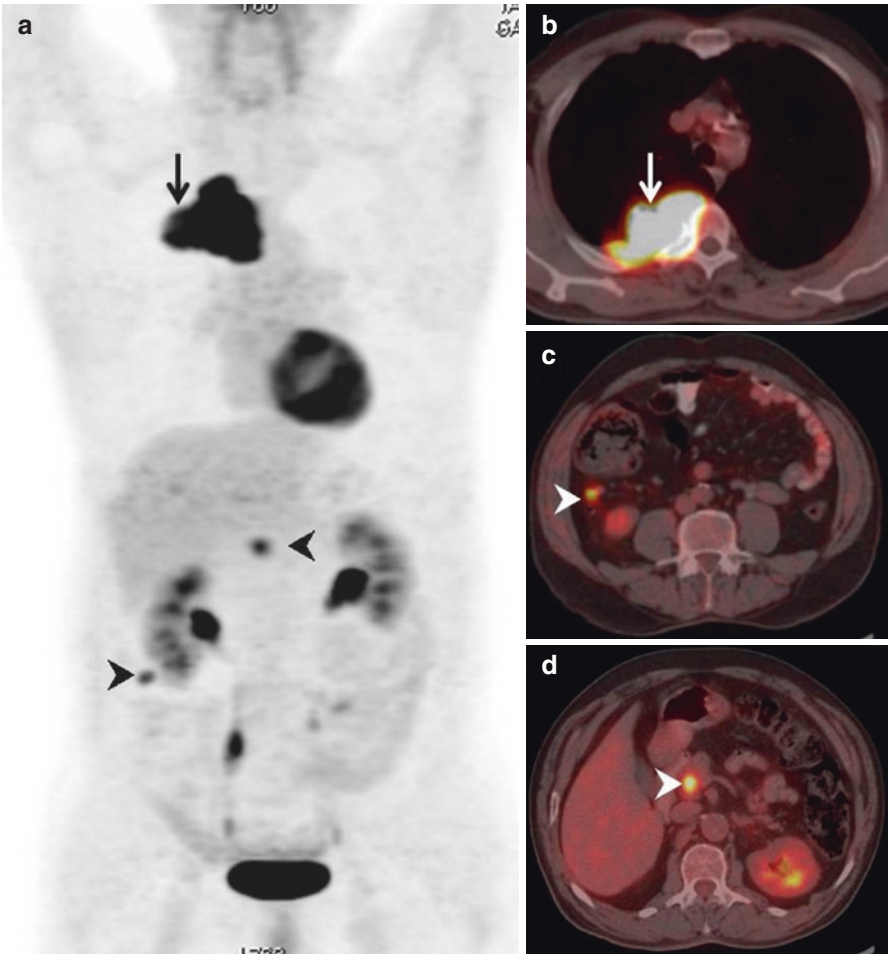

Fig. 8.5 Whole body MIP image and fusion PET/CT images show a FDG-avid mass in the right lung (arrows in **a**, **b**). Foci of FDG avidity in the abdomen seen in the MIP image (arrowheads in **a**) correspond to metastatic peritoneal deposits on fusion PET/CT images (arrowheads in **c**, **d**)

8.6 Case 6: Staging PET/CT in Lung Cancer Detects Asymptomatic Distant Metastases

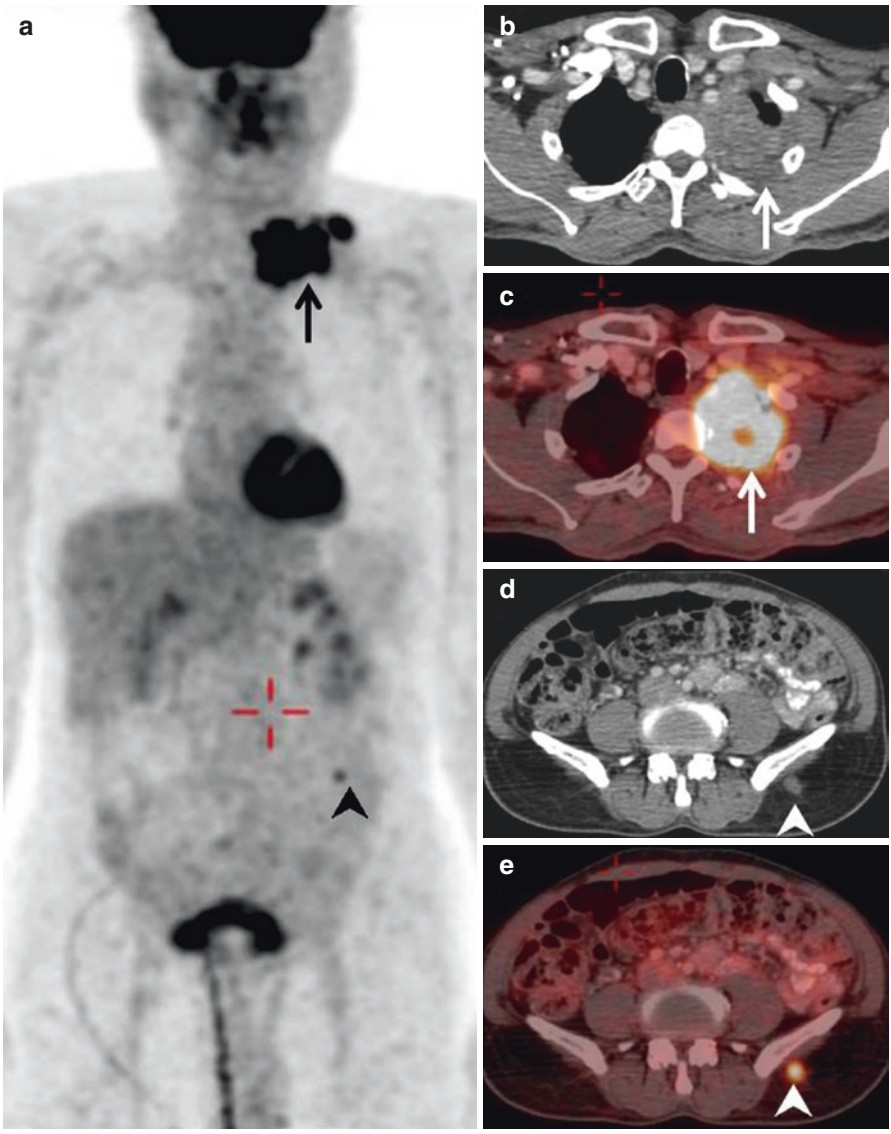

Fig. 8.6 Whole body MIP image axial CT and fusion PET/CT images show a FDG-avid Pancoast tumor in the left lung apex (arrows in **a**–**c**). Focus of FDG avidity in the lower abdomen seen in the MIP image (arrowheads in **a**) corresponds to metastatic soft tissue deposit in the gluteal region on CT and fusion PET/CT images (arrowheads in **d**, **e**)

8.7 Case 7: Staging PET/CT in Lung Cancer Detects a Second Primary Malignancy in the Urinary Bladder

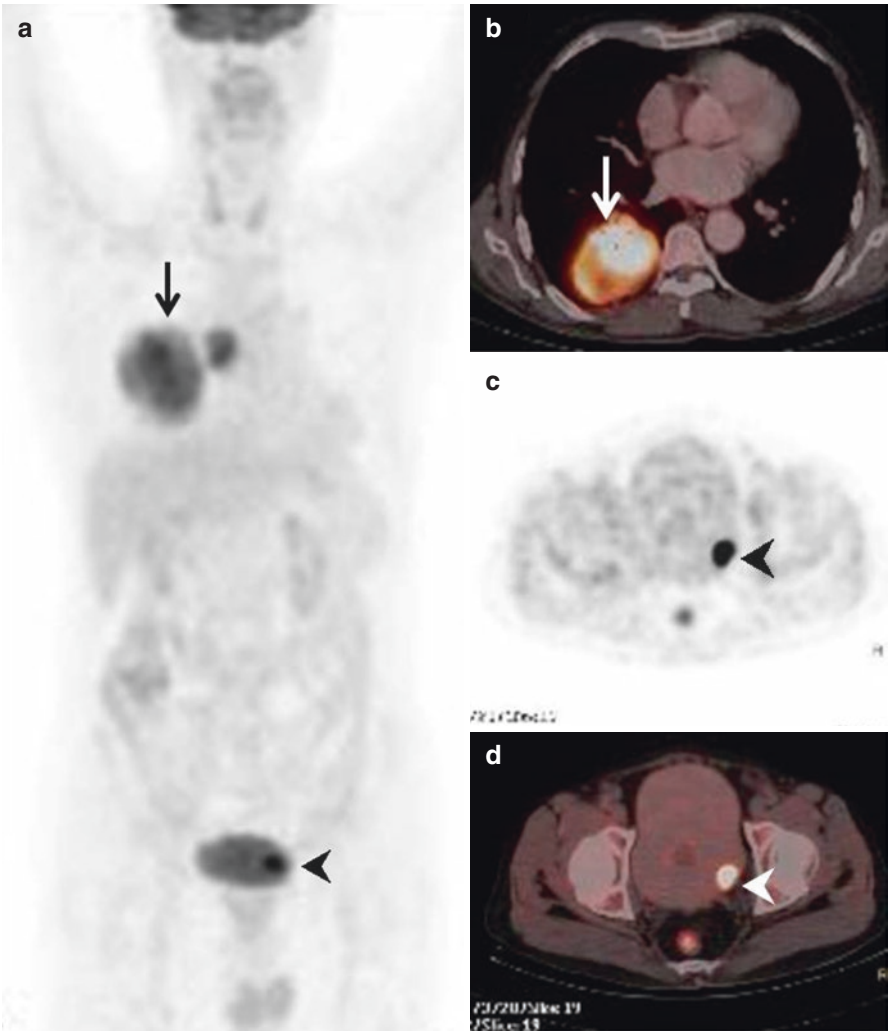

Fig. 8.7 Whole body MIP image and fusion PET/CT images show a FDG-avid mass in the right lung (arrows in **a**, **b**). Focus of FDG avidity in the pelvis seen in the MIP and axial PET image (arrowheads in **a**, **c**) corresponds to a second primary malignancy in the urinary bladder on fusion PET/CT image (arrowhead in **d**)

8.8 Case 8: Staging PET/CT in Lung Cancer Detects a Second Primary Malignancy in the Cecum

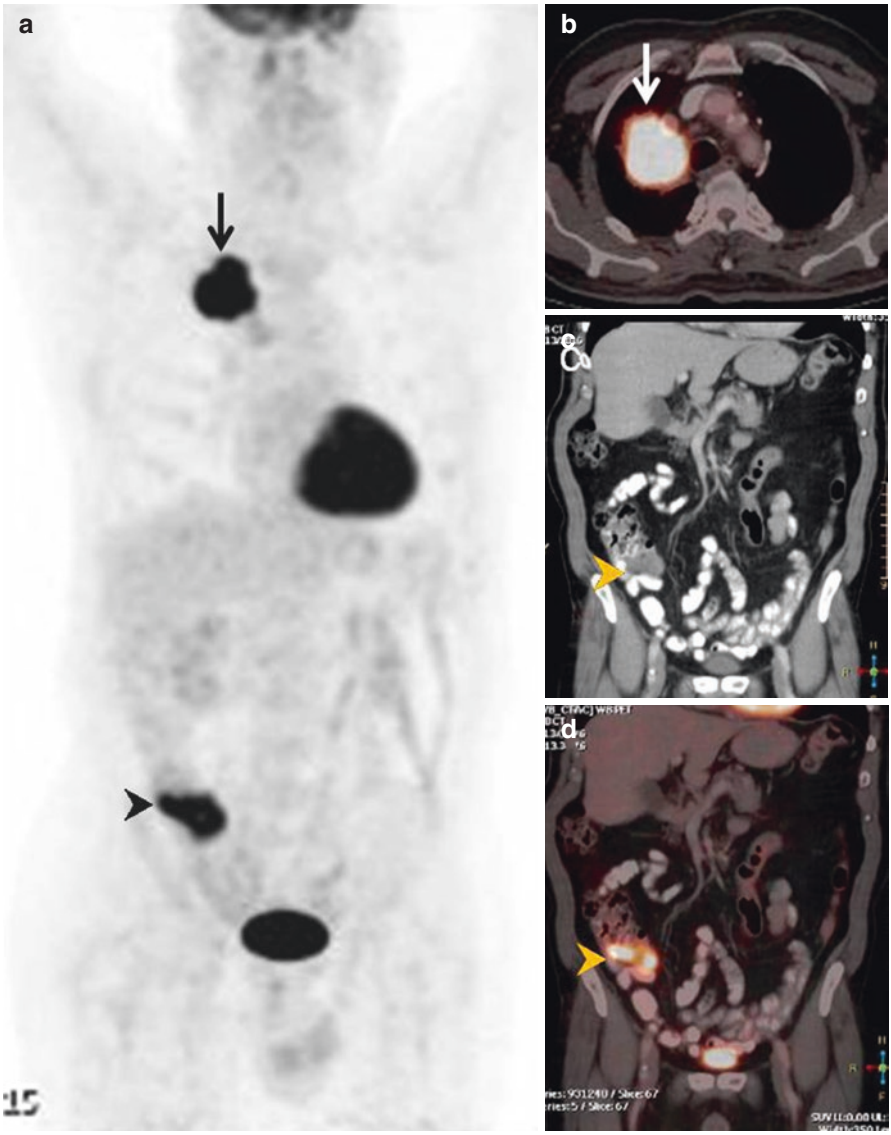

Fig. 8.8 Whole body MIP image and fusion PET/CT images show a FDG-avid mass in the right lung (arrows in **a**, **b**). Focus of FDG avidity in the lower abdomen seen in the MIP image (arrowhead in **a**) corresponds to a second primary malignancy in the cecum on coronal CT and fusion PET/CT image (arrowhead in **c**, **d**)

8.9 Case 9: Staging PET/CT in Lung Cancer with False-Positive Tuberculous Mediastinal Adenopathy

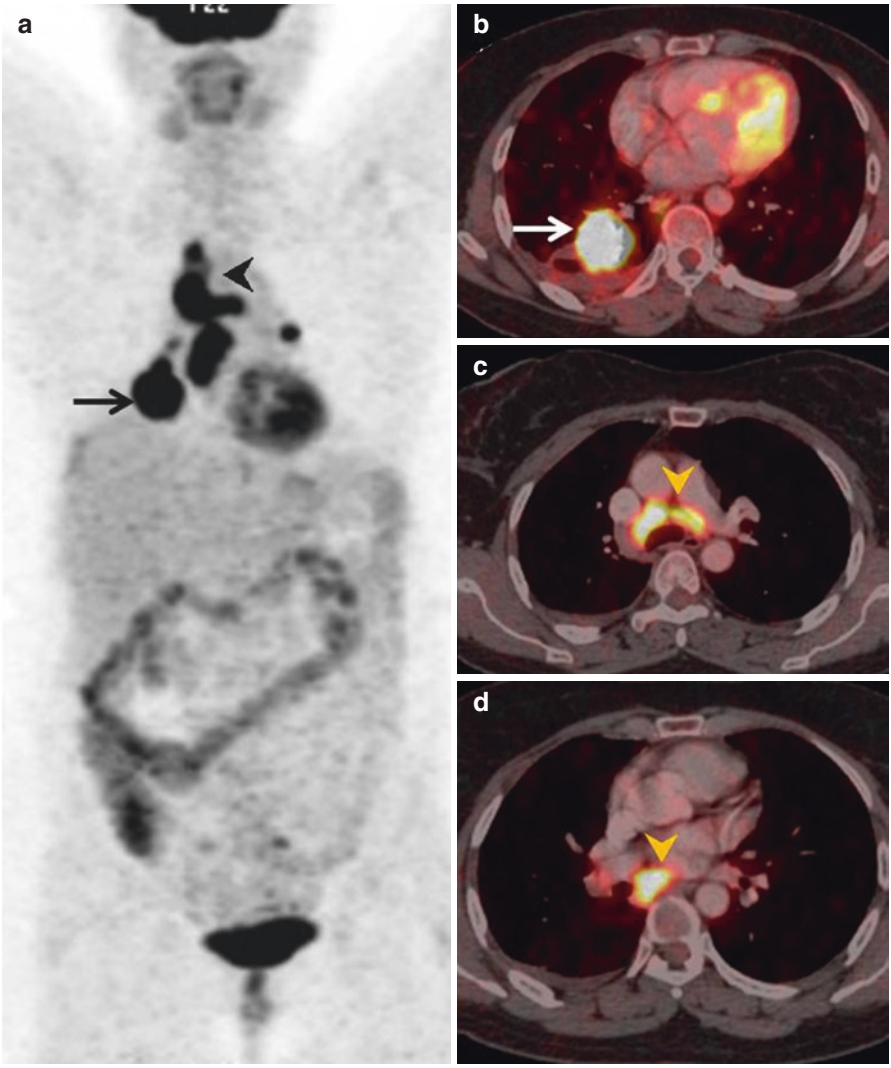

Fig. 8.9 Whole body MIP image and fusion PET/CT images show a FDG-avid mass in the right lung (arrows in **a**, **b**). FDG-avid foci in the mediastinum seen in the MIP image (arrowhead in **a**) correspond to multistation mediastinal nodes on fusion PET/CT images (arrowheads in **c**, **d**) suggesting nodal spread of disease. Biopsy from the mediastinal nodes revealed tuberculosis

8.10 Case 10: Postradiation Therapy Changes in Lung Cancer

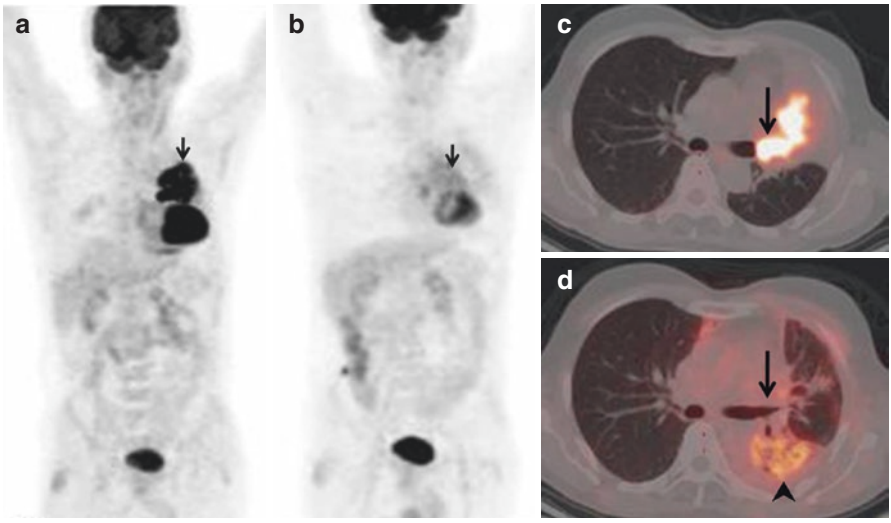

Fig. 8.10 Pretreatment whole body MIP and fusion PET/CT images show a FDG-avid endobronchial soft tissue mass in the left lung (arrows in **a**, **c**). PET/CT performed 12 weeks after radiation therapy shows complete metabolic and morphologic regression of the lung mass (arrows in **b**, **d**). Note: FDG-avid postradiation pneumonitis (arrow in **d**) seen distinct from the site of primary mass

8.11 Case 11: Locoregionally Advanced Lung Cancer After Chemoradiation Therapy, Solitary Distant Failure with Complete Response at Primary Site

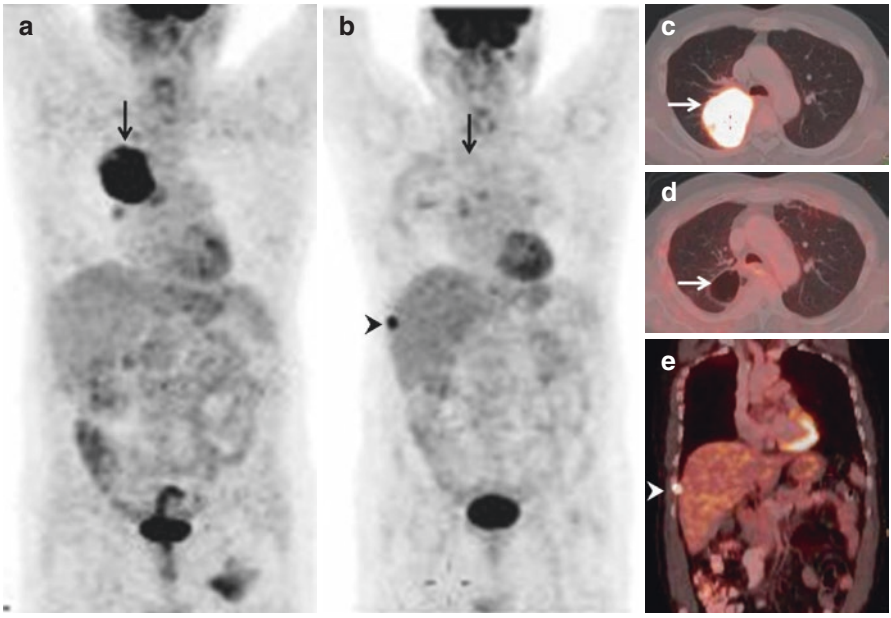

Fig. 8.11 Pre- and post-therapy whole body MIP studies (arrows in **a**, **b**) and fusion PET/CT studies (arrows in **c**, **d**) show complete morphologic and metabolic response at the primary site. Post-therapy whole body MIP study and fusion PET/CT studies (arrowheads in **b**, **e**) show a solitary metastatic site in the chest wall

8.12 Case 12: Metastatic Lung Cancer Treated with Chemotherapy, Solitary Distant Failure with Stable Locoregional Disease

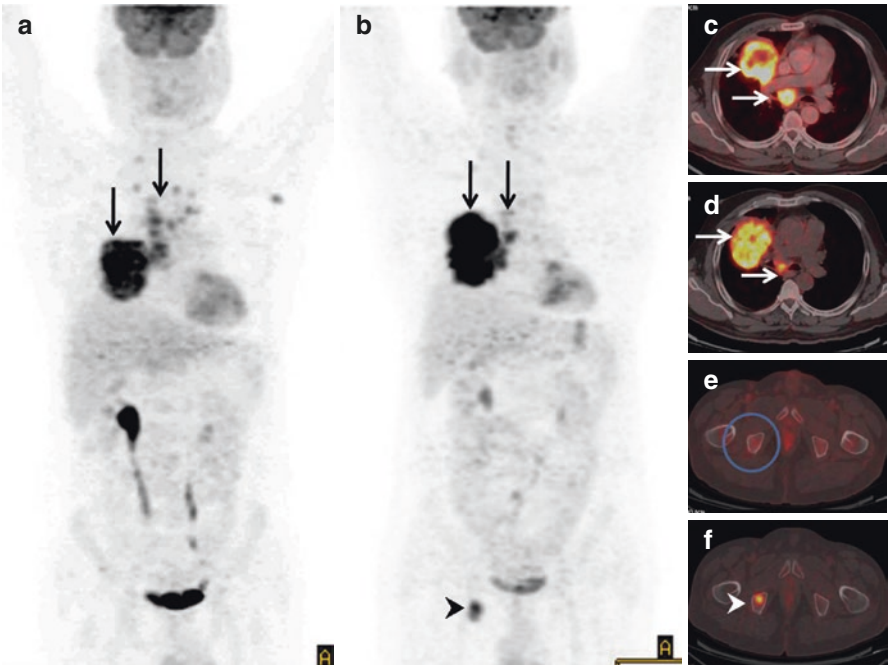

Fig. 8.12 Pre- and post-therapy whole body MIP studies (arrows in **a**, **b**) and fusion PET/CT studies (arrows in **c**, **d**) show persistent disease at the primary site and mediastinal nodes. Post-therapy whole body MIP study and fusion PET/CT studies (arrowheads in **b**, **f**) show a solitary marrow metastases in the ischial tuberosity. Note: Normal-appearing ischial tuberosity in pretreatment PET/CT (circle in **e**)

Index

A. Agrawal, V. Rangarajan (eds.), *PET/CT in Lung Cancer*, Clinicians' Guides to Radionuclide Hybrid Imaging, https://doi.org/10.1007/978-3-319-72661-8